

MOSTAFA KIAMEHR

# Induced Pluripotent Stem Cell-Derived Hepatocyte-Like Cells

*The lipid status in differentiation, functionality,  
and de-differentiation of hepatic cells*



MOSTAFA KIAMEHR

Induced Pluripotent  
Stem Cell-Derived  
Hepatocyte-Like Cells

*The lipid status in differentiation, functionality,  
and de-differentiation of hepatic cells*

ACADEMIC DISSERTATION

To be presented, with the permission of  
the Faculty Council of Faculty of Medicine and Life Sciences  
of the University of Tampere,  
for public discussion in the auditorium F114  
of the Arvo building, Arvo Ylpön katu 34, Tampere,  
on 8 February 2019, at 12 o'clock.

# ACADEMIC DISSERTATION

Tampere University, Faculty of Medicine and Health Technology  
Finland

<i>Responsible supervisor or/and Custos</i>	Professor Katriina Aalto-Setälä Tampere University Finland	
<i>Supervisor(s)</i>	Professor Katriina Aalto-Setälä Tampere University Finland	
<i>Pre-examiner(s)</i>	Docent Matti Jauhiainen University of Helsinki Finland	Professor Kenji Osafune CiRA, Kyoto University Japan
<i>Opponent(s)</i>	Professor Edward A. Fisher New York University United States	

The originality of this thesis has been checked using the Turnitin OriginalityCheck service.

Copyright ©2019 author

Cover design: Roihu Inc.

ISBN 978-952-03-0988-6 (print)

ISBN 978-952-03-0989-3 (pdf)

ISSN 2489-9860 (print)

ISSN 2490-0028 (pdf)

<http://urn.fi/URN:ISBN:978-952-03-0989-3>

PunaMusta Oy  
Tampere 2019

To my wife Katri,  
and my son Daniel



# ACKNOWLEDGEMENTS

The research for this dissertation was carried out in Heart Group at the Institute of Biosciences and Medical Technology (BioMediTech) and Faculty of Medicine and Life Sciences, University of Tampere, during years 2013-2018. I am grateful to the former and current deans of institute and faculty, Hannu Hanhijärvi and Professor Tapio Visakorpi for maintaining excellent research facilities and collaborative working environment during my studies.

I would like to thank all the financial supporters of the thesis: the EU-FP7 RiskyCAD (Personalized diagnostics and treatment for high risk coronary artery disease), the EU-FP7 Athero-Flux (Targeting novel lipid pathways for treatment of cardiovascular disease), the Tampere Graduate Program in Biomedicine and Biotechnology (TGPBB), Instrumentarium Science Foundation, Aarne Koskelo Science Foundation, Ålands Cultural Foundation, Finnish Foundation for Cardiovascular Research, and Finnish Atherosclerosis Society for financially supporting my research and the travels to the international conferences.

Most importantly, my deepest appreciation goes to my kind and proficient supervisor Professor Katriina Aalto-Setälä M.D., Ph.D. for believing in me and granting the opportunity of working and learning in her research group. Katriina, all these years my first priority has been to answer your trust with dedication, hard work and performing good quality science. Thank you for supporting me endlessly and giving me the freedom to do research and yet always finding the time to provide guidance and help. Also I thank you for your advises regarding both scientific career and personal life.

I would like to acknowledge the members of the thesis committee, Professor Olli Silvennoinen M.D., Ph.D.; Professor Timo Otonkoski, M.D., Ph.D.; and Docent Susanna Miettinen, Ph.D. for their support and helpful guidance during the annual meetings. I also express my gratitude to Professor Kenji Osafune and Dr. Matti Jauhiainen for the careful review of my thesis manuscript and for their valuable comments.

All the co-authors of the original communications included in this thesis are acknowledged for their precious work, contribution, and collaboration. The staff in Zora Bioscience, Helsinki University Lipidomics Unit (HiLIPID), and

Hummingbird Diagnostics are also acknowledged for analyzing the samples and for their technical support and guidance. I would like to offer my special thanks to Dr. Reijo Käkälä, for his comments on the original articles and fruitful discussions. Thank you Reijo for sharing your knowledge and expertise with us, it has been invaluable for this dissertation.

A special thank should be given to Professor Kenji Osafune, Dr. Maki Kotaka, and MSc. Azuma Kimura for their guidance and warm hospitality during my two-week visit to the Center for iPS Cell Research and Application (CiRA), Kyoto University in Japan. I also would like to acknowledge all the great people and collaborators in the EU-FP7 RiskyCAD project for the fruitful and fun annual meetings. It was my pleasure to get to know you all and learn from you. I specially would like to name Professor Reijo Laaksonen, Dr. Stefano Manzini, and Dr. Marco Busnelli for their positive attitude and creating the enjoyable moments during the RiskyCAD meetings.

All the former personnel of Regea and current colleagues in Arvo building, 4<sup>th</sup> floor - particularly people in Adult Stem Cell Group, Neuro Group and Eye Group - are thanked for the nice talks during coffee breaks and for their help in the Lab.

A huge thank you to all the former and present members of the Heart Group for their help and support. I warmly thank you for creating a nice and friendly working environment and all the everlasting beautiful memories during the fun activities and trips. A sincere thank you to the dedicated and brilliant technicians of the Heart Group, Henna Lappi, Markus Haponen, and Merja Lehtinen for the constant assistance during my entire studies, and for maintaining the laboratories in such high standard, assuring a great environment for good science. I offer my special thanks to the Old Gang, Markus Haponen and Disheet Shah, for their friendship and positive energy, making my life easier through the hard moments. A big thank you to Chandra Prajapati, Janne Koivisto, and Risto-Pekka Pölönen for their genuine support and great company. A warm thank you to Eeva Laurila, Reeja Maria Cherian, and Marta Hakli for all the shared moments in the office, nice discussions and laughter which kept me going and helped me to deal with the challenging times.

I am eternally grateful to my family in Iran, my caring mother, Fatemeh Meybodi, for her support, unconditioned love and patience during all these years. My father who recently left us to another world. Dad, you always encouraged me to study and now it deeply burns my heart that at this very moment of the highest accomplishment, you are not among us to celebrate this special day with me. But, I am sure that up there, you are happy and proudly looking at me, like you always did, and that keeps my heart warm. My sisters Shahnaz, Marjan, and Sara Kiamehr and



my brother, Abbas Kiamehr, who endlessly supported me during the years being far from home. Thank you for your love and for compensating my absence during all these years and taking care of mom and dad while I was away and busy with my studies. I couldn't have accomplished this heavy task without your support. I am also very thankful to Amir, Shayan, and Aria Tabatabaei, Mohammad Babayousef, Raziye Kouchakipour and Amin Kiamehr for their love and support. I am grateful to Lauri, Sirkka, Hanna, Suvi and Matti Karjalainen and Eeva Uuksulainen for their care and constant support along the way.

And Finally, from the deepest part of my heart, I would like to express my love and appreciation to my wife, Katri Kiamehr, and my dear son, Daniel Kiamehr, without whom I could not have imagined going through this journey. Daniel, you brought a lot of joy to my life and from time to time, took my mind away from the stress towards what really matters in life. Katri, you gave me the most needed mental support in the hard moments and I cannot thank you enough for that and your patience, understanding, and all the sacrifices you made during those times and above of all, for your love! I also want to acknowledge you for helping me with writing the Finnish abstract of this book and all the proofreading of the English texts. You and Daniel are my world!

Tampere, November 2018

*Mostafa*



# ABSTRACT

Primary human hepatocytes (PHHs) are currently considered the “gold standard” cell model for investigating the liver physiology, toxicity, and lipid homeostasis. However, PHHs are scarce and functionally heterogeneous, and when cultured, they lose their liver-specific functions relatively fast within a few days. Induced pluripotent stem cell-derived hepatocyte-like cells (iPSC-HLCs) provide a relevant alternative model for PHHs to study the lipid derangements of the liver. Unlike PHHs, the cell source to generate iPSC-HLCs is unlimited and they can be advantageously generated from selected individuals with different genetic backgrounds. Since lipid defects play central roles in the pathogenesis of several common diseases such as non-alcoholic fatty liver disease and atherosclerotic cardiovascular disease, iPSC-HLCs could serve as a novel platform for studying the basic mechanisms of the lipid metabolism and its dysregulation in a truly patient-specific manner. Additionally, this cell model could be utilised in drug discovery and especially in studying the drug induced hepatotoxicity. To maximise the utilisation of HLCs for such valuable purpose, it is critical to characterise their detailed lipid profile in relation to the human adult liver cells.

Lipids are a major class of molecules, which play critical roles in cellular structure, function, and signalling. It has been shown that certain fatty acids (FAs) promote neuronal and adipocyte differentiation. Therefore, in-depth knowledge of changes in lipid and FA profile of the hepatocytes during differentiation and de-differentiation could assist us to generate matured target cells, which resemble the lipid profile of PHHs even closer. In addition, this knowledge can be utilised to optimise the culture environment according to the cellular need and subsequently prolong the life span and functionality of both the iPSC-HLCs and the PHHs in culture.

Major aims of this thesis were to first study the alterations in the lipid and FA profile of the cells during the hepatic differentiation in order to identify the lipid species that may play important roles in the differentiation and maturation of hepatocytes. For this purpose, detailed lipidomic analysis and gene expression profiling of a set of key genes involved in the metabolism of lipids were performed at several time points during the entire differentiation process from iPSC to HLCs.

The second aim was to comprehensively characterise the lipid and FA profile of HLCs against current standard hepatic cell models. HLCs were generated by five different methods and their lipid profile as well as their ability to synthesise, elongate, and desaturate FAs were thoroughly assessed and compared to the profiles of widely used hepatocyte models, PHHs and HepG2 cells. In addition, the effect of various conditions or stimuli introduced by each method were evaluated on HLCs' phenotype and functionality. The third aim focussed on the mechanisms behind the hepatic de-differentiation by studying the alterations in the lipid profile of the PHHs during their prolonged two-dimensional (2D) culture. In addition, we complemented our results from lipidomics with miRNA analysis to further identify the differentially expressed miRNAs that may regulate changes in the lipid profile of PHHs during the process of de-differentiation.

Taken together, our findings illustrate that HLCs differentiated from iPSCs provide a relevant and functional cell model to explore human lipid homeostasis at both cellular and molecular levels. Additionally, this thesis provides novel findings on the possible role of lipids, FAs, and miRNAs in the process of differentiation and/or de-differentiation and may be applied in designing culture environments that would improve the maturity of HLCs. Since hepatocytes in 2D culture lose their metabolic competence and viability relatively fast, this thesis offers some new ideas and strategies to improve the culture systems for maintaining hepatocytes in long-term culture.

# TIIVISTELMÄ

Ihmisen maksasta eristettyjä soluja (PHH) pidetään ns. ”kultaisena standardina” maksan fysiologian, toksisuuden ja lipidien homeostaasin tutkimiseksi. Nämä solut ovat vaikeasti saatavia sekä toiminnoiltaan heterogeenisiä ja viljeltynä menettävät maksalle spesifit toiminnot suhteellisen nopeasti jo muutamassa päivässä. Uudelleen ohjelmoiduista kantasoluista (iPS-solut) tuotetut maksasolujen kaltaiset solut (HLC) tarjoavat vaihtoehtoisen mallin maksan normaalin ja poikkeavan rasva-aineenvaihdunnan tutkimiseksi. Näiden kantasoluista tuotettujen maksasolujen etuna on rajoittamaton saatavuus sekä mahdollisuus tuottaa niitä eri geenitaustan omaavien yksilöiden soluista. Koska rasva-aineenvaihdunnan häiriöillä on keskeinen rooli monien yleisten tautien kuten ei-alkoholiperäisen rasvamaksan sekä ateroskleroottisen sydän- ja verisuonitaudin patogeenisissä, kantasoluista tuotetut maksasolut tarjoavat uuden potilasspesifisen keinon rasva-aineenvaihdunnan ja sen häiriöiden perusmekanismien tutkimiseksi. Lisäksi tätä solumallia on mahdollista hyödyntää lääkekehityksessä ja erityisesti lääkkeiden aiheuttaman maksatoksisuuden tutkimisessa. Jotta näitä maksasoluja voidaan hyödyntää maksimaalisesti, on tärkeää selvittää niiden yksityiskohtainen lipidiprofiili ja verrata sitä ihmisen maksasta eristettyihin soluihin.

Rasvat ovat merkittävä molekyyli luokka, ja niillä on tärkeä tehtävä solun rakenteessa, toiminnassa ja signaloinnissa. On myös osoitettu, että tietyt rasvahapot edistävät hermo- ja rasvasolujen erilaistumista. Siksi maksasolujen lipidi- ja rasvahappoprofiilien muutoksien syvälinen tuntemus sekä erilaistumisen (differentiaation) että spesifisten ominaisuuksien vähenemisen (dedifferentiaation) aikana auttaisi meitä tuottamaan kantasoluista kypsiä maksasoluja, joiden lipidiprofiili muistuttaisi maksasta eristettyjen solujen lipidiprofiilia entistä paremmin. Lisäksi tämän tiedon avulla viljely-ympäristö voitaisiin optimoida solujen tarpeiden mukaiseksi ja sen seurauksena pidentää niiden elinkaarta ja funktionaalisuutta.

Tämän väitöskirjatyön päätavoitteina oli ensin tutkia lipidi- ja rasvahappoprofiilien muutoksia maksasolujen erilaistumisen aikana ja pyrkiä tunnistamaan tässä erilaistumisessa ja kypsymisessä tärkeitä lipidejä. Tätä tarkoitusta varten tehtiin yksityiskohtainen lipidomikka-analyysi ja rasva-aineenvaihduntaan osallistuvien aineiden ilmentymisen profilointi useina eri ajankohtina

erilaistumisprosessin aikana. Toinen tavoite oli kuvata kattavasti kantasoluista tuotettujen maksasolujen lipidi- ja rasvahappoprofiili ja verrata sitä tämänhetkisiin standardimaksasolumalleihin. Maksasolujen tuottamiseen iPS-soluista käytettiin viittä eri menetelmää ja näiden maksasolujen lipidiprofiili samoin kuin niiden kyky syntetisoida ja prosessoida rasvahappoja tutkittiin perusteellisesti ja verrattiin laajasti käytettyihin maksasolumalleihin. Lisäksi tarkasteltiin kunkin menetelmän avulla tuotettujen erilaisten kasvatusolosuhteiden vaikutusta solujen ilmiäsuun sekä toiminnallisuuteen. Kolmas tavoite keskittyi maksasolujen dedifferentiaation, eli soluviljelmissä tapahtuvan maksasoluominaisuuksien menettämisen, taustalla olevien mekanismien tutkimiseen seuraamalla ihmisen maksasta eristettyjen solujen lipidiprofiilin muutoksia soluviljelyn aikana. Lipidomiikka-analyysistä saatuja tuloksia täydennettiin mikroRNA-analyysillä, jotta voitiin tunnistaa eri tavoin ilmentyneet mikroRNA:t, jotka voisivat säädellä tuota prosessia.

Yhteenvedona voidaan todeta, että iPS-soluista tuotetut maksasolut tarjoavat asianmukaisen ja toimivan solumallin ihmisen rasva-aineenvaihdunnan tutkimiseksi sekä solu- että molekyyalitasolla. Lisäksi tämä tutkimus tarjoaa uusia havaintoja lipidien, rasvahappojen ja mikroRNA:n mahdollisesta roolista differentiaatio- ja/tai dedifferentiaatioprosessissa, joita voidaan soveltaa kantasoluista tuotettujen maksasolujen kypsymistä parantavien viljely-ympäristöjen suunnittelussa. Koska maksasolut menettävät soluviljelmissä merkittäviä metabolisia toimintojaan suhteellisen nopeasti, tämä tutkimus tarjoaa uusia ideoita ja strategioita kasvatusjärjestelmien parantamiseksi maksasolujen pitämiseksi toiminnallisina pitkäaikaisissakin soluviljelmissä.

# TABLE OF CONTENTS

1	Intoduction .....	21
2	Literature review .....	23
2.1	Human liver .....	23
2.2	Liver development .....	24
2.3	Lipid and fatty acid synthesis in hepatocytes .....	26
2.4	Functions of lipids and fatty acids .....	28
2.5	Liver cell models.....	30
2.5.1	Primary human hepatocytes .....	31
2.5.2	Hepatoma cell lines .....	32
2.5.3	Stem cell-derived hepatocytes .....	32
2.6	Differentiation of HLCs from pluripotent stem cells .....	33
2.7	Challenges in using iPSC-derived hepatic cells .....	34
2.8	Three-dimensional culture of hepatic cells.....	35
2.9	De-differentiation of hepatic cells .....	36
2.10	MicroRNAs.....	37
3	Aims of this thesis .....	39
4	Materials and methods.....	40
4.1	Ethical consideration.....	40
4.2	Reprogramming of hiPSC .....	40
4.3	Culture of hiPSC .....	40
4.4	Characterization of hiPSC .....	41
4.5	Culture of the human primary hepatocytes.....	42
4.6	Culture of HepG2 cells.....	42
4.7	Hepatic differentiation from hiPSCs .....	42
4.8	The characterization of cells during hepatic differentiation and maturation.....	44
4.8.1	Morphology.....	44
4.8.2	Real-time quantitative PCR.....	45
4.8.3	Immunofluorescence.....	47
4.8.4	Flow cytometry.....	47
4.9	Biochemical methods.....	48

4.10	Mass spectrometry lipidomics.....	48
4.11	Fatty acid analysis by gas chromatography .....	49
4.12	miRNA analysis.....	49
4.13	Statistical analysis.....	49
5	Summary of the results .....	50
5.1	Hepatic differentiation.....	50
5.1.1	Cell morphology during the hepatic differentiation .....	50
5.1.2	Gene and protein expression during the hepatic differentiation .....	51
5.1.3	Functionality assessment during the hepatic differentiation .....	51
5.1.4	Fluctuation in the lipid species content of cells during hepatic differentiation .....	52
5.1.5	Gene-lipid interactions.....	54
5.2	Comparison of hepatic differentiation methods .....	54
5.2.1	Morphology.....	54
5.2.2	Gene and protein expression.....	55
5.2.3	Functional assays .....	55
5.2.4	Lipid species profiles and fatty acid synthesis.....	56
5.3	Comparison of hiPSC-HLCs with HepG2 and primary human hepatocytes .....	56
5.3.1	Morphology.....	56
5.3.2	Gene and protein expression.....	56
5.3.3	Functional assays .....	57
5.3.4	Lipid species and fatty acid profiles .....	57
5.3.5	Fatty acid metabolic regulation pathway .....	58
5.4	De-differentiation of primary human hepatocytes in culture.....	58
5.4.1	The morphology, gene expression, and the functionality of de-differentiating PHHs.....	58
5.4.2	Lipid profile of de-differentiating PHHs .....	60
5.4.3	Fatty acid and glucose metabolism in de-differentiating PHHs.....	61
5.4.4	miRNA profile of de-differentiating PHHs.....	61
6	Discussion.....	62
6.1	The differentiation of hiPSCs towards HLCs.....	62
6.2	hiPSCs-HLCs as cell models for investigating the lipid aberrations of the liver.....	64
6.3	Lipids and the de-differentiation of the PHHs.....	66
6.4	The role of miRNAs in de-differentiation of PHHs.....	68
6.5	Limitations and future perspective .....	69
7	Conclusions and future aspects.....	71



8	References.....	73
---	-----------------	----

# ABBREVIATIONS

AFP	Alpha-fetoprotein
APOA1	Apolipoprotein A-I gene
APOB	Apolipoprotein B gene
ASAH	Acid ceramidase
ASGPR	Asialoglycoprotein receptor
bFGF	Basic fibroblast growth factor
BMP4	Bone morphogenic protein 4
BSA	Bovine serum albumin
CE	Cholesteryl ester
Cer	Ceramide
CerS	Ceramide synthase
DAG	Diacylglycerol
DAPI	6-diamidino-2-phenylindole
DE	Definitive endoderm
EGF	Epidermal growth factor
ELOVL	Fatty acid elongase
ER	endoplasmic reticulum
FA	Fatty acid
FADS	Fatty acid desaturase
FASN	Fatty acid synthase
Gb3	Globotriaosylceramide
GCK	Glucokinase
Glc/GalCer	Glucosyl/galactosylceramide
GSL	Glycosphingolipid
HGF	Hepatocyte growth factor
hiPSC	Human induced pluripotent stem cell
HLC	Hepatocyte-like cell
hLTR	Human Liver Total RNA
KO-DMEM	Knock-out Dulbecco's Modified Eagle's Medium
LacCer	Lactosylceramide

LCFA	Long-chain fatty acid
Lyso-PC	Lysophosphatidylcholine
Lyso-PE	Lysophosphatidylethanolamine
Lyso-PL	Lysophospholipid
M1	Method 1
M2	Method 2
M3	Method 3
M4	Method 4
M5	Method 5
MEF	Mouse embryonic fibroblast
MSC	Mesenchymal stem cell
miRNA	MicroRNA
MUFA	Monounsaturated fatty acid
OSM	Oncostatin M
PC	Phosphatidylcholine
PCR	Polymerase chain reaction
PCA	Principal Component analysis
PC-O	Alkyl-linked phosphatidylcholine
PC-P	Alkenyl-linked phosphatidylcholine
PCK1	Phosphoenolpyruvate carboxykinase 1
PE	Phosphatidylethanolamine
PE-O	Alkyl-linked phosphatidylethanolamine
PE-P	Alkenyl-linked phosphatidylethanolamine
PHH	Primary human hepatocyte
PI	Phosphatidylinositol
PKLR	Liver-type pyruvate kinase
PL	Phospholipid
PPAR	Peroxisome proliferator activated receptor
PS	Phosphatidylserine
PUFA	Polyunsaturated fatty acid
qPCR	Quantitative PCR
SCD	Stearoyl-CoA desaturase
SFA	Saturated fatty acid
SGMS	Sphingomyelin synthase
SL	Sphingolipid
SM	Sphingomyelin

SMPD	Sphingomyelin phosphodiesterase
SMS	Sphingomyelin synthase
TAG	Triacylglycerol
UGCG	UDP-glucose ceramide glucosyltransferase
VLCFA	Very-long chain fatty acid

# ORIGINAL PUBLICATIONS

This dissertation is based on the original peer-reviewed publications listed below and referred as **Study I-III** in the text. Articles are reprinted with permissions from the copyright holders (publishers).

Publication I **Kiamehr M\***, Viiri L\*, Vihervaara T, Koistinen K, Hilvo M, Ekroos K, Käkälä R, Aalto-Setälä K. Lipidomic profiling of patient-specific iPSC-derived hepatocyte-like cells. *Disease Models & Mechanisms*. 2017; 10:1141-1153.

Publication II **Kiamehr M**, Alexanova A, Viiri L, Heiskanen L, Vihervaara T, Kauhanen D, Ekroos K, Laaksonen R, Käkälä R, Aalto-Setälä K. hiPSC-derived hepatocytes closely mimic the lipid profile of primary hepatocytes: A future personalised cell model for studying the lipid metabolism of the liver. *Journal of Cellular Physiology*. 2018; doi: 10.1002/jcp.27131.

Publication III **Kiamehr M**, Heiskanen L, Laufer T, Düsterloh A, Kahraman M, Käkälä R, Laaksonen R, Aalto-Setälä K. Dedifferentiation of primary hepatocytes is accompanied with reorganisation of lipid metabolism indicated by altered molecular lipid and miRNA profiles. Under review at *Scientific Reports*.

\* These authors contributed equally

The current dissertation also includes unpublished data.



# 1 INTRODUCTION

Liver is the main metabolic and synthetic organ, which regulates many critical physiological functions in the human body. Approximately 70% of the liver mass is composed of hepatocytes (Blouin et al., 1977), which carry out most of the metabolic functions of the liver such as detoxification of a wide variety of molecules, synthesis of plasma proteins, regulation of amino acids and carbohydrates, and activation of inflammatory and immune responses (Si-Tayeb et al., 2010a). In addition, hepatocytes control the energy/fuel homeostasis by regulating the synthesis of glucose/glycogen and fatty acids (FAs). Moreover, hepatocytes are the major cells for synthesis of many lipids including cholesterol, cholesteryl esters (CEs), triacylglycerols (TAGs) and phospholipids (PLs), which are further utilized by hepatocytes to assemble and secrete lipoprotein particles to the general circulation (Godoy et al., 2013; Gordillo et al., 2015).

The use of primary hepatocytes as the “gold standard” model system to study the liver physiology and drug-induced liver injury has escalated in recent years. However, since primary human hepatocytes (PHHs) are obtained from organ donors, they are scarce and functionally variable due to genetic variation of the donors. In addition, when PHHs are isolated and cultured, they progressively lose their liver-specific functions (Elaut et al., 2006; Godoy et al., 2013), which dramatically limits their utility especially in the long-term toxicity studies. Due to these limitations, other cell models such as human hepatoma cell lines (e.g. HepG2) have been widely used since they demonstrate unlimited life span and stable phenotype. However, the key morphological and metabolic features are often repressed or absent in hepatoma cell lines and they may typically represent a cancer metabolic profile. Therefore, they do not faithfully represent the metabolic activities of healthy hepatic cells (Olsavsky et al., 2007; Steenbergen et al., 2018). Animal models have also abundantly been used, but information gained from animal primary hepatocytes is not fully translatable to humans due to significant interspecies variations e.g. in their physiology, gene expression profile, lipoprotein distribution and drug metabolism (Kvilekval et al., 1994; Uhl and Warner, 2015).

The invention of human induced pluripotent stem cells (hiPSCs) have opened new avenues for the research in the field of regenerative medicine (Takahashi et al., 2007). hiPSCs can be easily reprogrammed from somatic cells, and then differentiated into hepatocyte-like cells (HLCs) that functionally resemble PHHs (Hu and Li, 2015). Therefore, hiPSC-derived HLCs (iPSC-HLCs) provide a good alternative for PHHs as they also circumvent the limited availability of the cells faced when working with the PHHs. hiPSC-HLCs could highly benefit us in understanding the molecular basis of liver cell differentiation, disease mechanisms, modelling inborn errors of hepatic metabolism, and in drug discovery and studying the hepatocellular toxicity effects as well as in developing personalised medicine.

Lipids, as a major class of biological molecules, play critical roles in energy storage, structure, function, and signalling (Van Meer et al., 2008). Lipids are the key components in plasma and nuclear membrane, endoplasmic reticulum (ER), Golgi apparatus, and trafficking vesicles such as endosomes and lysosomes (Muro et al., 2014). Lipoproteins in circulation are vehicles operating the transfer of lipids between the organs and peripheral cells.

In addition, lipid defects have central role in the pathogenesis of many diseases, such as atherosclerotic cardiovascular disease (Meikle et al., 2011; Stübiger et al., 2012) and non-alcoholic fatty liver disease (Ruhanen et al., 2017; Younossi et al., 2016), and hiPSC-HLCs offer a relevant platform to investigate the basic mechanisms of lipid metabolism and its dysregulation in a patient-specific manner. In order to maximise the utilisation of HLCs as a cell model, it is essential to know their lipid profile in relation to their native counterparts and the currently used cell models, such as PHHs and hepatoma cell lines. Until recently, studying the lipids in molecular levels was dramatically hampered due to their complexity and lack of suitable analytical technology. However, by the emergence of the advanced lipidomic technologies together with the recent cutting-edge computational techniques, today it is possible to study the complex cellular lipidome, making this field a promising area for biomedical research. The lipidomic data can be further combined with genotype/phenotype information on the individual level.

The main objectives of this dissertation were to generate a functional patient-specific hepatic cell model suitable for investigating human lipid homeostasis, to characterise the lipid and FA profile of generated hepatocytes comprehensively in comparison to their native counterparts, and to investigate the role of various molecular lipid species and FAs both in the differentiation and in de-differentiation of hepatic cells.



## 2 LITERATURE REVIEW

### 2.1 Human liver

Liver is the largest metabolic organ in the human body and regulates more than 500 various functions including the synthesis and storage of lipids, amino acids, proteins, and vitamins as well as the detoxification of a wide variety of molecules (Si-Tayeb et al., 2010a) (Gordillo et al., 2015). In addition, liver is responsible for the synthesis and transport of cholesterol and triglycerides, the metabolism of urea, and the production and secretion of bile. Hepatocytes are the main cell type in the liver and are responsible for most of its physiological function (Blouin et al., 1977). The liver is traditionally structured in highly organised functional units called lobules which in addition to hepatocytes contain many other cell types such as cholangiocytes, endothelial cells, pit cells, Kupffer cells, and stellate cells (Ishibashi et al., 2009; Si-Tayeb et al., 2010b) (**Figure 1**). In the lobules, blood from the portal vein and hepatic artery flows toward the central vein through sinusoids. On the other hand, the bile acid secreted by the hepatocytes flows in the opposite direction than the blood and towards the bile ducts (Godoy et al., 2013). In this structure, hepatocytes are organised in a highly polarised manner and have sinusoidal and the apical surfaces. The sinusoidal surface is faced towards sinusoidal endothelial cells and apical surface is faced towards the bile canaliculi (Treyer and Müsch, 2013). This organisation and polarization is critical for the proper function of hepatocytes (Gissen and Arias, 2015).

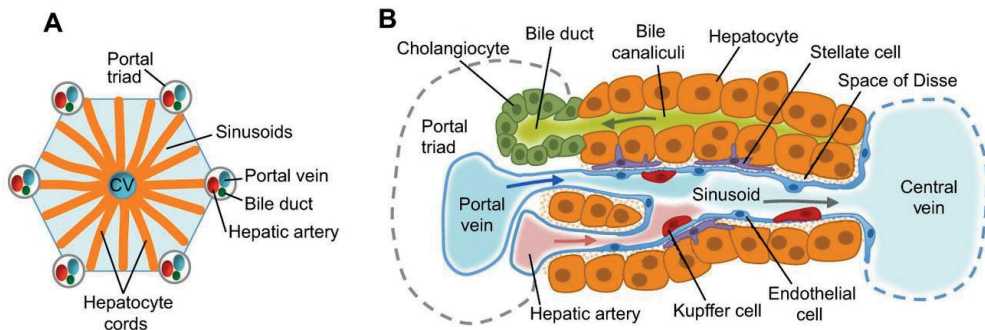


**Figure 1.** The structure of the liver lobule and its composing cell types. **A)** Demonstrates a liver lobule including the central vein (CV) and portal triad consist of hepatic artery, portal vein, and biliary duct. Hepatocytes are structured as cords separated by sinusoids. **B)** Demonstrates the organised hepatic cells along with the non-parenchymal cells (NPCs) within a liver lobule. The sinusoids carry blood from the portal triad towards the central vein while the secreted bile moves in the opposite direction in the bile canaliculi towards the bile ducts. Image is adapted with permission from Gordillo et al., 2015 (Gordillo et al., 2015).

## 2.2 Liver development

During embryogenesis, the inner cell mass goes through gastrulation and forms three germ layers of endoderm, mesoderm, and ectoderm. At this stage, endoderm is a single cell layer thick on the ventral site of the developing embryo. The definitive endoderm (DE) then forms the primitive gut tube patterned into three progenitor domains of foregut, midgut and hindgut (Tremblay and Zaret, 2005). Through inductive signals from surrounding tissues, the foregut differentiates into the liver as well as many other tissue types such as pancreas, thyroid, lungs, and gastrointestinal tract (Wells and Melton, 1999).

Liver development is tightly regulated by signals and growth factors in both time- and concentration-dependent manner (Gordillo et al., 2015; Zaret, 2002) and cell signalling during the hepatocyte differentiation process is of utmost importance (Vasconcellos et al., 2016). Wnt/ $\beta$ -catenin signalling together with bone morphogenic proteins (BMPs) and fibroblast growth factors (FGFs) activate Nodal signalling (Haramoto et al., 2004; Lade and Monga, 2011), which is critical for the initiation of gastrulation and early endoderm development as well as the segregation of endoderm and mesoderm from the bipotential mesendoderm (Vincent et al., 2003). The first sign of liver formation is seen when the cells in ventral foregut endoderm express alpha-fetoprotein (*AFP*) (Tremblay and Zaret, 2005). The FGFs

secreted from early cardiac mesoderm and BMPs secreted from the septum transversum mesenchyme (STM) initiate hepatic induction in a concentration-dependent manner (Calmont et al., 2006; Rossi et al., 2001). FGFs activate phosphatidylinositol 3-kinase (PI3K) independent MAPK pathway and BMPs activate the *albumin* gene as well as the expression of GATA4 transcription factor which all participate in the specification of hepatic endoderm (Rossi et al., 2001; Wandzioch and Zaret, 2009). When the ventral foregut endoderm cells commit to the hepatic fate, Wnt/ $\beta$ -catenin signalling is repressed to allow the activation of hematopoietically-expressed homeobox protein (HHEX), an important transcription factor regulating the hepatic commitment and development (Bort et al., 2006). The newly committed hepatic endoderm cells then thicken and form the liver diverticulum which further proliferates and forms a multilayer of hepatoblasts surrounded by a laminin-rich basal membrane. Hepatoblasts then delaminate into the STM and proliferate to give rise to the liver bud (Bort et al., 2006). At this stage, FGFs, BMPs, and hepatocyte growth factor (HGF) promote the hepatoblast migration and hepatic bud growth (Calmont et al., 2006; Medico et al., 2001). Hepatoblasts differentiate into hepatocytes and start to polarize and arrange into cords lined by bile canaliculi and sinusoidal epithelial cells (**Figure 1A**).

A complex transcriptional network and a combination of several growth factors secreted from the surrounding cells regulates the maturation of the newly formed hepatocytes. Wnt/ $\beta$ -catenin and HGF signalling together with oncostatin M (OSM) coordinate the maturation of hepatocytes (Nejak-Bowen and Monga, 2008). In addition, the dynamically changing extra cellular matrix (ECM) surrounding the hepatoblasts also plays an important role in the hepatic fate determination (McClelland et al., 2008).

In addition to the growth factors, several transcription factors (TFs) regulate the liver development. Forkhead box (Fox) A and GATA binding factor (Gata) -4 bind to the *Albumin* enhancer region, which opens the chromatin structure and assists the access of the other transcription factors to the promoter site (Kaestner, 2005). Hhex is initially involved in the regulation of the hepatic endoderm cell proliferation and later it controls the completion of the liver bud morphogenesis as well as the hepatocyte maturation (Bort et al., 2006; Hunter et al., 2007; Martinez Barbera et al., 2000). Hepatocyte nuclear factor 4 alpha (HNF4 $\alpha$ ) regulates the morphological and functional differentiation of hepatocytes as well as the formation of the hepatic epithelium (Li et al., 2000; Parviz et al., 2003). HNF4 $\alpha$  is shown to be critical in the generation of correct liver architecture and its polarised structure (Santangelo et al., 2011).

## 2.3 Lipid and fatty acid synthesis in hepatocytes

Hepatocytes can directly uptake lipids in the form of lipoproteins and FAs from their culture medium using low-density lipoprotein receptor (LDL-R), LDL receptor-related protein-1 (LRP-1), and scavenger receptor B1 (SR-B1). Simultaneously, they can produce FAs (*de-novo* lipogenesis) by hydrolysing glucose to acetyl-CoA through tricarboxylic acid (TCA) cycle, which links glycolysis to lipogenesis (**Figure 2A**). Concurrently, acetyl-CoA can be synthesised from other precursors than glucose such as glutamine (Currie et al., 2013). Acetyl-CoA is then used by a multifunctional enzyme called fatty acid synthase (FASN) to synthesize FA 16:0 (palmitic acid) (Jensen-Urstad and Semenkovich, 2012). FA 16:0 is then elongated by fatty acid elongase (ELOVL) members to generate long-chain FAs (LCFAs, >16 carbon). LCFAs are further desaturated by stearoyl-CoA desaturase (SCD) and fatty acid desaturase (FADS) to produce diverse spectrum of mono- and poly-unsaturated LCFAs. Human cells are not able to produce unsaturated FAs with a double bond positioned on their  $\omega$ -3 and  $\omega$ -6 acyl chain. Therefore, these essential FAs, alpha-linolenic acid (18:3  $\omega$ -3) and linoleic acid (18:2  $\omega$ -6), need to be obtained from the diet or the medium in case of cell culture.

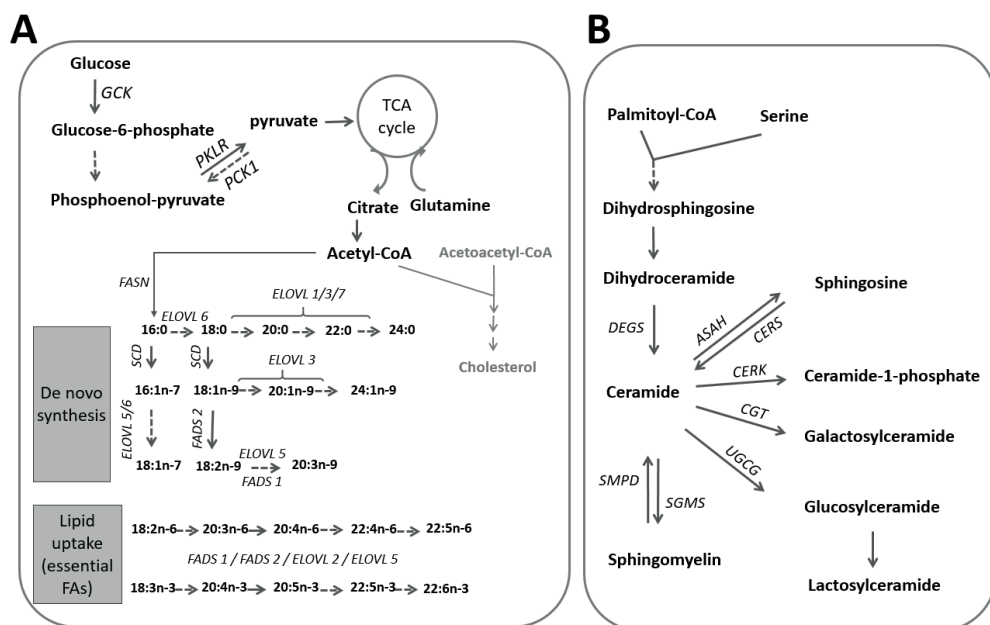


**Figure 2.** A) Demonstrates a simplified pathway of *de-novo* synthesis of fatty acids (FAs) as well as imported essential polyunsaturated FAs (PUFAs) alongside the responsible genes such as

*FASN, SCD, ELOVL, FADS* regulating the pathway. **B)** Demonstrates a simplified pathway of sphingolipids (SLs) alongside the responsible key genes.

FAs are further used by the cells to generate different types of lipids. Via the glycerol phosphate pathway, FAs are converted into diacylglycerols (DAGs) and triacylglycerol (TAGs), which are mainly utilized by cells for energy storage in the form of lipid droplets. In addition, the intermediates of the glycerol phosphate pathway can be converted into PLs such as PC, PE and PI, which are important for membrane functions (Baenke et al., 2013; Ntambi and Miyazaki, 2004). Sterols such as cholesterol and cholesteryl esters (CEs) - another important component of the cellular membrane- are synthesised from acetyl-CoA (discussed in Liscum 2008 (Liscum, 2008)).

Sphingolipids (SLs) form a class of lipids defined by their C18 amino-alcohol backbones and are synthesised from non-sphingolipid precursors coupled to serine. This basic structure is further modified to produce the immense family of SLs such as ceramides (Cer), glycosphingolipids (GSLs) and sphingomyelins (SMs). SLs are bioactive molecules in several cellular activities including cell division, differentiation, gene expression and apoptosis and are the structural components of biological membranes (Gault et al., 2010). In addition, SLs contribute to cell signalling and regulation of inflammation (Hannun & Obeid 2008; Maceyka & Spiegel 2014). The metabolism of SLs is a complex process with ceramide playing as a central key molecule (Delgado et al., 2006) (**Figure 2B**). Cer synthesis is orchestrated by six ceramide synthases (CerS), each of which produces ceramides with distinct FA chain lengths (Cingolani et al., 2016; Levy and Futerman, 2010; Park et al., 2014). The expression pattern of CerS is cell specific and CerS2 is the dominant CerS isoform found in the liver (Laviad et al., 2008; Levy and Futerman, 2010). Cers are degraded to sphingosines and free FAs by ceramidases encoded by distinct genes like acid ceramidase (*ASAH1* and *ASAH2*).

SM is metabolised from ceramides by SM synthase (SMS). SM is the most abundant SL in human cells and its synchronised breakdown is also an important part of membrane homeostasis. Regulated by SMase family (SMPD), SM can be degraded to Cer and free phosphorylcholine (Kim et al., 2008). SMase are organised into acidic, alkaline, and neutral SMases depending on the pH in which their enzymatic activity is optimal.

Glycosphingolipids are complex carbohydrate-containing SLs and UDP-glucose:ceramide glucosyltransferase (UGCG) gene encodes the enzyme which catalyses the first glycosylation step in GSL biosynthesis (**Figure 2B**) (Gault et al., 2010). GSLs are characteristic components of plasma membranes, residing

specifically in the membrane microdomains called lipid rafts (**Figure 3**). The lipid rafts are relatively small and specialised regions of the plasma membrane enriched in cholesterol and very-long and saturated SLs, unlike the surrounding bulk membrane, which is dominated with unsaturated PLs (Ishibashi et al., 2013; Simons and Gerl, 2010).

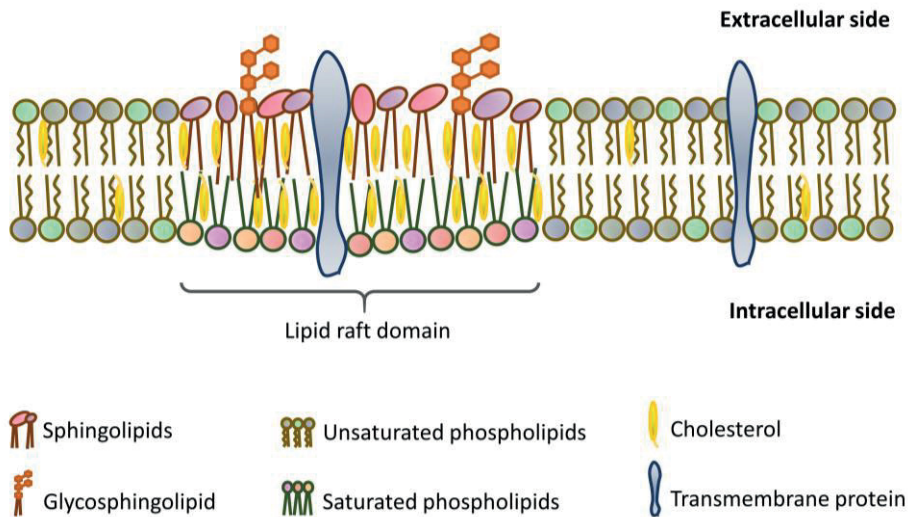


**Figure 3.** A simplified model of cell membrane lipid rafts domain. The phospholipids and cholesterol are located in both outer and inner leaflets, while sphingolipids such as sphingomyelin (SM) and glycerophospholipids (GPLs) are enriched in the outer leaflet of the membrane bilayer. The bulk (non-raft) membrane is enriched with unsaturated glycerophospholipids (GPLs) such as phosphatidylcholine.

## 2.4 Functions of lipids and fatty acids

Mammalian cells contain more than 1000 of different lipids, mostly comprise of a polar head and hydrophobic tails. This complex mixture of lipids execute a wide variety of functions in the cells from forming the bilayer matrix and shaping cellular and ultimately tissue architecture to storing energy (principally as triacylglycerol and steryl esters in the form of lipid droplets) and regulating membrane protein activity, mediating membrane trafficking, facilitating signal transduction, and forming the basis for creating dynamic subcompartments within membranes (Ekroos, 2012). The composition of lipids in different organelles, cell types, and tissues can vary



considerably, which suggests that different lipids are required for different functions (Muro et al., 2014). In addition, the local concentration of each lipid varies between the cells, cellular organelles, and even between the two leaflets of the lipid bilayer, which determines their function (Van Meer, 2005).

Cholesterol is a fundamental structural component in the cell membranes of most vertebrates (Ikonen, 2008) and contribute in forming a semipermeable barrier between the cellular compartments. Cholesterol also regulates the membrane fluidity. In addition, it modulates the membrane proteins function and participates in many membrane trafficking and transmembrane signalling processes.

Sphingolipids are essential constituents of eukaryotic cells. Besides playing structural roles in cellular membranes, some of the SLs metabolites, including ceramide, are considered as bioactive signalling molecules involved in the regulation of cell growth, proliferation, differentiation, senescence, necrosis, and apoptosis. SLs dynamically cluster with sterols to form lipid rafts, which function as hubs for effective signal transduction and protein sorting (Bartke and Hannun, 2008). Interestingly, some SLs such as ceramide and sphingosine 1-phosphate (S1P) exhibit opposing functions in the regulation of cell survival and death, and therefore the relative balance between ceramide/S1P determines the fate of cells in response of particular stimuli (Morales et al., 2007).

Phospholipids play key roles in the structure and function of mammalian cell membranes and account for approximately 70% of the total membrane lipid content and the PC alone covers approximately 50% of the phospholipids in most eukaryotic membranes (Leventis and Grinstein, 2010). As was mentioned above, the composition of lipids varies between the two leaflets in Golgi, plasma and endosomal membranes, where in the outer leaflet (luminal side) PC, SM, and PE are the dominating lipids, whereas in the inner leaflet (cytoplasmic side), PS, PE, and PI are abundant (Van Meer et al., 2008). This asymmetric distribution of lipids is important for the function of the cellular membrane e.g. in vesicle budding (Marsh, 2007; Pomorski and Menon, 2006). In hepatocytes, phospholipids also take part to assemble very low density lipoprotein (VLDL) particles, a 30-70 nm diameter spherical complexes, with approximately 50% triglycerides, 20% cholesterol, 20% phospholipids and 10% protein (with apoB-100 as the major apolipoprotein) (Ikonen, 2008).

Fatty acids are one of the most fundamental classes of biological lipids, which serve as the basic building blocks of the complex lipids. In form of triacylglycerol, they represent a major form of storage energy containing fatty acyl groups in their structure largely in white adipose tissue. Glycerophospholipids provide an essential

structural component of membranes, and are able to regulate and modify the properties of many proteins through direct covalent linkage. FAs can also be metabolized to lipid signalling molecules that perform important role as metabolic intermediates used for lipid synthesis and protein modification. In addition, through mitochondrial beta-oxidation, FAs can be broken down to generate ATP via oxidative phosphorylation (Puzio-Kuter, 2011). Furthermore, FAs can directly regulate cellular processes via controlling of gene transcription, or via binding to membrane-bound receptors. For example,  $\omega$ 3-unsaturated FAs bind to G protein-coupled receptor 120 (GPR120) and exert anti-inflammatory effects in macrophages (Ichimura et al., 2012; Oh et al., 2010). FAs also regulate the expression of a range of genes involved in lipid metabolism. For instance, it has been shown that PUFAs interacts directly with nuclear receptors such as peroxisome proliferator activated receptors (PPARs). PPAR $\alpha$  is the predominant isoform of PPARs in the liver and plays a major role in the fatty acid-induced regulation of hepatic gene transcription (Montagner et al., 2011).

## 2.5 Liver cell models

Physiologically relevant predictive *in vitro* hepatocyte models are needed to develop and test different drugs and to mimic diseases. There are several cell sources available when constructing *in vitro* human liver cell culture models and depending on the study aim, various sources may be utilised in hepatic *in vitro* research (**Figure 4**). Below some of the main cell sources commonly used as *in vitro* hepatic cell models are discussed.



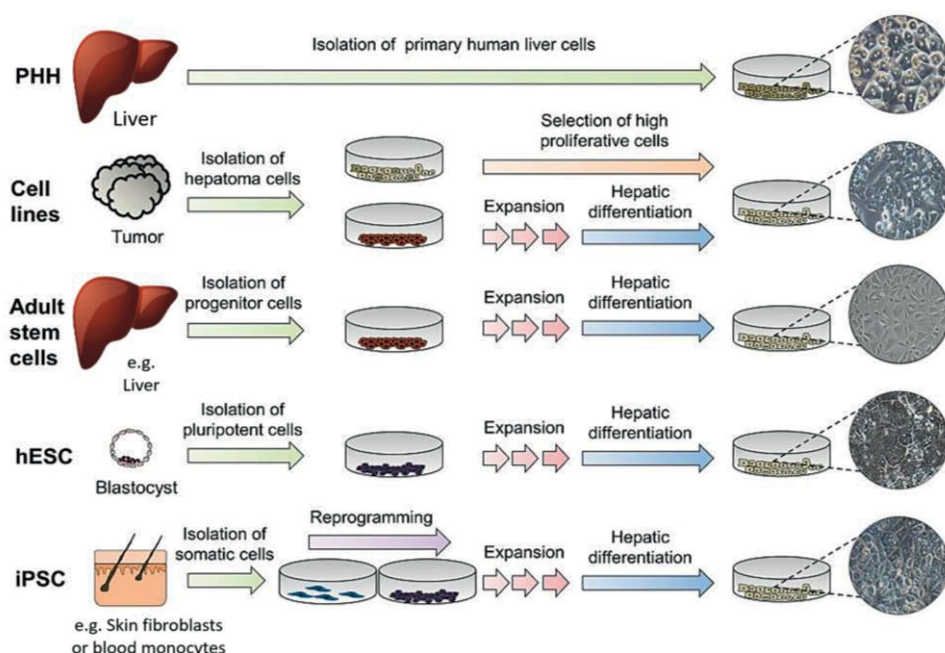


**Figure 4.** Major cell sources used for generation of human *in vitro* liver cell models and their processing steps. Image is adapted with permission from Zeilinger et al., 2016 (Zeilinger et al., 2016).

## 2.5.1 Primary human hepatocytes

Freshly isolated primary hepatocytes are a faithful representative of *in vivo*-like hepatic physiology and currently is considered as the “gold standard” cell model to study liver physiology (Kakisaka et al., 2012; Ling et al., 2013; Sahi et al., 2010). PHHs express the drug transporter enzymes at considerably higher levels than e.g. many hepatoma cell lines (Westerink and Schoonen, 2007). In addition, cultured hepatocytes are able to maintain high levels of their functionality in short-term, which makes them a well-accepted platform for studying liver-related diseases and drug toxicity (Godoy et al., 2013). However, their routine implementation in long-term studies is hampered by the progressive loss of liver-specific phenotype (Elaut et al., 2006). In addition, PHHs are usually obtained from cadaveric donors; therefore, they are expensive, limited and hard to access.

### 2.5.2 Hepatoma cell lines

In order to overcome the limitations of primary human hepatocytes, several human hepatoma cell lines such as HepG2, Huh7, Fa2N4, and HepaRG cells have been developed and utilised (Godoy et al., 2013). Hepatoma cell lines are abundant, have unlimited life span and stable phenotype, and are easy to handle, which explains their wide application as *in vitro* cell models in both academia and industry. However, they do not faithfully represent the metabolic activities of healthy hepatic cells and as a result have failed to correctly predict many hepatotoxic side-effects of the new drugs (Olsavsky et al., 2007). Moreover, most cell lines exhibit low or partial expression of key hepatic-specific factors and particularly drug-metabolizing enzymes (i.e. CYPs) in comparison to the primary hepatocytes (Donato et al., 2008). Recently, several studies have tried to improve the phenotype of hepatoma cell lines. For instance, treating proliferating HepaRG cells with differentiating factors such as DMSO have shown to improve their drug-metabolizing activities (Kanebratt 2008). However, compared with human hepatocytes, the CYP expression in hepatoma cell lines remains low and even the most promising cell line is not yet an ideal alternative system for human primary hepatocytes (Sivertsson et al., 2010). Additionally, these cell models also differ substantially in their potential to secrete apoB-100 and apoA-I containing nascent lipoproteins (Meex et al., 2011; Sasaki et al., 2017).

### 2.5.3 Stem cell-derived hepatocytes

Hepatic cells have been derived from both human embryonic stem cells (hESCs) and hiPSCs in numerous studies and the differentiated hepatic cells derived from both cell sources have reported to be morphologically, genetically, and functionally identical (Godoy et al., 2013). Stem cell-derived HLCs show very similar characteristics to PHHs and are able to circumvent the limited availability of the PHHs. HLCs secrete albumin, urea and TAG and to some levels express drug transporters and cytochrome P450 enzymes (Kia et al., 2012). HLCs are able to produce, secrete, and uptake cholesterol *in vitro* and robustly express apolipoprotein genes, e.g. *APOA1*, *APOA2*, *APOB-100*, *APOC*, and *APOE* (Rasmussen, 2015). HLCs also respond to statin treatment *in vitro* by decreasing their cholesterol secretion (Krueger et al., 2013). Another advantage of HLCs is that unlike the rodent hepatocytes and some human hepatoma cells, they are sensitive to hepatitis C virus infection and support viral replication, similar to PHHs (Schwartz et al., 2012). In addition, iPSC-derived HLCs can be generated from patients of different genetic

backgrounds, a pre-requisite for personalised medicine development. Furthermore, generating hiPSC-HLCs in large quantities facilitates the modelling of inborn errors of hepatic metabolism, understanding the molecular basis of liver cell differentiation, studying disease mechanisms, and discovering novel and safe drugs. iPSC-HLCs have been already utilised as cell models to study several liver disease such as hepatitis C virus infection (Zhou et al., 2014), liver-stage malaria (Ng et al., 2015), and systemic amyloidosis (Leung et al., 2013). In addition, iPSC-HLCs have been used to recapitulate the human cholesterol homeostasis (Krueger et al., 2013), the pathophysiology of familial hypercholesterolemia (Cayo et al., 2012), and Tangier disease, a rare autosomal recessive disorder with almost full absence of HDL (Bi et al., 2017). Furthermore, iPSC-HLCs have proven to be of great value in developing novel therapeutics (Medine et al., 2013; Szkolnicka et al., 2014).

## 2.6 Differentiation of HLCs from pluripotent stem cells

To date, several protocols for differentiating hepatocytes from hESCs or iPSCs have been published (Cameron et al., 2015; Chen et al., 2012; Gerbal-Chaloin et al., 2014; Hannan et al., 2013; Hu and Li, 2015; Mallanna and Duncan, 2013; Schwartz et al., 2014; Si-Tayeb et al., 2010a; Sullivan et al., 2010; Takayama et al., 2012). Nonetheless, most can be divided into three-step differentiation protocols proceeding from stem cells through DE phase, hepatoblast stage, and finally hepatocyte-like cells using various growth factors and cytokines known to be necessary for liver development. In addition, protocols for direct reprogramming of somatic cells (human fetal and adult fibroblasts) to functional hepatocytes have also been reported (Huang et al., 2017; Simeonov and Uppal, 2014).

Activin A is commonly used during the DE induction as it activates the Nodal signal necessary for the DE formation (D'Amour et al., 2005; Kubo, 2004). Alternatively, Wnt3a is crucial for the specification of cell fates during embryonic development (Cohen and Friedman, 2004). CHIR99012 is a small molecule and is an inhibitor of human glycogen synthase kinase 3  $\beta$  (GSK-3 $\beta$ ). GSK3 is also inhibited in response to Wnts during liver development. It has been shown that CHIR99021 enhances cell survival at low density but also induces non-neural differentiation (Ying et al., 2008). NaB is an epigenetic modifier, more specifically a short chain FA that inhibits histone deacetylases (HDACs), leading to hyperacetylation of histones. NaB together with Activin A induces DE formation, possibly through promoting epigenetic changes that consequently make cells more

prone for Activin A-mediated induction of endoderm-specific genes (Jiang et al., 2007).

Bone morphogenic protein 4 (BMP4) and basic fibroblast growth factor (bFGF) are used to promote hepatic differentiation from DE cells. Low concentration of FGF induces hepatic gene expression through activation of the MAPK pathway. In some protocols, DMSO is used instead of FGF and BMP4 to induce hepatic differentiation. DMSO has histone deacetylase inhibitor activity and significantly increases the expression of BMP2 and BMP4 but decreases the expression of stem cell markers such as Oct4 (Behbahan et al., 2011; Choi et al., 2015; Czysz et al., 2015; Santos et al., 2003). Finally, for the maturation of hepatocytes, HGF and OSM, and dexamethasone are used. OSM suppresses the differentiation towards the hematopoietic lineage and promotes the liver progenitor cells to differentiate to hepatocytes (Kamiya et al., 1999). The combination of HGF and OSM enhances hepatocyte proliferation (Si-Tayeb et al., 2010b) and inhibits the progression of the cells into the cholangiocytic lineage by blocking the Notch signalling. Dexamethasone reduces hepatocyte growth by suppressing many growth-associated molecules in the liver including IL-6. In addition, it induces phenotypic maturation of hepatocytes by HNF4 and C/EBP- $\alpha$  induction, which are essential transcription factors for hepatic differentiation (Michalopoulos et al., 2003).

## 2.7 Challenges in using iPSC-derived hepatic cells

While there are many advantages in using iPSC-derived hepatocytes, there are yet some limitations and challenges to overcome. Despite the great advances in hepatic differentiation methods, none of the existing protocols is yet producing fully mature hepatocytes (Baxter et al., 2015). Additionally, variabilities exist between the iPSC lines generated from different donors or in different laboratories (Kim et al., 2011; Rouhani et al., 2014). This variation could be due to many reasons including differences in epigenetic cell memory (Ruiz et al., 2012), or “lab-specific” gene expression patterns (Newman and Cooper, 2010). The variation between the iPSC lines could affect the differentiation potential of the cell lines to a certain cell types other than hepatocytes. Therefore, more consistent iPS cell cultures are needed in order to generate uniform hepatic cells with fully comparable phenotype. Moreover, the criteria for characterisation and functional assessment of the HLCs is currently varying between the laboratories and needs to be standardised (Gerbai-Chaloin et al., 2014).

Even in the most efficient hepatic differentiation, residual undifferentiated iPSCs might remain in the culture, which brings the risk of tumour formation in case of cell transplantation. One solution is sorting the hepatic or hepatic progenitor cells using specific cell surface markers such as asialoglycoprotein receptor (ASGPR) (Goldman et al., 2013; Peters et al., 2016). Recently, Kang et al have suggested that addition of YM155 – a small molecule- to the cell culture during the differentiation could remove the undifferentiated iPSCs and eliminate the risk of teratoma formation upon *in vivo* transplantation (Kang et al., 2017).

Even though the purified hepatic cells can highly affect the functionality of a cell model, an ideal cell model should also include the non-parenchymal cells (NPCs) along with the hepatocytes. The interaction between the hepatocytes and NPCs e.g. endothelial and Kupffer cells are important particularly when testing unknown mechanisms of a disease or potential toxicity of a drug (Godoy et al., 2013). This arises another challenge of culturing HLCs in co-culture with NPCs or in 3D format, which require development of suitable culture environments and optimal biomaterials or hydrogels able to support the growth and differentiation of HLC (see chapter 2.8 below).

## 2.8 Three-dimensional culture of hepatic cells

The conventional 2D culture is the most common approach for culturing and differentiating the hepatic cells due to its ease of achievement. However, the 2D system does not fully support the natural organisation and polarization of hepatic cells, which is necessary for their correct organotypic cell differentiation and proper function (Gissen and Arias, 2015; Godoy et al., 2013; Schyschka et al., 2013). Therefore, the 3D cultivation of hepatocytes has recently gained increasing attention and in this concept, various strategies have been utilised to improve the hepatocytes maturity, functionality, and life-span by re-establishing the physiological microenvironment of the liver including cell-cell contacts and cell-matrix interactions.

A simple approach like the sandwich culture of hepatocytes in type I collagen or Matrigel (a mixture of basal membrane components derived from mouse sarcoma) have shown to enhance the long-term functionality, drug metabolism activity and formation of canalicular networks (Gieseck et al., 2014; Kim and Rajagopalan, 2010; Swift et al., 2010). Numerous studies have also reported the 3D culture of hepatic cells in various matrixes such as collagen (Gieseck et al., 2014), alginate (Ramasamy

et al., 2013), Matrigel (Takayama et al., 2013), heparin (Foster et al., 2015) or nanofibrillar cellulose (NFC, commercially available as GrowDex™) (Malinen et al., 2014), leading to improved liver-specific parameters including CYP expression and albumin and urea secretion. In addition, some recent reports have utilised bioreactors for 3D culture of hepatic cells (Freyer et al., 2016; Heidariyan et al., 2018). In order to further improve the physiological relevance of the hepatic culture environments, different co-culture systems have been also investigated (often in 3D format). For instance, several studies have reported successful co-culture of stem cell-derived hepatocytes with endothelial cells and mesenchymal stem cells (MSCs) (Du et al., 2014; Takebe et al., 2014; Zhong et al., 2015), and fibroblasts (Berger et al., 2015; Nagamoto et al., 2012), all of which significantly increased the expression of hepatic marker genes and overall hepatic functionality. In a more complex approach, a dynamic 3D culture of hepatic cells is created using advanced biofabrication techniques or patterned culture of cells combined with microfluidics systems to create Liver-On-Chip constructs (Bhise et al., 2016; Ma et al., 2016; Skardal et al., 2015). In this system, hepatic cells alone or alongside the NPCs are printed (often with a support hydrogel) on a platform connected to a perfusion system.

The 3D structure could also be achieved through a scaffold-free approach based on the self-aggregation of the hepatic cells known as spheroids. Spheroids can be formed either by seeding the cells in low-attachment culture vessels (Bell et al., 2016) or by gravity-enforced cellular assembly in a hanging drop (Messner et al., 2013). In this perspective, stem cell-derived liver organoids have been recently developed (Kruitwagen et al., 2017; Nantasanti et al., 2015), which provides the nonparenchymal cells (NPCs) and essential tight cell-cell interactions for proper function of hepatocytes.

## 2.9 De-differentiation of hepatic cells

When primary hepatocytes are isolated and cultivated in culture, a number of liver-specific phenotypes are progressively lost with time, which is known as “de-differentiation”. De-differentiation can already be started during the isolation procedure in which the polarised and organised cellular structure of the liver is disrupted and an ischemia-perfusion injury happens, which triggers both a proliferative and inflammatory response. Consequently, liver-enriched transcription factors such as CYP enzymes are negatively affected and hepatocytes rapidly



deteriorate (Baker et al., 2001; Elaut et al., 2006; Godoy et al., 2009). The de-differentiation process continues upon the *in vitro* culture and the hepatic cells are not able to recover to a stable state particularly in current suboptimal 2D culture environments that lack the significant survival factors (Cohen et al., 2015; Elaut et al., 2006; Godoy et al., 2009).

The de-differentiation limits the usability of primary hepatocytes to typically a few days, far from the minimum two-weeks required for long-term toxicity studies (Elaut et al., 2006; Gouliarmou et al., 2015). To date, intensive research has been conducted to understand the mechanism of de-differentiation. For instance, it has been reported that proteins responsible for carbohydrate, amino acid and lipid metabolism networks are affected during the de-differentiation (Rowe et al., 2010). On the other hand, different approaches have been adopted to prevent or decelerate the de-differentiation of primary hepatocytes in culture. Classical approaches have tried to mimic the *in vivo* hepatic environment by using bioreactors, liver spheroids, microfabricated co-culture, and 3D sandwich cultures as well as a wide variety of soluble differentiating-promoting medium components (Darnell et al., 2012; No et al., 2012; Tostões et al., 2012). Although these efforts could delay the de-differentiation process they are not yet able to counteract it completely. Therefore, the ideal hepatocyte-based culture model, which could preserve the long-term expression of hepatocellular phenotype, is still lacking.

## 2.10 MicroRNAs

MicroRNAs (miRNAs) are short (approximately 22 nucleotides), non-coding RNA molecules acting as post-transcriptional regulators of gene expression by inhibiting translation and increasing mRNA degradation (Schmiedel et al., 2015). Single miRNAs are able to regulate multiple genes and conversely, individual genes can be regulated by multiple miRNAs. To date, more than 1,000 miRNAs have been identified in human and approximately 50% of human mRNAs are predicted to be miRNA targets (Shomron and Levy, 2009). miRNAs are cell- or tissue-specific and are shown to play important roles in e.g. the regulation of cell replication and differentiation. miR-122 is abundantly expressed in the liver tissue, composing about 70% of all hepatic miRNAs (Ørom et al., 2008). miR-122 regulates up to 200 genes in the liver (**Figure 5**) and its knockdown results in the reduction of the biosynthesis of hepatic cholesterol (Elmén et al., 2008).

miRNAs have been previously shown to play critical roles in the de-differentiation of PHHs (Fraczek et al., 2013; Lauschke et al., 2016). Emerging evidence also shows that miRNAs regulate the lipoprotein formation and secretion as well as the lipid synthesis and FA oxidation (Yang et al., 2015).

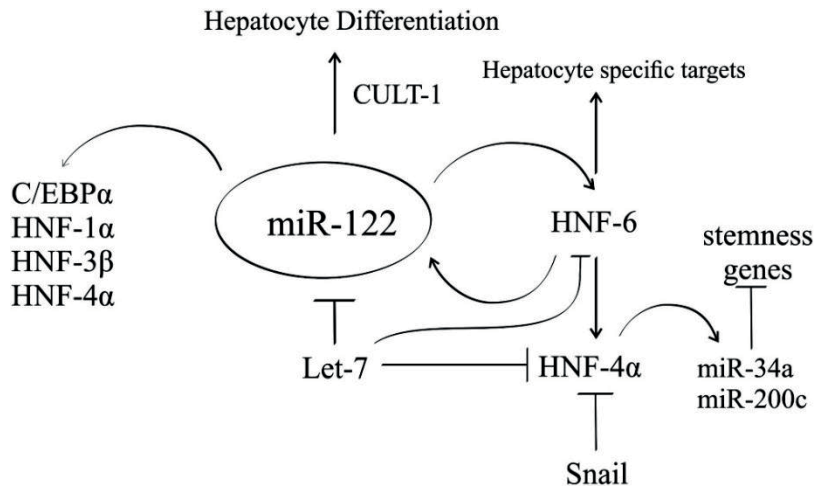


**Figure 5.** MicroRNA-122 signalling. An example of the role of microRNAs in regulation of genes involved in the liver function and differentiation. The figure was adapted with permission from Vasconcellos et al. (Vasconcellos et al., 2016).



### 3 AIMS OF THIS THESIS

The objective of this PhD thesis was to establish HLCs as patient-specific cell models for studying lipid metabolism and derangements. Therefore, it was crucial to investigate the similarities between the lipid profiles of matured HLCs and human primary hepatocytes. In addition, considering the important structural and signalling function of lipids, we investigated the role of lipids in both hepatic differentiation (in iPSC-HLCs) and de-differentiation (in PHHs). The step-by-step aims of this dissertation are outlined as follows:

1. To study the lipid alterations in differentiating HLCs and investigate the possible role of lipids in hepatic differentiation and maturation (**Study I**).
2. To compare the hepatic differentiation methods and investigate the effect of various differentiating conditions and biological stimuli on the phenotype of HLCs (**Study II**).
3. To comprehensively characterise the lipid and FA profile of HLCs and compare it with both PHHs and HepG2 cells (**Study II**).
4. To study the lipid alterations in de-differentiating PHHs and investigate the possible role of lipids in the de-differentiation process and its mechanism (**Study III**).
5. To study the alterations in the miRNA profile of de-differentiating PHHs and identify the differentially expressed miRNAs that may regulate those changes in the lipidome of PHHs (**Study III**).

## 4 MATERIALS AND METHODS

### 4.1 Ethical consideration

The study and the recruitment of the patients have been approved by the Ethics Committee of Pirkanmaa Hospital District (Tampere University Hospital) with the approval number: R12123. All recruited participants were adults over 18 years old, who had signed an informed consent form after receiving both written and oral descriptions of the research.

### 4.2 Reprogramming of hiPSC

Three hiPSC lines (UTA.11104.EURCAs, UTA.10100.EURCAs, and UTA.11304.EURCCs) were used in the original publications (**Studies I** and **II**) and cell lines were derived directly from the fibroblasts of three individuals. The collected fibroblasts were induced to pluripotency by Sendai reprogramming kit (CytoTune; Life Technologies), based on the protocol described by Takahashi et al. (Ohnuki et al., 2009; Takahashi et al., 2007). The induction of cell lines was performed according to the manufacturer's instruction. Induced cells were cultured on mitotically inactivated mouse embryonic fibroblast (MEF, Applied StemCell) feeders until characterisation.

### 4.3 Culture of hiPSC

hiPSC lines were maintained at +37 °C in 5% CO<sub>2</sub> on MEFs in a basic hiPSC culture medium containing Knock-Out Dulbecco's Modified Eagle's Medium (KO-DMEM) supplemented with 20% Knock out Serum Replacement (Ko-SR), 0.1 mM 2-mercaptoethanol (2-ME), 2 mM Glutamax (all from Gibco®), 1% nonessential amino acids (NEAA), 50 U/ml penicillin/streptomycin (both from LONZA), and 4 ng/ml human basic fibroblast growth factor (bFGF, R&D system).

Undifferentiated colonies were enzymatically passaged onto fresh feeder layers on weekly bases. Cell lines were routinely checked for mycoplasma contamination.

# 4.4 Characterization of hiPSC

All the hiPSC lines were characterised for their pluripotency at both gene and protein levels. In addition, their ability to generate derivatives of all three embryonic germ layers was evaluated by the formation of embryoid bodies (EBs). Furthermore, normal karyotype of the hiPSC lines was confirmed by performing genome-wide screening for gross chromosomal abnormalities with KaryoLite BoBs (Product number 4501–0010, Perkin Elmer) as described elsewhere (Lund et al., 2012). The details of the characterisations have been described before (Manzini et al., 2015). A summary of the hiPSC characterisation methods is demonstrated in the **Table 1**.

**Table 1.** An overview of the assays used in this thesis for characterisation of the iPSC lines.

Methods/assays	Markers
PCR	
Exogenes	<i>OCT4, SOX2, c-MYC, KLF4</i>
Endogenes	<i>NANOG, REX1, OCT3/4, SOX2, c-MYC</i>
Embryoid bodies (EBs)	
Endoderm	<i>SOX17, AFP</i>
Mesoderm	<i>KDR, ACTC1</i>
Ectoderm	<i>Nestin, Musashi</i>
Immunocytochemistry (ICC)	
Pluripotency markers	<i>NANOG, OCT3/4, SSEA4, SOX2, TRA1-60, TRA1-81</i>
Karyotype analysis	

Abbreviations: *OCT*, octamer-binding transcription factor; *SOX*, (sex determining region Y)-box; *KLF*, kruppel-like factor; *NANOG*, nanog homeobox; *REX1*, *ZFP42* zinc finger protein; *AFP*, alpha fetoprotein; *KDR*, kinase insert domain receptor; *ACTC1*, alpha actin cardiac muscle 1; *SSEA*, stage-specific embryonic antigen; *TRA*, tumour rejection antigen.

## 4.5 Culture of the human primary hepatocytes

Cryopreserved PHHs (Lots. Hu8209 & Hu8210) (**Studies I, II, and III**) were purchased from Gibco®. PHHs were cultured in monolayer on collagen-I-coated plates (CellAffix™), with the density of  $2.5 \times 10^5$  cells/cm<sup>2</sup>, and maintained in William's E medium (Gibco®) supplemented with cocktail B (CM 4000, Gibco; including ITS [insulin, transferrin, selenium], bovine serum albumin (BSA), GlutaMAX™, and linoleic acid) as well as dexamethasone.

## 4.6 Culture of HepG2 cells

Hepatocellular carcinoma cells (HepG2) (**Study II**) were purchased from ATCC™ and were thawed and plated according to the manufacturer's instructions. HepG2 cells were cultured in DMEM medium supplemented with 10% FBS (Biosera) and 50 U/ml penicillin/streptomycin (LONZA). HepG2 cells were passaged on weekly bases and normally used at passages 5-10.

## 4.7 Hepatic differentiation from hiPSCs

To generate HLCs, iPSCs were adapted to feeder free condition on pre-coated plates either with Geltrex (Gibco®) or Laminin 521 (BioLamina, Lot: 80104) in mTeSRT™ medium before starting the hepatic differentiation. In this thesis, HLCs have been differentiated by five different methods (**Studies I and II**). **Figure 6** demonstrates a schematic view of methods used.

	Pluripotent	Definitive endoderm	Hepatic specification		Hepatic maturation	
Method 1	iPSCs on Geltrex 3-4 days	Act. A, <b>CHIR 99021</b> , NaB 2 days	Act. A, NaB 3-4 days	RPMI, <b>BMP4</b> <b>bFGF</b> , B27 3 days	RPMI, HGF 5 days	HCM (no EGF) , HGF, OSM Up to day 20
Method 2	iPSCs on Geltrex 3-4 days	Act. A, Wnt3, NaB 5-6 days		Ko-DMEM, Ko-SR, $\beta$ ME, NEAA, DMSO 7 days		<b>L-15</b> , HGF, OSM Up to day 20
Method 3	Seeding <b>single</b> iPSCs on Geltrex	Act. A, Wnt3, ROCK 1 day	Act. A, Wnt3, <b>NaB</b> 3-5 days	Ko-DMEM, Ko-SR, $\beta$ ME, NEAA, DMSO 7 days		HCM , HGF, OSM Up to day 20
Method 4	Seeding single iPSCs on <b>Laminin 521/111</b>	Act. A, Wnt3, ROCK 1 day	Act. A, Wnt3, <b>NaB</b> 3-5 days	Ko-DMEM, Ko-SR, $\beta$ ME, NEAA, DMSO 7 days		HCM , HGF, OSM Up to day 20
Method 5	iPSCs on Geltrex for <b>24 hrs</b>	<b>STEMdiff™ DE Kit</b> 4 days		Ko-DMEM, Ko-SR, $\beta$ ME, NEAA, DMSO 7 days		HCM , HGF, OSM Up to day 20

**Figure 6.** A schematic illustration of the five hepatic differentiation methods used in the **Studies I** and **II** for generating hepatocyte-like cells (HLCs).

The details of the differentiation methods are described below:

**Method 1 (M1) (Study II)** is based on a protocol originally introduced by Si-Tayeb et al. (Si-Tayeb et al., 2010a). In this protocol, hiPSCs were cultured in RPMI+Glutamax (Gibco®) supplemented with 1×B27 (Gibco®), 100 ng Activin A (Peprotech), 3  $\mu$ M CHIR99021 (Stemgent), 1 mM NaB (Sigma) for 1 day and 0.5 mM for 5-6 days until definitive endoderm (DE) formation. Medium was switched to RPMI/B27 supplemented by 20 ng/ml BMP4 and 10 ng/ml of bFGF for hepatic induction for 3 days. Then, BMP4 and bFGF were replaced by 20 ng/ml of hepatocyte growth factor (HGF) for 5 days. From this stage onward, cells were cultured in HBM (cc-3199, Lonza) supplemented with Single Quotes (no epidermal growth factor [EGF]) complemented with 40 ng/ml HGF (life technologies) and 20 ng/ml oncostatin M (OSM, R&D systems) for further maturation.

**Method 2 (M2) (Studies I and II)** is according to a study performed by Hay et al. (Hay et al., 2008). The DE stage was similar to M1 except that 75 ng/ml Wnt3 (R&D systems) was used instead of CHIR99021. The hepatic differentiation was initiated by switching the medium to KO-DMEM+20% KO-SR, 1 mM Glutamax, 1% NEAA, 0.1%  $\beta$ -ME, and 1% DMSO for 7 days. From this point, cells were cultured in Leibovitz's L-15 medium (Invitrogen), supplemented by 8.3% BSA (Biosera), 8.3% Tryptose phosphate broth (Sigma-Aldrich), 10  $\mu$ M Hydrocortisone 21- hemisuccinate, 1 mM Insulin (both from Sigma-Aldrich), 2 M Glutamax, 25 ng/ml HGF, and 20 ng/ml OSM.

**Method 3 (M3) (Study II)** is an alteration of both M1 and M2 and was described by Kajiwarra et al. (Kajiwarra et al., 2012). After reaching 70% confluency, hiPSCs were detached by Versene (Gibco) and re-suspended in RPMI+Glutamax supplemented with 1 $\times$ B27, 100 ng/ml Activin A, 50 ng/ml Wnt3, and 10  $\mu$ M Rock inhibitor and seeded with 5-10  $\times$  10<sup>4</sup> /cm<sup>2</sup> density. Next day Rock inhibitor was replaced with 0.5  $\mu$ M NaB until day 5-6 of differentiation. Hepatic specification stage was carried out as in M2 and hepatic maturation stage was carried out according to M1, however, EGF was included in HCM, and HGF was reduced to 25 ng/ml.

**Method 4 (M4) (Study II)** is similar to M3 except that the plates were coated with a mix of Laminin 111/521 (3:1 ratio) instead of Geltrex<sup>TM</sup> used in other methods.

**Method 5 (M5) (Study II)** is similar to M3 except that the DE stage in M3 was substituted by a commercial kit (STEMdiff<sup>TM</sup>). The differentiation in DE stage was performed according to the manufacturer's instructions.

## 4.8 The characterization of cells during hepatic differentiation and maturation

### 4.8.1 Morphology

During the hiPSC-HLCs differentiation, cell growth and morphology were regularly monitored using either Nikon Eclips TS100 phase contrast or EVOS FL (Life technology) microscope.

## 4.8.2 Real-time quantitative PCR

Real-time quantitative polymerase chain reaction (qPCR) was used to evaluate the stages of differentiation (**Studies I and II**) or de-differentiation (**Study III**), functionality (**Studies I, II, and III**), and efficiency of differentiation methods (**Study II**). Total RNA extraction and cDNA synthesis are described in details in the original publications. cDNA was multiplied either by Power SYBR Green PCR Master Mix (Life Technologies) and gene specific primers or Taqman Fast Advanced Master Mix (applied Biosystems) and gene specific TaqMan probes. The qPCR reactions were run in triplicates using the 7300 Real-time PCR system (Applied Biosystems, Foster City, CA) (**Study I**) or Real Time PCR Detection System (BioRad, CFX384™ Optics Module, Singapore) (**Studies II and III**). The studied genes and respective primers are presented in **Tables 2 and 3**.

**Table 2.** List of the studied genes using SYBR Green-based real-time quantitative PCR (qPCR). *GAPDH* was used as the endogenous control gene.

Gene	Target	Forward primer 5'-3'	Reverse primer 5'-3'	Study
<i>OCT3/4</i>	iPSCs	TTGGGCTCGAGAA GGATGTG	TCCCTCTCGTTGTGC ATAGTCG	<b>I, II</b>
<i>SOX17</i>	Endoderm	CCGAGTTGAGCAA GATGCTG	TGCATGTGCTGCA CGCGCA	<b>I, II</b>
<i>FOXA2</i>	Endoderm	AAGACCTACAGGC GCAGCT	CATCTGTGTGGGG CTCTGC	<b>I, II, III</b>
<i>AFP</i>	Immature HLCs	CGCTGCAAACGAT GAAGCAG	AATCTGCAATGAC AGCCTCAAG	<b>I, II, III</b>
<i>ALB</i>	Matured HLCs	GAAAAAGTGGGCAG CAAATGT	GGTTCAGGACCAC GGATAGA	<b>I, II, III</b>
<i>GAPDH</i>	Housekeeping gene	AGCCACATCGCTC AGACACC	GTACTCAGCGCCA GCATCG	<b>I, II, III</b>

Abbreviations: iPSCs, induced pluripotent stem cells; HLCs, hepatocyte-like cells

**Table 3.** List of the studied genes using TaqMan-based real-time quantitative PCR (qPCR). Both *B2M* and *GAPDH* were used as the endogenous control genes.

Gene symbol	Gene product	TaqMan assay ID	Study ID
<i>FASN</i>	Fatty acid synthase	Hs01005622_m1	<b>II, III</b>
<i>SCD</i>	Stearoyl-CoA desaturase	Hs01682761_m1	<b>II, III</b>
<i>FADS1</i>	Fatty Acid Desaturase 1	Hs01096545_m1	<b>II, III</b>

<i>FADS2</i>	Fatty Acid Desaturase 2	Hs00927433_m1	II, III
<i>ELOVL1</i>	Elongation of very-long chain fatty acids 1	Hs00967951_g1	II, III
<i>ELOVL2</i>	Elongation of very-long chain fatty acids 2	Hs00214936_m1	II, III
<i>ELOVL3</i>	Elongation of very-long chain fatty acids 3	Hs00537016_m1	II, III
<i>ELOVL5</i>	Elongation of very-long chain fatty acids 5	Hs01094711_m1	II, III
<i>ELOVL6</i>	Elongation of very-long chain fatty acids 6	Hs00907565_m1	II, III
<i>ELOVL7</i>	Elongation of very-long chain fatty acids 7	HS00405151_m1	II, III
<i>GCK</i>	Glucokinase	Hs01564555_m1	II, III
<i>PKLR</i>	Liver-type pyruvate kinase	Hs00176075_m1	III
<i>PCK1</i>	Phosphoenolpyruvate carboxykinase	Hs00159918_m1	III
<i>CERS1</i>	Ceramide synthase 1	Hs04195319_s1	I, III
<i>CERS2</i>	Ceramide synthase 2	Hs00371958_g1	I, III
<i>CERS3</i>	Ceramide synthase 3	Hs00698859_m1	I
<i>CERS4</i>	Ceramide synthase 4	Hs00226114_m1	I, III
<i>CERS5</i>	Ceramide synthase 5	Hs00908759_m1	I, III
<i>CERS6</i>	Ceramide synthase 6	Hs00826756_m1	I, III
<i>SGMS1</i>	Sphingomyelin synthase 1	Hs00983630_m1	I, III
<i>SGMS2</i>	Sphingomyelin synthase 2	Hs00380453_m1	I, III
<i>UGCG</i>	UDP-glucose ceramide glucosyltransferase	Hs00234293_m1	I, III
<i>SMPD1</i>	Sphingomyelin phosphodiesterase 1	Hs03679347_g1	I, III
<i>SMPD2</i>	sphingomyelin phosphodiesterase 2	Hs00906924_g1	I
<i>SMPD3</i>	sphingomyelin phosphodiesterase 3	Hs00920354_m1	I
<i>SMPD4</i>	sphingomyelin phosphodiesterase 4	Hs04187047_g1	I
<i>ASAH1</i>	N-acylsphingosine amidohydrolase (acid ceramidase) 1	Hs00602774_m1	I, III
<i>ASAH2</i>	N-acylsphingosine amidohydrolase (non-lysosomal ceramidase) 2	Hs01025305_m1	I, III
<i>ASAH2B</i>	N-acylsphingosine amidohydrolase (non-lysosomal ceramidase) 2B	Hs00184096_m1	I
<i>APOB</i>	apolipoprotein B-100	Hs00181142_m1	I, II
<i>APOA1</i>	apolipoprotein A-I	Hs00985000_g1	I, II
<i>B2M</i>	Beta-2-microglobulin	Hs99999907_m1	III
<i>GAPDH</i>	Glyceraldehyde-3-phosphate dehydrogenase	Hs99999905_m1	I, II, III



### 4.8.3 Immunofluorescence

Protein expression of the putative markers for the stem cells, definitive endoderm, and hepatocytes were evaluated in iPSCs, differentiating, immature and matured HLCs as well as in PHHs and HepG2 cells using immunofluorescence (**Studies I and II**). The primary and secondary antibodies are presented in **Table 4**. The staining protocol is described in detail in the original publication (**Study I**).

**Table 4.** Primary and secondary antibodies used in **Studies I and II**.

Primary antibody	Target	Origin	Dilution	Manufacturer
OCT3/4	iPSCs	Goat	1:400	R&D
SOX17	Endoderm	Mouse	1:200	R&D
FOXA2	Endoderm	Goat	1:300	Abcam
LDL-R	HLCs	Rabbit	1:300	Cayman
ASGPR1	HLCs	Mouse	1:100	Novus Biologicals
AFP	Immature HLCs	Rabbit	1:500	Dako
ALB	Mature HLCs	Mouse	1:400	R&D
Secondary antibody	Target	Origin	Dilution	Manufacturer
Anti Goat	OCT3/4, FOXA2	Donkey	1:800	Life Technology
Anti rabbit	LDL-R, AFP	Donkey	1:800	Life Technology
Anti mouse	SOX17, ASGPR1, ALB	Donkey	1:800	Life Technology

Abbreviations: OCT, octamer-binding transcription factor; SOX17, (sex determining region Y)-box 17; FOXA2, forkhead box protein A2; LDL-R, low-density lipoprotein receptor; ASGPR 1, asialoglycoprotein receptor 1; AFP, alpha fetoprotein; ALB, albumin; iPSCs, induced pluripotent stem cells; HLCs, hepatocyte-like cells.

### 4.8.4 Flow cytometry

To determine the efficiency of the DE differentiation (**Studies I and II**), cells were stained by a DE surface marker, CXCR4 conjugated antibody (R&D Systems), and the number of CXCR4-positive cells were analysed using the Accuri™ C6 device (BD Biosciences, Franklin Lakes, NJ). The detailed protocol can be found in the original publications.

## 4.9 Biochemical methods

HLCs were evaluated for their functionality during the differentiation (**Study I**) and maturation (**Studies I and II**) and the results were then compared with the data from the PHHs and HepG2 cells, which were cultured in parallel with the HLCs. PHHs were also evaluated for their functionality during the process of de-differentiation (**Study III**). The albumin, triacylglycerol (TAG), and urea content of the culture conditioned medium were determined, with the human albumin ELISA quantitation kit (Bethyl Laboratory, USA), the triglyceride quantification kit (BioVision Inc.), and the QuantiChrom™ urea assay kit (BioAssay Systems), respectively, according to the manufacturers' instructions. The values were normalised to the cell numbers.

## 4.10 Mass spectrometry lipidomics

Lipids (cholesterol, sphingolipids, glycerolipids, and glycerophospholipids) were extracted from iPSCs (**Study I**), DEs (**Study I**), immature HLCs (**Study I**), matured HLCs (**Studies I and II**), PHHs (**Studies I, II, and III**) and HepG2 cells (**Study II**) by Hamilton Microlab Star system (Hamilton Robotics AB, Kista, Sweden), and studied by using shotgun lipidomics.

In the shotgun lipidomics, lipid extracts [cholesteryl ester (CE), diacylglycerol (DAG), lysophosphatidylcholine (Lyso-PC), lysophosphatidylethanolamine (Lyso-PE), lysophosphatidylglycerol (LPG), lysophosphatidylserine (LPS), lysophosphatidylinositol (LPI), and sphingomyelin (SM)] were examined on a hybrid triple quadrupole/linear ion trap mass spectrometer (QTRAP 5500) equipped with a robotic nanoflow ion source (NanoMate, Advion Biosciences Inc., Ithaca, NJ). Molecular lipids were analysed in positive ion mode using lipid class-specific precursor ion or neutral loss scans (Ekroos et al., 2002, 2003). Sphingolipids [ceramide (Cer), lactosylceramide (LacCer), glucosyl/galactosylceramide (Glc/GalCer), and globotriaosylceramide (Gb3)] and molecular phospholipids [phosphatidylcholines (PC), phosphatidylethanolamines (PE), and phosphatidylinositols (PI)] were analysed using ultra-high pressure liquid chromatography-mass spectrometry (UHPLC-MS) with a targeted approach (Merrill et al., 2005). Identified lipids were normalized against their respective internal standard (Ejsing et al., 2006) as well as their total protein concentrations in the cell samples. The total protein concentrations were determined by the Micro BCA™ Protein Assay kit (Thermo Scientific Pierce Protein Research Products) according to

the manufacturer's instructions. The detailed procedure of analysis is described in the original publications.

## 4.11 Fatty acid analysis by gas chromatography

The FA composition and concentrations in the cell culture media used at iPSC-stage and at different stages of hepatocyte differentiation (**Study I**), as well as in the matured HLCs, PHHs, and HepG2 cells and their media (**Study II**) were analysed by gas chromatography. The calculations of the FA compositions and concentrations followed standard procedures and the FAs were named by using the abbreviations: [carbon number]:[number of double bonds] n-[position of the first double bond calculated from the methyl end] (e.g. 18:2n-6). The detailed analytical procedure is described in the original publications.

## 4.12 miRNA analysis

The expression profiles of all miRBase release v21 human miRNAs were determined using Agilent Sureprint G3 Human miRNA microarray slides. RNA was labelled and hybridized using the Agilent's miRNA Complete Labelling and Hybridization Kit according to manufacturer's protocol. After hybridization, the slides were scanned using Agilent's High Resolution Microarray Dx Scanner. Data was normalised by quantile normalization (Bolstad et al., 2003) using the robust multi-array average (RMA) algorithm (Irizarry et al., 2003). Log2 fold change 1 was applied as a cut off value for determining the up- or downregulation of miRNAs in PHHs.

## 4.13 Statistical analysis

The results were compared using one-way ANOVA, followed by Bonferroni's multiple-comparison test (**Studies I and II**). Data are presented as means  $\pm$  SD with  $n$  representing the number of independent experiments. Analysis was carried out in GraphPad Prism version 5.02 software and results were considered significant if  $p$ -value  $< 0.05$ .

## 5 SUMMARY OF THE RESULTS

### 5.1 Hepatic differentiation

#### 5.1.1 Cell morphology during the hepatic differentiation

The cells underwent a dramatic morphological changes during the hepatic differentiation process: round and dense iPSCs gradually lost their morphology and start migrating outwards from the colonies to form new network of DE cells. By second week, cells gradually increased in size, particularly in cytoplasm, and formed hepatoblasts/immature hepatocytes. During the third week of differentiation, immature hepatic cells became mature and formed polygonal cells with distinct canalculated borders (**Figure 7A**).

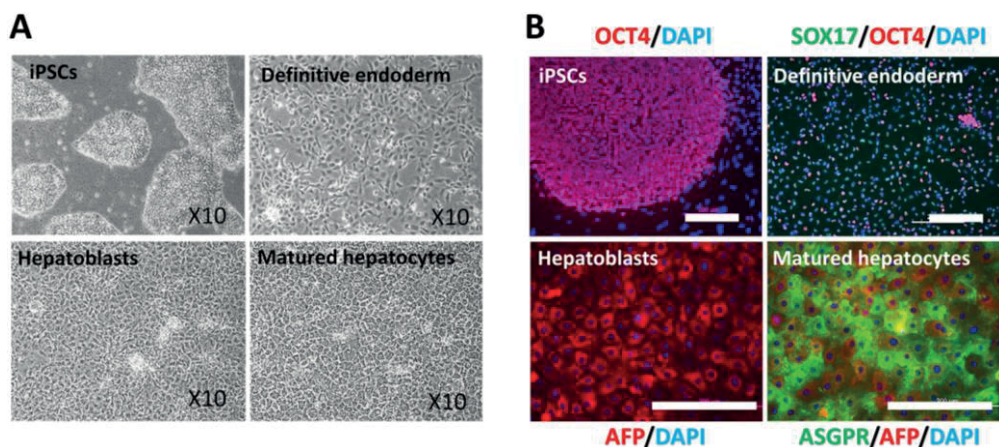


**Figure 7.** The differentiation of iPSCs towards HLCs and their characterisations at different stages. **A)** Phase contrast images showing the morphological changes from iPSCs to definitive endoderm, hepatoblasts, and finally matured hepatocyte. **B)** Characterization of cells by immunocytochemistry at various stages of hepatic differentiation. OCT, octamer-binding transcription factor; SOX17, (sex determining region Y)-box 17; AFP, alpha fetoprotein; ASGPR, asialoglycoprotein receptor; DAPI, 6-diamidino-2-phenylindole. Scale bar 200  $\mu$ m.

## 5.1.2 Gene and protein expression during the hepatic differentiation

Consistent with the morphological changes, dramatic changes in gene expression was also observed during the differentiation process. The expression of *OCT3/4* was downregulated at day 5, while the DE markers, *SOX17* and *FOXA2*, were highly expressed. As the cells differentiated further, *AFP* started to be expressed around day 10 and the expression of mature liver marker, *ALB*, increased significantly around day 15 and peaked at day 20 or 25.

Immunocytochemical staining further confirmed the results from gene expression. The cells at DE stage expressed only low levels of pluripotency marker *OCT3/4* but were positive for the DE markers, *SOX17* and *FOXA2* (**Study II, Fig. S2A**). In addition, alpha-fetoprotein (AFP), albumin (ALB) as well as asialoglycoprotein receptor (ASGPR) were all expressed in differentiated HLCs, further confirming their hepatic phenotype (**Figure 7B**).

## 5.1.3 Functionality assessment during the hepatic differentiation

Several experiments were performed to evaluate the functionality of the differentiated HLCs. Our results showed that HLCs were able to synthesise and release albumin into the culture medium by the end of second week, with a maximum secretion at day 20 (**Figure 8A**). In addition, the expression of apolipoprotein B (*APOB*) and apolipoprotein A-I (*APOA1*) were measured as a surrogate for estimating VLDL and HDL production levels of the cells which further demonstrated that the cells are differentiating and maturing towards functional hepatocytes (**Study II, Fig. 2C**). Furthermore, HLCs showed to be able to efficiently uptake labelled LDL particles from the culture medium and produce and store lipid droplets in a FA rich medium supporting the role of functional LDL receptors and molecular machinery to generate lipid droplets (**Figure 8 B&C**).

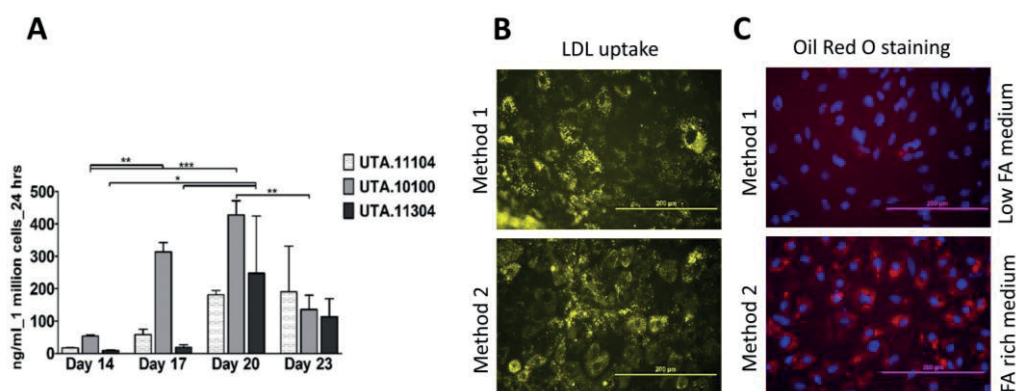


**Figure 8.** The assessment of functionality of HLCs during the differentiation. **A)** Albumin secretion by HLCs generated from three individual cell lines at 4 time points of days 14, 17, 20, and 23. Bars represent mean $\pm$ SD of three biological replicates. **B)** Uptake of labeled LDL by HLCs at day 16 of differentiation generated by Method 1 and Method 2. **C)** Oil Red O staining of HLCs at day 16 of differentiation generated in low FA medium (Method 1) and FA rich medium (Method 2). HLCs were able to generate lipid droplets in FA rich medium. Scale bar 200  $\mu$ m.

#### 5.1.4 Fluctuation in the lipid species content of cells during hepatic differentiation

We followed the changes in the cellular lipid content and composition during the entire differentiation process and overall, more than 160 molecular lipid species were detected using a shotgun mass spectrometry. Our results showed that the cellular lipid contents were constantly altered during the hepatic differentiation from iPSCs to matured HLCs and the alterations were mostly a reflection of the lipid or FA content of the culture medium (**Figure 9A**). At DE stage, the concentrations of the majority of lipid classes reduced in the cells, whereas three classes of SM, CE and PI were increasing independent of the lower or undetectable levels of those lipids in the DE medium. In hepatic commitment stage, a sudden increase in all lipid classes was evident, which mirrored the abundant lipid and FA in the medium at this stage. During the hepatic maturation, changes in the lipid levels were more subtle in agreement with the constant FA level of the medium during this stage. In addition, PCA showed that the cellular lipid composition of iPSC and DE cells clearly differ from that in hepatoblasts and HLCs (**Study II, Fig. 2 C&D**)

Studying the lipids in molecular levels showed that the majority of CEs peaked at day 12. At later time points, however, the concentration of most CEs decreased



except those containing very-long chain unsaturated fatty acids (VLCUFA) such as CE 22:6, the concentration of which increased by maturation of HLCs (**Figure 9B**). In addition, we detected an overall increase in the FA chain length of SLs during hepatic differentiation and maturation. The largest changes in PLs occurred in polyunsaturated fatty acid (PUFA)-containing species such as PC 18:0/20:4 and PC 18:0/22:6, and their concentration drastically increased in HLCs (**Study I, Fig. 3C**). On the other hand, PLs containing saturated or monounsaturated FAs (SFA or MUFA) were more constant during the differentiation. We detected, in total, 41 molecular lipids that statistically significantly changed during the maturation stage (**Figure 9B**).

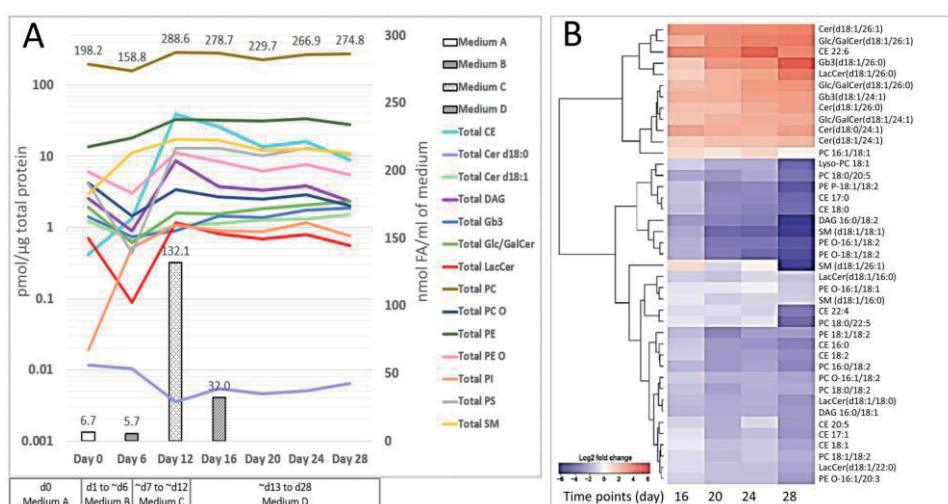


**Figure 9.** Alterations in the lipidome during the iPSC-HLC differentiation in **Study I**. **A)** Lines define the total concentration of different lipid classes in HLCs at seven time points during the differentiation. Bars show the total FA concentration of different media used for the hepatic differentiation. **B)** Lipidomic heat map showing the fold-increase of molecular lipid species that differed statistically significantly ( $p < 0.05$ ) between day 12 and day 28. CE, cholesteryl ester; Cer, ceramide; DAG, diacylglycerol; Gb3, globotriaosylceramide; Glc/GalCer, glucosyl/galactosylceramide; LacCer, lactosylceramide; Lyso-PC, lysophosphatidylcholine; Lyso-PE, lysophosphatidylethanolamine; PC, phosphatidylcholine; PC O, alkyl-linked phosphatidylcholine; PE, phosphatidylethanolamine; PE O, alkyl-linked phosphatidylethanolamine; PI, phosphatidylinositol; PS, glycerophosphoserine; SM, sphingomyelin.

### 5.1.5 Gene-lipid interactions

In **Study I**, several SLs with very-long chain FAs increased during the hepatic maturation phase independent of the exogenous lipid supplies. Concurrently, a number of genes including *CERS2*, *UGCG*, *SGMS1*, and *SGMS2* involved in the synthesis of SLs were upregulated in matured HLCs (**Study I, Fig. 5A**). In addition, positive correlations between several SLs and their corresponding genes (e.g. Cer d18:1/24:0 and *CERS2*; Glc/GalCer d18:1/26:0 and *UGCG*; and SM d18:1/24:1 and *SGMS2*) were detected. Unlike SMs with very-long chain fatty acids (VLCFAs), the shorter-chain SMs (e.g. SM d18:1/18:0) decreased at hepatic maturation stage. SMs can be degraded by many different sphingomyelinase enzymes. The expression of two out of four studied sphingomyelinases, *SMPD1* and *SMPD3*, were increased during the hepatic differentiation. On the other hand, the expression of several other genes such as *CERS3*, *CERS5*, *ASAH2b*, *SMPD2*, and *SMPD4* remained constant during the hepatic differentiation.

## 5.2 Comparison of hepatic differentiation methods

### 5.2.1 Morphology

In all five hepatic differentiation methods used in **Study II**, dramatic morphological changes happened during the differentiation, particularly at DE stage (**Figure 4** displays the five methods). In all methods except M5, migrating DE cells possessed a spiky morphology, while in M5, DEs were instead more square-shaped. Furthermore, the amount of cell death in M5 was considerably lower than in the rest of the methods. The choice of CHIR 99021 (used in M1) or Wnt3 (used in M2–4) seemed to have no effect on the morphology of the DE cells. At the hepatic specification stage, cells treated with BMP4, bFGF, and HGF (used in M1) possessed a different morphology compared to the cells treated with DMSO (used in M2–5). In addition, the HLCs differentiated by M4 showed the highest binuclearity (16%), the closest to the binuclearity observed in PHHs (**Study II, Fig. 2b**).

Initiating differentiation with single cells in M3 and M4 did not result in a higher efficiency of DE formation compared to M1 and M2, which were started with



colonies. However, DE cells were observed one or even two days earlier in methods initiated with single cells compared to methods initiated with colonies.

### 5.2.2 Gene and protein expression

*SOX17* in M2-HLCs and *FOXA2* in M4-HLCs were expressed lower than HLCs differentiated by other methods, however, this difference was not found statistically significant. On the other hand, the expression of *AFP* in the M2-HLCs was statistically significantly higher than in the M1-HLCs and the expression of *ALB* in the M5-HLCs was significantly higher than in the M1-HLCs and M3-HLCs (**Study II, Fig. 2c**).

The analysis from flow cytometry showed that the expression of CXCR4, a surface DE marker, is higher in M1-, M2-, and M3- HLCs compared to that in M4- and M5-HLCs. Estimated by immunocytochemistry, matured HLCs differentiated by M4 contained the highest number of ALB positive cells (37.7%), while M1 contained the lowest (9.8%). Additionally, in M2-, M3-, M4-, and M5-HLCs, more than 90% of cells showed to be positive for ASGPR, a mature hepatic marker.

### 5.2.3 Functional assays

The liver is responsible for producing albumin, the major protein in human serum. All the HLCs generated in **Study II**, were able to secrete albumin and no major differences were observed between the differentiation protocols. On the other hand, the levels of secreted urea by the M3- and M4-HLCs was significantly higher compared to the M1-, M2-, and M5-HLCs. Conversely, the TAG secretion in M1- and M2-HLCs was considerably higher than that in M3-, M4-, and M5-HLCs. The expression of both *APOA1* and *APOB* in the HLCs was comparable in some points to HepG2 cells, PHHs, and hLTR, which further indicated the functionality of the HLCs (**Study II, Fig. 2c**). Interestingly, the expression of *APOB* in M2 correlated well with TAG secretion, whereas M5 showed high *APOB* expression but low TAG secretion. Unfortunately, the secreted apoB and apoA-I were not measured in the culture medium. All HLCs were able to uptake the fluorescently-labelled LDL from the culture medium, which was also supported by positive immunostaining of LDL receptors (LDL-R) by monoclonal antibody.

## 5.2.4 Lipid species profiles and fatty acid synthesis

Since the HLCs differentiated by M3, M4, and M5 showed superior functionality, we selected the HLCs differentiated by those methods for the lipidomic analysis by a shotgun mass spectrometry. Overall, 15 major lipid classes – including CE, DAG, PC, Lyso-PC, PI, LPI, PE, Lyso-PE, SM, Cer, LacCer, Glc/GalCer, and Gb3 – were investigated, and altogether more than 150 molecular species were detected in **Study II**. The lipid profile of M3-, M4-, and M5-HLCs closely resembled each other with the exception of three PC species (PC 16:1–20:4, PC 17:0–18:1, and PC 17:0–20:4) (**Study II, Fig. 3a**). When the total levels of lipid classes were compared between the methods, only the concentration of Cer was at significantly lower levels in the M5-HLCs compared to the M4-HLCs (**Study II, Fig. 5b**).

## 5.3 Comparison of hiPSC-HLCs with HepG2 and primary human hepatocytes

### 5.3.1 Morphology

The morphology of differentiated HLCs in **Study I** and **II** resembled the morphology of PHHs very well. HLCs possessed a polygonal structure with dense nuclei and high cytoplasm/nuclei ratio. In addition, similar to PHHs, it was common to observe binuclear HLCs. However, among all, M4-HLCs displayed the closest morphology and characteristic binuclearity to PHHs.

### 5.3.2 Gene and protein expression

All the HLCs expressed *SOX17* higher than that in the PHHs and HepG2 but interestingly at the same levels as in the hLTR. In addition, the level of *FOXA2* in the HLCs was comparable to those shown in PHH, hLTR, and HepG2. Furthermore, due to the immature characteristic of the HLCs, the expression of *AFP* was considerably higher while the expression of *ALB* was considerably lower in HLCs compared to those expression levels seen in the three studied reference samples.

### 5.3.3 Functional assays

HLCs differentiated by all the methods displayed the hepatic functional aspects observed in PHHs. However, the levels of functionality varied in HLCs depending on the protocols and the functionality assays. For instance, all HLCs secreted lower amounts of albumin than the PHHs or even the HepG2 cells. M3- and M4-HLCs secreted TAG and urea in the same levels as those in PHHs. Additionally, the expression of *APOA1* and *APOB* in M3- and M4-HLCs were the closest to the expression of those in the PHHs.

### 5.3.4 Lipid species and fatty acid profiles

The levels of PC and PI classes were similar among HLCs, PHHs, and HepG2 cells. The level of PE was, however, detected lower in the HLCs compared to the PHHs, mostly due to the lower levels of PE 18:0-18:2 and PE 18:0-20:4 in the HLCs. We observed that the concentration of PLs containing PUFAs were significantly lower in HLCs compared to the PHHs, particularly in the species that a SFA was coupled with 18:2 FA or its derivative 20:4. The concentrations of Lyso-PLs in the HLCs and the PHHs were in similar levels, whereas HepG2 cells contained considerably higher levels of Lyso-PLs compared to both HLCs and PHHs (**Study II, Fig. 3**).

Similar to PLs, DAGs containing FA 18:2 were found in higher levels in the PHHs compared to HLCs. On the other hand, DAGs with FA 18:1 were lower in PHHs when compared to the HLCs. The CE concentration turned out to be lowest in PHHs, intermediate in HLCs, and the highest in HepG2 cells (**Study II, Fig. 4**).

HLCs mimicked the SM profile of PHHs very well except that both the HLCs and HepG2 cells contained significantly higher levels of SM d18:1/16:0 compared to the PHHs. In addition, HepG2 also contained statistically significantly higher concentrations of SM d18:1/15:0 and SM d18:1/16:1 compared to both the HLCs and PHHs. In general, HLCs mimicked the ceramide profile in PHHs very well, however, the ceramide levels as total in HLCs were closer to HepG2 cells as PHHs contained higher levels of ceramides with long- and very-long chain SFAs (e.g. Cer d18:0/22:0, Cer d18:1/22:0, and Cer d18:1/24:0). Conclusively, HLCs contain lower levels of ceramide but higher levels of LacCer, Glc/GalCer, and Gb3 [members of glycosphingolipid (GSL) family] compared to the PHHs (**Study II, Fig. 5**).

The FA analysis of HLCs, PHHs, and HepG2 cells in **Study II (Fig. 6)** showed that PHHs contained the highest and HepG2 cells the lowest amount of cellular PUFAs. In PHHs, this was mostly a reflection of high concentration of FA 18:2n-6

in their media. HLCs seemed to compensate the shortage of PUFAs receiving from their medium by efficiently synthesising VLCUFAs from the derivatives. For instance, the levels of 20:4n-6 (arachidonic acid), a bioactive metabolite of 18:2n-6, in HLCs was very close to that found in PHHs, while HepG2 did not show such efficiency. Comparing the MUFAs, the total levels of MUFAs in the HLCs were higher than in the PHHs, but lower than HepG2. FA 18:1n-9, generated from FA 18:0 via stearoyl-CoA desaturase (SCD) function, was the major MUFA in the HLCs. HepG2 cells, on the other hand, contained high levels of 18:1n-7, clearly indicating a difference from the HLCs and the PHHs. Comparing the SFAs, the levels of SFAs in HLCs was also closer to PHHs than to HepG2 cells. In summary, the most abundant FAs detected in the studied cell types were as follows: HLCs: 18:1n-9>16:0>18:0; PHHs: 16:0>18:0>18:2n-6; and HepG2: 16:0>18:1n-9>18:1n-7.

### 5.3.5 Fatty acid metabolic regulation pathway

In **Study II**, the expression of six key genes important in the synthesis of FAs were also studied by qPCR. *GCK*, *FASN*, *ELOVL2*, and *ELOVL5* were expressed in HLCs mostly in similar levels as in PHHs. In half of the differentiated HLCs, the expression of *FADS2* was similar to that in the PHHs, and the other half expressed *FADS2* in the levels detected in HepG2 and hLTR samples. *FADS1* was also expressed in HLCs at similar levels as in hLTR and the HepG2 cells but in significantly lower levels compared to the PHHs (**Study II, Fig. 7**).

## 5.4 De-differentiation of primary human hepatocytes in culture

### 5.4.1 The morphology, gene expression, and the functionality of de-differentiating PHHs

In **Study III**, the morphology of cultured PHHs remained unchanged for first two days of the culture but they started to lose their typical polygonal morphology from day 3 and presented weakly defined cell-to-cell borders (**Figure 10A**). The expression of *FOXA2* and *ALB*, *CYP1A2*, and *CYP51A1* was dramatically downregulated in PHHs within the first day of culture (**Figure 10D**), all confirming that the PHHs were going through the de-differentiation process. The secretion of TAG and urea by PHHs did not show any change between day2 and day 5. Interestingly, PHHs

seemed to slightly adapt to their new culture environment as their ability to secrete ALB was improved to some extent at day 5 compared to day 2, which correlated well with our observation from the expression of *ALB* at gene level.

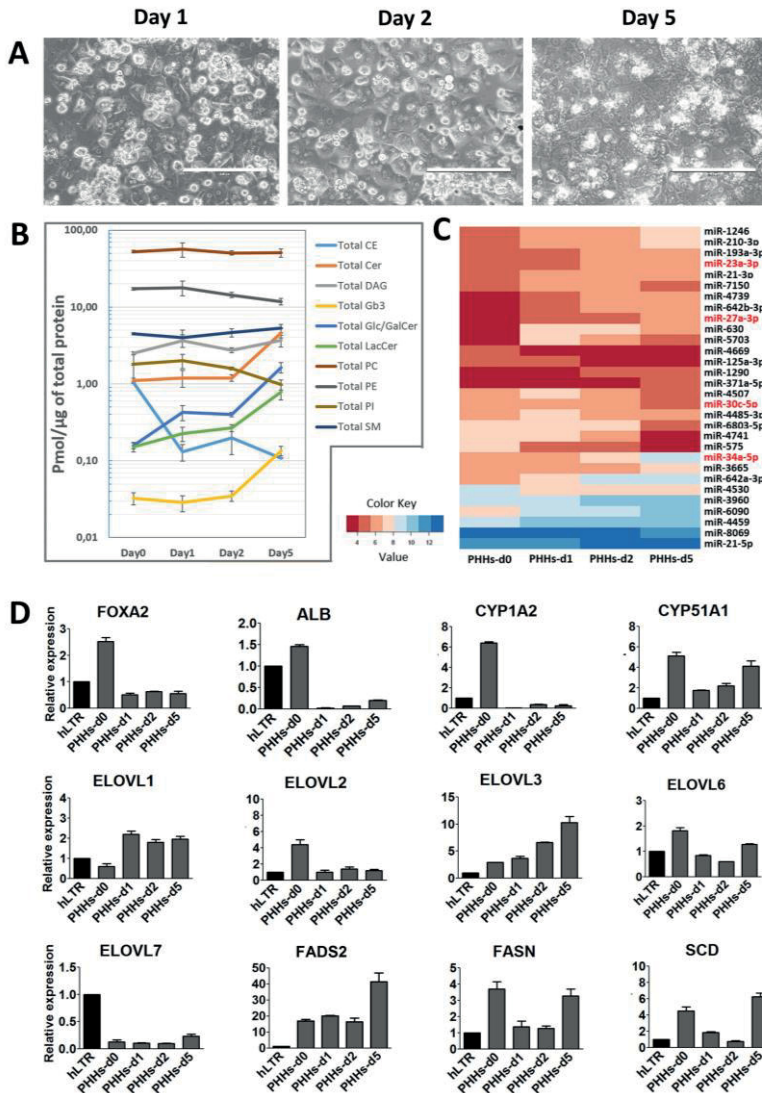


**Figure 10.** Alteration in morphology, lipid profile, miRNAs, functionality as well as metabolism of FAs in de-differentiating PHHs. **A)** Phase contrast images displaying the morphology of the PHHs in the culture on days 1, 2, and 5. Scale bar 200 μm. **B)** Lines describe the detected total concentration of different class of lipids in cultured PHHs on days 1, 2, and 5. **C)** Heatmap presenting the expression changes of top 30 miRNAs in cultured PHHs on days 1, 2, and 5.

miRNAs that have already been associated with regulation of lipids are presented in Red. **D)** Real-time qPCR analysis of genes important in the functionality (*CYP1A2* and *ALB*) or metabolism of FAs (*ELOVL1*, *ELOVL2*, *ELOVL3*, *ELOVL6*, *ELOVL7*, *FADS2*, *FASN*, and *SCD*) in PHHs on time points day 0, day 1, day2, and day5. The values are calculated relative to the human liver total RNA (hLTR) sample. Each sample was run in triplicate and bars represent mean $\pm$ SD of the biological replicates.

#### 5.4.2 Lipid profile of de-differentiating PHHs

The lipidomics data from **Study III** showed that the levels of ceramide, LacCer, Glc/GalCer, and Gb3 increased while the levels of PE and PI decreased in de-differentiating PHHs (**Figure 10B**). In addition, the total CE content of PHHs was dramatically reduced after 1 day of the culture. The total PC and DAG, however, remained relatively constant during the culture of the PHHs.

All the molecular SL species increased in PHHs-d5 particularly SLs containing LCFAs. The only exceptions were Glc/GalCer d18:1/23:0, SM d18:1/23:0, SM d18:0/23:0, SM d18:1/23:1 and SM d18:1/26:2, which decreased in PHHs-d5 (**Study III, Fig. 2B**). Using qPCR, we carefully studied the expression of several genes related to the synthesis of SLs in the de-differentiating PHHs. In line with the lipidomics results, *CERS5*, *CERS6*, *UGCG*, *SGMS1* and *SGMS2* were all upregulated, while *ASAH2* was downregulated in the cultured PHHs. *CERS7* expression was first elevated and then down-regulated during the culture of the PHHs. The expression of *CERS2*, *ASAH1*, *SMPD1* remained relatively constant throughout the culture (**Study III, Fig. 3**).

Lipidomics results also showed that the concentration of the PLs containing FA 18:1 decreased during the first day of the culture of PHHs, while species containing FA 18:0 and FA 16:0 increased from day 0 to day 1. The PL species that contained PUFAs (specially 18:2) or highly unsaturated fatty acids (HUFAs with 4-6 double bonds) coupled with a SFA (e.g. PC 16:0-22:6) decreased in PHHs from day 2 to day 5. On the other hand, the PCs consisting of SFAs and MUFAs (e.g. PC 16:0-18:1) mainly increased between day 2 and day 5.

### 5.4.3 Fatty acid and glucose metabolism in de-differentiating PHHs

Studying the expression of key genes in metabolism of FAs showed an upregulation in the genes involved in *de-novo* lipogenesis of SFAs and MUFAs but downregulation in the genes synthesising the enzyme modifying PUFAs structures (**Figure 10D**). In fact, we observed an upregulation in the expression of *ELOVL1*, *ELOVL3*, *ELOVL7*, and *FADS2*. On the other hand, the expression of *ELOVL2* was downregulated in the de-differentiating PHHs. *FADS1* and *ELOVL5* remained relatively unchanged. In addition, *FASN*, *SCD*, and *ELOVL6* showed the same pattern of expression downregulated at days 1 and 2 but upregulated at day 5.

Since the FA synthesis in hepatocytes is highly affected by glucose homeostasis, we also investigated 3 key genes involved in both glycolysis and gluconeogenesis in the liver. The expression of both glucokinase (*GCK*) and phosphoenolpyruvate carboxykinase 1 (*PCK1*) was constantly downregulated in cultured PHHs. Liver-type pyruvate kinase (*PKLR*) however, was temporally downregulated in PHHs-d1, but then upregulated in PHHs-d2 and recovered to its original level of expression of day 0 at day 5 of the culture (**Study III, Fig. 4B**).

### 5.4.4 miRNA profile of de-differentiating PHHs

In total, 382 miRNAs were detected in the cultured PHHs. Our analysis showed major alterations in the expression of miRNAs in PHHs during the course of de-differentiation. Comparing the miRNA profile of PHHs-d5 to that in PHHs-d0 it was demonstrated that 23 miRNAs were upregulated in de-differentiated PHHs from which miR-34a, miR-27a-3p, and miR-1246 were the most upregulated miRNAs. On the other hand, 22 miRNAs were downregulated in PHHs-d5 and miR-575, miR-4741, and miR-8069 were the most downregulated miRNAs. Those 30 miRNAs that showed the largest temporal variations during the PHH de-differentiation are presented in a heatmap (**Figure 10C**).



## 6 DISCUSSION

### 6.1 The differentiation of hiPSCs towards HLCs

In **Study I**, we performed a comprehensive lipidomic fingerprint of differentiating HLCs in conjunction with transcriptional, biochemical and functional measurements and HLCs demonstrated the expected functionality and phenotype of hepatic cells. We observed that the concentrations of most lipid classes, including functionally important PLs and SLs increased after commitment of the cells to hepatic lineage. However, PCs and PEs, the main building blocks of bulk membrane, showed less variation. At the same time, the levels of storage lipids such as CEs were elevated. Similarly, DAGs that are intermediary lipid class between the storage and structural lipids were elevated indicating the enhanced lipid metabolism in the cells. Unfortunately, TAGs, which are the major lipids in hepatic LDs were not measured in the HLCs. Along with the significant influence of exogenous supplies of FAs and PUFAs, we also detected endogenous cellular responses in generating very-long chain and polyunsaturated FAs. Correlations were detected between the distinct SL species levels and their specific SL metabolism-regulating genes.

Medium C (used in the hepatic commitment stage) contained high concentration of FAs which exceeded the sufficient amount needed for cells consumption. This excess amount of FAs resulted in formation of lipid droplets (LDs) during the second week of differentiation (see **Figure 8C**) in HLCs. LDs are the main reservoir for neutral lipids (majorly TAGs) in hepatocytes and can be used for e.g. membrane and steroid synthesis as well as for lipoprotein biosynthesis (Martin and Parton, 2006). These observations were giving confidence that lipid metabolism in HLCs resembles that of genuine hepatocytes.

It has been shown that the VLCFA-containing SLs are critical for the liver function (Park et al., 2014). During the HLCs differentiation and maturation, the concentration of several VLCFA-containing SLs increased, confirming that the stepwise hepatic differentiation protocol produced HLCs with a lipid phenotype resembling that of the PHHs. Ceramides can be degraded to sphingosine and free FA by ceramidases (encoded by the *ASAH* genes) (Mao and Obeid, 2008).



Concurrent with increase in VLCFA-containing Cer in differentiating HLCs, the expression of *ASAH2* was also upregulated, suggesting a balancing mechanism between Cer production and degradation during differentiation, which could partly explain why Cer levels remain constant during the late maturation stage.

The expression of sphingomyelin synthases, *SGMS1* and *SGMS2*, was upregulated in differentiating HLCs, correlating with increase in several molecular SM species (particularly those containing FAs C23-26). Simultaneously, *SMPD1*, a lysosomal acid sphingomyelinase, was upregulated during the differentiation. It is known that the SM coordinated breakdown is an essential part of membrane homeostasis (Kim et al., 2008) and ceramide as one of the products of SM catabolism is critical to the vital cellular processes (Delgado et al., 2006; Gault et al., 2010). Therefore, our data suggested that lysosomal degradation of SM might be crucial for balancing proper differentiation, maturation or functional structure of the HLCs.

The levels of several VLCFA-containing GSLs were also increasing during the maturation of HLCs in **Study I** correlating with the expression of *UGCG* in HLCs. It has been shown that GSL products play critical roles in cell growth and differentiation, and mediate cell adhesion and modulate signal transduction (Gault et al., 2010). Our finding emphasizes the important role of active UGCG enzyme function in hepatic maturation. We also detected an overall increase in the FA chain lengths in the studied SLs classes during the differentiation. This might suggest that as the cells differentiate towards HLCs, SLs with longer chain FAs are incorporated in the lipid rafts affecting the membrane lateral lipid organisation. Complex SLs have various roles in lipid rafts for example for cell-cell contact and efficient membrane trafficking (Wassall et al., 2004). In addition, cell-adhesion and signalling molecules are localised in lipid rafts, implicating that these membrane domains may form platforms for cell adhesion and signal transduction.

We detected a strong increase in PUFA-containing PL species during the hepatic differentiation in **Study I**. The increase in the polyunsaturated PLs affect the bulk membrane properties, such as flexibility, fluidity, and permeability (Rawicz et al., 2008) and changing in these properties affects membrane vesicle formation and thereby lipid and protein trafficking, which needs to be efficient as the cells grow, differentiate and make more membranes (Van Meer et al., 2008). PC species containing FA 20:4 increased more drastically than PCs containing the other PUFAs. This increase was concurrent with the highest expression of apolipoprotein B-100 and emergence of the lipid droplets in the cells. Studies showed that defects in efficient incorporation of 20:4n-6 into ER membranes, reduces TAG secretion from hepatic cells (Rong et al., 2015; Ruhanen et al., 2017). Thus, it appears that PC species

containing FA 20:4n-6 from the  $\omega$ -6 FA pathway are crucial for the assembly and secretion of TAG containing lipoprotein particles, and likely needed for the proper function of the HLCs.

Taken together, in **Study I**, it was demonstrated that how the lipidome of stem cells is remodelled in response to the external stimuli as they differentiate and mature towards functional HLCs. In addition, independent elevation in the production of VLCFA-containing SLs and PUFA-containing PLs during the hepatic maturation clearly showed that cells efficiently uptake FAs from the media, incorporate them, and modify simple lipids into more complex ones, which in turn can modify the membrane architecture mirrored in the altered cellular functions.

## 6.2 hiPSCs-HLCs as cell models for investigating the lipid aberrations of the liver

In **Study II**, we generated functional hiPSC-HLCs using five hepatic differentiation protocols and compared the differentiated HLCs comprehensively for their morphology, gene and protein expression, lipid composition, and functional traits to each other and to the two common hepatic cell models, PHHs and HepG2 cells. In this study, we performed a thorough characterisation of the metabolic features of HLCs and investigated their potential as a new cell model for lipid studies.

First, we examined the effect of various conditions and stimuli on the phenotype of the cells during the hepatic differentiation. Determining the correct initial cell density for each cell line and method was found to be a key factor in success for the DE differentiation process. This was more critical than e.g. the type of the DE inducer such as CHIR 99021 or Wnt3. Furthermore, initiating the differentiation with single cells instead of colonies resulted in an earlier emergence of the DE cells but not the efficiency of the differentiation. In line with previous studies (Cameron et al., 2015), coating the culture plates with a mixture of Laminin 521/111 instead of Geltrex™ increased the number of ALB-positive cells by 82% and the binuclearity of the HLCs by 65%, however, this coating did not see any affect on the functionality of the HLCs. Conclusively, M3, M4, and M5 showed to differentiate HLCs with superior characteristics for studying the liver function and lipid metabolism compared to the M1 and M2 (see **Figure 6**).

PUFAs and their bioactive derivatives play important roles during the cell proliferation and differentiation (Bieberich, 2012; Kim et al., 2009) and the PHHs possess an excellent capacity to metabolise diet-derived PUFAs (Sprecher, 2000). In

**Study II**, it was shown that the HLCs express the key enzymes in the metabolism of FAs at similar levels to those in the PHHs. In addition, HLCs showed to be superior cell models for studying the overall FA metabolism of the liver compared to HepG2 cells.

*FASN* determines the *de-novo* synthesis of FAs in the cells by synthesising palmitate (FA 16:0) (Jensen-Urstad and Semenkovich, 2012). The relative activities of SCD and ELOVL dictate whether the metabolism of 16:0 follows the route 16:0 – 16:1n-7 – 18:1n-7, or the route 16:0 – 18:0 – 18:1n-9 (Glück et al., 2016) (see **Figure 2A**). Our results showed that HepG2 cells may prefer the route forming 18:1n-7 and this clearly distinguished them from HLCs and PHHs. HepG2 cells also significantly differed in the expression of most other genes involved in the synthesis of FAs such as *FASN*, *ELOVL2*, *FADS1*, and *FADS2*. The high expression of *FASN* in the HepG2 cells has also been reported elsewhere (Huang and Lin, 2012).

Due to the rich supply of the FA 18:2n-6 in their medium, PHHs contained a considerably larger proportion of PUFAs, part of which was apparently converted to 20:4n-6 by the cells using the *FADS1*, *FADS2*, *ELOVL2*, and *ELOVL5* enzymes. Consequently, the PLs composed of 16:0-18:2, 18:0-18:2, 16:0-20:4, and 18:0-20:4 were abundant in the PHHs. HLCs, despite the very low supply of 18:2n-6 in their medium, were able to efficiently produce FA 20:4n-6, suggesting the proper function of corresponding enzymes in the HLCs. However, the presence of 2–3 mol% n-9 PUFAs (produced from MUFAs) in both HLCs and HepG2 cells showed that both cell types suffered from essential PUFA deficiency (Kamada et al., 1999). It is considered that a high supply of n-6 PUFA to PHHs inhibits their endogenous MUFA synthesis from SFAs (Ntambi, 1999). Therefore, considering the important role of PUFAs in HLCs' maturation shown in **Study I**, we speculate that reformulating the HLCs' medium to a PUFA-rich medium may help to produce hepatic cells with improved functionality and a lipid profile better resembling that shown in the PHHs.

The HLCs showed a mild accumulation of neutral lipids, which is likely due to their treatment with a FA-rich medium at the hepatoblast stage (discussed in **Study I**). The PHHs contained low levels of CE due to their low FA medium. HepG2 cells, on the other hand, were grown in FA rich medium and accumulated a large amount of the neutral lipids (preferentially TAGs). Therefore, results in the **Studies I and II** reveal the need to revise the generally overlooked FA content of culture media and to tailor it according to the cell's needs. In addition, developing a standardised medium may bring added value in the accuracy of the results and prevent wrong interpretations particularly in the comparison studies.

In conclusion, data in **Study II** showed the detailed lipid profile of the HLCs in parallel to PHHs and HepG2 cells and evaluated their ability to metabolise FAs. iPSC-HLCs closely mimicked the lipid profile of PHHs and showed to be a more relevant liver cell model than HepG2 cells for studying cellular and molecular mechanisms that regulate lipid homeostasis in the liver.

## 6.3 Lipids and the de-differentiation of the PHHs

Hepatocytes undergo rapid de-differentiation in 2D culture and lose their phenotype, which particularly hampers their utility in long-term *in vitro* studies. In **Study III**, the mechanisms behind the de-differentiation and the possible role of lipids and miRNAs in the loss of the phenotype of PHHs were investigated. Here, a comprehensive lipidomic and lipid-related gene analysis as well as miRNA analysis on de-differentiating PHHs over 5 days of their culture was performed. Major alterations in both lipid and miRNA profiles of the cultured PHHs were observed. Despite the abundant PUFA 18:2-n6 in the culture medium of PHHs, the lipidome of PHHs showed increasing concentrations of SLs and MUFA-containing PLs and concurrently decreasing levels of PUFA-containing PLs. In line with this, the high expression levels of *FASN*, *SCD*, and *ELOVL6* at day 0 created the prerequisite for *de-novo* synthesis of SFAs and MUFAs, although the genes related to the desaturases (*FADS1*, *FADS2*) and elongases (*ELOVL2*, *ELOVL5*), required for PUFA modifications were also expressed in the de-differentiating PHHs.

It is previously reported that the viability of the PHHs decreases by 50% after 3 days in culture (Ling et al., 2013). Conversely, we did not observe a dramatic cell death in 5 days culture of PHHs. One reason can be attributed to the density of the cultured PHHs. In our study, PHHs were cultured with high density, and therefore they formed a confluent monolayer, which could provide the cells with the critical cell-cell interactions. In Ling et al. study, however, the cell density was considerably lower. Alternatively, Ling et al. used RPMI+10% FBS medium for culturing the PHHs which differed from the defined medium used in the present study.

Interestingly, as PHHs morphologically de-differentiated, they showed partial adaptation to the new 2D environment as the expression of both *ALB* and *CYP* genes were slightly improved at day 2 or 5. It is known that de-differentiation is an active, complex and differentially controlled process (Heslop et al., 2017) (Elaut et al., 2006; Gault et al., 2010). Therefore, while some features are diminishing, some other features might become over-expressed during the de-differentiation of the

PHHs. Therefore, even though the PHHs were de-differentiating, some functional features could still improve through adaptation to the new culture environment.

We found that the concentration of almost all SL species increased during the de-differentiation of PHHs. We confirmed this observation in gene expression levels and observed that several genes involved in the synthesis of SLs (such as *UGCG* and *SGMS1*) were upregulated, while the genes involved in the degradation of SLs (such as *ASAH2*) were downregulated in the de-differentiated PHHs. The concentration of SMs increased during the de-differentiation of PHHs. It is known that in the cells, approximately two-thirds of the total SM is located on the plasma membrane, 65% of which are found in the structure of the lipid rafts (Li et al., 2007). As discussed in chapter 2.3, lipid rafts are enriched with very-long chain and saturated SLs, surrounded with the bulk membrane containing unsaturated PLs (Ishibashi et al., 2013; Simons and Gerl, 2010). We also observed a clear increase in very-long and saturated SLs (e.g. SLs with FA 22:0) and MUFAs containing PLs. These changes may implicate the alteration of the cellular membrane and the lipid rafts during the process of de-differentiation. This can subsequently affect lateral lipid packing membrane fluidity and permeability as well as cellular trafficking, signalling, and functionality.

*CERS1* and *CERS5* were upregulated but *CERS4* was downregulated in the cultured PHHs. Different *Cers* are known to be involved in regulating the balance between cell death and survival (Mesicek et al., 2010). We speculate that up- or down-regulation of specific ceramides may be attributable to the activation of anti-apoptotic or pro-survival mechanisms in PHHs (Cingolani et al., 2016; Heslop et al., 2017; Saddoughi et al., 2008). These alterations could act as a double-edged sword, on one hand preventing the cell death, while on the other hand, causing the loss of the liver-specific functions in PHHs.

In the de-differentiating PHHs, the *de-novo* synthesis of SFAs and MUFA synthesis (see **Figure 2**) was upregulated but the synthesis pathway of PUFAs was downregulated. *FASN*, *ELOVL6*, and *SCD* genes showed a tight co-regulation displaying similar pattern of expression: all downregulated on day1 and 2, but upregulated on day 5 suggesting that they regulated *de-novo* FA synthesis in a concerted manner during the prolonged culture of the PHHs. *ELOVL1* and *ELOVL3* were upregulated during the de-differentiation of the PHHs, matching with the observation from the increase in the lipids harbouring SFAs and MUFAs. On the other hand, *ELOVL2* was downregulated in line with our observations of the reduced levels of PL species with a very-long PUFA chain in the de-differentiating PHHs.

The increased degree of intrahepatic lipid saturation could affect the cell fate as SFAs may play an important role in “lipotoxic” mechanisms and in the initiation of apoptosis in hepatic cells. In addition, it could trigger the detrimental unfolded protein response (UPR) signalling pathways (Leamy et al., 2013). In the de-differentiating PHHs, however, the reduction in the polyunsaturated PL content was compensated by an increase of PL species with MUFAs, which should balance the overall fluidity of the membrane bulk lipids (Ntambi, 1999). The MUFA production from SFA precursors may also have protected the cells from accumulation of high levels of toxic SFAs. Nevertheless, by reduction in PUFAs, PHH membrane dynamics, requiring polyunsaturated PE (van der Veen et al., 2017), and signalling pathways, requiring PI precursors (Balla, 2013), may have been hampered in de-differentiating PHHs.

## 6.4 The role of miRNAs in de-differentiation of PHHs

Alongside the lipidomics, we analysed the miRNA profile in de-differentiating PHHs to identify the miRNAs that possibly regulate the lipid alterations during this process. We mainly focused on those miRNAs whose role in the regulation of lipids or FAs is already established or have been linked to the functionality of the cells (Novák et al., 2015; Takagi et al., 2010; Yang et al., 2015; Zhang et al., 2017). Several miRNAs were identified that were either up- or downregulated in the de-differentiated PHHs and which were connected to the regulation of lipid metabolism or PHHs functionality. miR-122 is a liver-specific miRNA and is the first miRNA reported to regulate lipid metabolism and its deletion results in the lower secretion of cholesterol and TG (Esau et al., 2006). This miRNA was downregulated in de-differentiated PHHs. On the other hand, miR-34a was upregulated in de-differentiated PHHs. It has been already shown that miR-34a plays multiple roles in the regulation of cell cycle, differentiation, migration and apoptosis (Yang et al., 2015). miR-34a can regulate bile acid-synthesizing enzymes such as CYP7A1, CYP26 family, and CYP3A4 (Goodwin et al., 2000; Oda et al., 2014; Takagi et al., 2010) as well as a series of genes and proteins involved in the lipid and glucose metabolism (Kim et al., 2013; Rodgers and Puigserver, 2007; Ye et al., 2017). In addition to miR-34a, miR-23a was another upregulated miRNA in the de-differentiated PHHs and reportedly it plays a role in suppression of gluconeogenesis in cells (Reyes et al., 2014; Wang et al., 2012). Therefore, it can be speculated that the upregulation of miR-34a



and miR-23a may be associated with the downregulation of *GCK*, *PCK1*, and *CYP* genes, and/or the loss of functionality observed in the de-differentiated PHHs.

miR-27a was another upregulated miRNA in de-differentiated PHHs. It has been shown that miR-27a regulates several enzymes connected to the metabolism of lipids including adenosine triphosphate-binding cassette transporter A1 (ABCA1), *FASN*, *SCD1*, sterol regulatory element-binding proteins (SREBP-1 and SREBR-2), PPAR $\alpha$  and PPAR $\gamma$ , APOA1, APOB100 and APOE3 (Ji et al., 2009; Shirasaki et al., 2013; Yang et al., 2015; Zhang et al., 2017). It has been suggested that miR-27a may regulate the metabolism of lipids by reducing lipid synthesis and increasing lipid secretion from the cells (Yang et al., 2015). The upregulation of miR-27a in **Study III** was simultaneous with the downregulation of both *FASN* and *SCD* in PHHs-d1 and PHHs-d2, but not in PHHs-d5 where the expression of those genes was upregulated. This observation proposes the possible involvement of other miRNA(s) in the regulation of *FASN* and *SCD*. Interestingly, we found that miR-30c, recently known to target *FASN* (Fan et al., 2017), was downregulated in PHHs-d5 which suggests that miR27a and miR-30c may work together to regulate the synthesis, accumulation, and secretion of lipids in PHHs during their de-differentiation.

## 6.5 Limitations and future perspective

iPSC-HLCs could serve as a powerful and functional cell model to study patient-specific mechanisms of the lipid aberrations leading to pathological conditions, such as fatty liver disease or atherosclerosis. They provide a valuable platform for both academia and pharmaceutical industry for screening novel drugs in a truly patient-specific manner and discovering the modes of action of molecules modulating the key lipids. Using iPSC-HLCs as a cell model, we can implicate the impact of genetic variations in developing metabolic diseases. iPSC-HLCs are also a promising cell source for regenerative medicine in hepatic replacement and managing of liver failure. However, more research is needed to improve the maturity of HLCs before they are widely applied in the clinic or drug screening. In fact, despite the huge progress, current efforts worldwide have not yet taken HLCs beyond a relatively immature phenotype (Baxter et al., 2015), and an integral part of this challenge is how we can capture the mature hepatic phenotype and prevent its deterioration. Crucially, increased understanding of both differentiation and de-differentiation process could be beneficial in developing a culture environment that improves the

maturity and maintains a hepatic phenotype from pluripotent cells *in vitro*. Our approach in **Study I** opens up new avenues in lipid-focused stem cell biology as it provides a novel tool in utilising the lipidome to follow the cell differentiation and maturation and how this is affected under altered conditions or stimuli. The stem cell lipidomic fingerprinting during HLC differentiation will assist in generating HLCs that more closely resemble the phenotype of primary human hepatocytes.

Both **Studies I** and **III** illustrated the importance of VLC PUFAs in maturation and proper function of the hepatic cells. We showed that HLCs are capable of metabolising highly unsaturated FAs in order to fulfil the complex biological functions mediated by those FAs. In addition, we illustrated that the de-differentiation of PHHs is accompanied by the reduction in their cellular PUFAs content. Therefore, it can be speculated that improving the PUFA homeostasis of hepatic cells either endogenously or exogenously, may help to improve their maturity and/or postpone their de-differentiation process in culture. In this respect, further studies in utilizing CRISPR-Cas9 technology to upregulate specific key genes important in synthesis of PUFAs could be applied in the future. In addition, improving the lipid formulation of the culture medium according to the HLCs need is worthwhile to be considered.

It is well accepted that the 3D culture of hepatocytes enhances the organization, metabolic activity, and life-span of the hepatocytes. (Gieseck et al., 2014; Vellonen et al., 2014). However, the effect of 3D culture on the lipid profile of hepatic cells is not yet known. Therefore, further investigations using more physiologically relevant 3D hepatic cell models are needed.



## 7 CONCLUSIONS AND FUTURE ASPECTS

This thesis provides a comprehensive study on iPSC-derived hepatic cells as a novel cell model for studying the lipid metabolism of liver. Here, the lipid profile of iPSC-HLCs is characterised and compared to their native counterparts (PHHs) and the role of molecular lipid species and FAs in both differentiation and maturation as well as the de-differentiation of hepatic cells in 2D cell culture is investigated. The following conclusions can be drawn based on the three collective studies presented in this thesis:

1. Three iPSC lines have been successfully differentiated to functional HLCs using various conditions described as five individual methods. HLCs resembled PHHs by expressing relevant hepatic markers as well as enabling secretion of lipoproteins, albumin, TAG and urea.
2. iPSC-HLCs closely mimicked the lipid and FA profile of PHHs and thus they are a relevant cell model to investigate human lipid homeostasis at both molecular and cellular levels.
3. The lipid profile of cells was dramatically altered during their differentiation from iPSC to HLCs, most of which was caused by exogenous supply of relevant lipids provided to the cells. However, several VLC SLs and PUFA-containing PLs increased during the hepatic maturation phase independent of the exogenous lipid supplies, which is proposed to be important for proper inherent hepatic function.
4. The de-differentiation of PHHs was accompanied with an upregulation in *de-novo* synthesis of SFAs and MUFAs, which was clearly mirrored in the increased levels of saturated and monounsaturated PLs and SLs. On the other hand, the levels of PLs containing PUFAs were reduced in the de-differentiated PHHs. All these changes could dramatically affect the cellular membrane fluidity and functionality.

5. We found that collectively 45 miRNAs were either up- or downregulated in the cultured dedifferentiated PHHs from which miR-34a, miR-27a-3p, and miR-1246 were the most upregulated while miR-575, miR-4741, and miR-8069 were the most downregulated miRNAs. Several up- or downregulated miRNAs in de-differentiating PHHs have been earlier associated with the regulation of genes involved in the lipid metabolism of hepatic cells.
6. Although a 3D culture of hepatic cells would be more ideal, the 2D platform developed in this study can still facilitate the generation of HLCs resembling PHHs to a great extent.

## 8 REFERENCES

- Baenke, F., Peck, B., Miess, H., and Schulze, A. (2013). Hooked on fat: the role of lipid synthesis in cancer metabolism and tumour development. *Dis. Model. Mech.* 6, 1353–1363.
- Baker, T.K., Carfagna, M.A., Gao, H., Dow, E.R., Li, Q., Searfoss, G.H., and Ryan, T.P. (2001). Temporal gene expression analysis of monolayer cultured rat hepatocytes. *Chem. Res. Toxicol.* 14, 1218–1231.
- Balla, T. (2013). ATP-binding cassette transporter A1 deficiency in human induced pluripotent stem cell-derived hepatocytes abrogates HDL biogenesis and enhances triglyceride secretion. *Physiol. Rev.* 93, 1019–1137.
- Bartke, N., and Hannun, Y.A. (2008). Bioactive sphingolipids: metabolism and function. *J. Lipid Res.* 50, 91–96.
- Baxter, M., Withey, S., Harrison, S., Segeritz, C.P., Zhang, F., Atkinson-Dell, R., Rowe, C., Gerrard, D.T., Sison-Young, R., Jenkins, R., et al. (2015). Phenotypic and functional analyses show stem cell-derived hepatocyte-like cells better mimic fetal rather than adult hepatocytes. *J. Hepatol.* 62, 581–589.
- Behbahan, I.S., Duan, Y., Lam, A., Khoobyari, S., Ma, X., Ahuja, T.P., and Zern, M.A. (2011). New approaches in the differentiation of human embryonic stem cells and induced pluripotent stem cells toward hepatocytes. *Stem Cell Rev.* 7, 748–759.
- Bell, C.C., Hendriks, D.F.G., Moro, S.M.L., Ellis, E., Walsh, J., Renblom, A., Fredriksson Puigvert, L., Dankers, A.C.A., Jacobs, F., Snoeys, J., et al. (2016). Characterization of primary human hepatocyte spheroids as a model system for drug-induced liver injury, liver function and disease. *Sci. Rep.* 6, 25187.
- Berger, D.R., Ware, B.R., Davidson, M.D., Allsup, S.R., and Khetani, S.R. (2015). Enhancing the functional maturity of induced pluripotent stem cell-derived human hepatocytes by controlled presentation of cell-cell interactions in vitro. *Hepatology* 61, 13701381.
- Bhise, N.S., Manoharan, V., Massa, S., Tamayol, A., Ghaderi, M., Miscuglio, M., Lang, Q., Zhang, Y.S., Shin, S.R., Calzone, G., et al. (2016). A liver-on-a-chip platform with bioprinted hepatic spheroids. *Biofabrication* 8, 014101.
- Bi, X., Pashos, E.E., Cuchel, M., Lyssenko, N.N., Hernandez, M., Picataggi, A., McParland, J., Yang, W., Liu, Y., Yan, R., et al. (2017). ATP-Binding Cassette Transporter A1 Deficiency in Human Induced Pluripotent Stem Cell-Derived Hepatocytes Abrogates HDL Biogenesis and Enhances Triglyceride Secretion. *EBioMedicine* 18, 139–145.
- Bieberich, E. (2012). It's a lipid's world: Bioactive lipid metabolism and signaling in neural stem cell differentiation. *Neurochem. Res.* 37, 1208–1229.
- Blouin, A., Bolender, R.P., and Weibel, E.R. (1977). Distribution of organelles and membranes between hepatocytes and nonhepatocytes in the rat liver parenchyma. A stereological study. *J. Cell Biol.* 72, 441–455.
- Bolstad, B.M., Irizarry, R. a, Astrand, M., and Speed, T.P. (2003). A comparison of normalization methods for high density oligonucleotide array data based on variance and bias. *Bioinformatics* 19, 185–193.

- Bort, R., Signore, M., Tremblay, K., Barbera, J.P.M., and Zaret, K.S. (2006). Hex homeobox gene controls the transition of the endoderm to a pseudostratified, cell emergent epithelium for liver bud development. *Dev. Biol.* 290, 44–56.
- Calmont, A., Wandzioch, E., Tremblay, K.D., Minowada, G., Kaestner, K.H., Martin, G.R., and Zaret, K.S. (2006). An FGF response pathway that mediates hepatic gene induction in embryonic endoderm cells. *Dev. Cell* 11, 339–348.
- Cameron, K., Tan, R., Schmidt-Heck, W., Campos, G., Lyall, M.J., Wang, Y., Lucendo-Villarin, B., Szkolnicka, D., Bates, N., and Kimber, S.J. (2015). Recombinant laminins drive the differentiation and self-organization of hESC-derived hepatocytes. *Stem Cell Reports* 5, 1250–1262.
- Cayo, M.A., Cai, J., Delaforest, A., Noto, F.K., Nagaoka, M., Clark, B.S., Collery, R.F., Si-Tayeb, K., and Duncan, S.A. (2012). JD induced pluripotent stem cell-derived hepatocytes faithfully recapitulate the pathophysiology of familial hypercholesterolemia. *Hepatology* 56, 2163–2171.
- Chen, Y.F., Tseng, C.Y., Wang, H.W., Kuo, H.C., Yang, V.W., and Lee, O.K. (2012). Rapid generation of mature hepatocyte-like cells from human induced pluripotent stem cells by an efficient three-step protocol. *Hepatology* 55, 1193–1203.
- Choi, S., Choi, J., Cui, L., Seo, H., Kim, J., Park, C., Joo, H., Park, J., Hong, S., and Yu, C. (2015). Mixl1 and Flk1 are key players of Wnt/TGF- $\beta$  signaling during DMSO-induced mesodermal specification in P19 cells. *J. Cell. Physiol.* 230, 1807–1821.
- Cingolani, F., Futerman, A.H., and Casas, J. (2016). Ceramide synthases in biomedical research. *Chem. Phys. Lipids* 197, 25–32.
- Cohen, P., and Friedman, J.M. (2004). Leptin and the control of metabolism: role for stearyl-CoA desaturase-1 (SCD-1). *J. Nutr.* 134, 2455S–2463S.
- Cohen, M., Levy, G., and Nahmias, Y. (2015). Coculture and long-term maintenance of hepatocytes. *Methods Mol Biol.* 1250, 161–173.
- Currie, E., Schulze, A., Zechner, R., Walther, T.C., and Farese, R. V. (2013). Cellular fatty acid metabolism and cancer. *Cell Metab.* 18, 153–161.
- Czysz, K., Minger, S., and Thomas, N. (2015). DMSO efficiently down regulates pluripotency genes in human embryonic stem cells during definitive endoderm derivation and increases the proficiency of hepatic differentiation. *PLoS One* 10, doi: 10.1371/journal.pone.0117689.
- D'Amour, K.A., Agulnick, A.D., Eliazer, S., Kelly, O.G., Kroon, E., and Baetge, E.E. (2005). Efficient differentiation of human embryonic stem cells to definitive endoderm. *Nat. Biotechnol.* 23, 1534–1541.
- Darnell, M., Ulvestad, M., Ellis, E., Weidolf, L., and Andersson, T.B. (2012). In vitro evaluation of major in vivo drug metabolic pathways using primary human hepatocytes and HepaRG cells in suspension and a dynamic three-dimensional bioreactor system. *J Pharmacol Exp Ther.* 343, 134–144.
- Delgado, A., Casas, J., Llebaria, A., Abad, J.L., and Fabrias, G. (2006). Inhibitors of sphingolipid metabolism enzymes. *Biochim. Biophys. Acta - Biomembr.* 1758, 1957–1977.
- Donato, M.T., Lahoz, A., Castell, J. V., and Gómez-Lechón, M.J. (2008). Cell lines: a tool for in vitro drug metabolism studies. *Curr Drug Metab.* 9, 1–11.
- Du, C., Narayanan, K., Leong, M.F., and Wan, A.C.A. (2014). Induced pluripotent stem cell-derived hepatocytes and endothelial cells in multi-component hydrogel fibers for liver tissue engineering. *Biomaterials* 35, 6006–6014.

- Ejsing, C.S., Duchoslav, E., Sampaio, J., Simons, K., Bonner, R., Thiele, C., Ekroos, K., and Shevchenko, A. (2006). Automated identification and quantification of glycerophospholipid molecular species by multiple precursor ion scanning. *Anal. Chem.* 78, 6202–6214.
- Ekroos, K. (2012). Lipidomics perspective: from molecular lipidomics to validated clinical diagnostics. In *Lipidomics Technologies and Applications*, K. Ekroos, ed. (Weinheim: Wiley-VCH Verlag & Co. KGaA), pp. 1–16.
- Ekroos, K., Chernushevich, I. V., Simons, K., and Shevchenko, A. (2002). Quantitative profiling of phospholipids by multiple precursor ion scanning on a hybrid quadrupole time-of-flight mass spectrometer. *Anal. Chem.* 74, 941–949.
- Ekroos, K., Ejsing, C.S., Bahr, U., Karas, M., Simons, K., and Shevchenko, A. (2003). Charting molecular composition of phosphatidylcholines by fatty acid scanning and ion trap MS3 fragmentation. *J. Lipid Res.* 44, 2181–2192.
- Elaut, G., Henkens, T., Papeleu, P., Snykers, S., Vinken, M., Vanhaecke, T., and Rogiers, V. (2006). Molecular mechanisms underlying the dedifferentiation process of isolated hepatocytes and their cultures. *Curr. Drug Metab.* 7, 629–660.
- Elmén, J., Lindow, M., Silahatoglu, A., Bak, M., Christensen, M., Lind-Thomsen, A., Hedtjærn, M., Hansen, J.B., Hansen, H.F., Straarup, E.M., et al. (2008). Antagonism of microRNA-122 in mice by systemically administered LNA-antimiR leads to up-regulation of a large set of predicted target mRNAs in the liver. *Nucleic Acids Res.* 36, 1153–1162.
- Esau, C., Davis, S., Murray, S.F., Yu, X.X., Pandey, S.K., Pear, M., Watts, L., Booten, S.L., Graham, M., McKay, R., et al. (2006). miR-122 regulation of lipid metabolism revealed by in vivo antisense targeting. *Cell Metab.* 3, 87–98.
- Fan, J., Li, H., Nie, X., Yin, Z., Zhao, Y., Chen, C., and Wen Wang, D. (2017). MiR-30c-5p ameliorates hepatic steatosis in leptin receptor-deficient (db/db) mice via down-regulating FASN. *Oncotarget* 8, 13450–13463.
- Foster, E., You, J., Siltanen, C., Patel, D., Haque, A., Anderson, L., and Revzin, A. (2015). Heparin hydrogel sandwich cultures of primary hepatocytes. *Eur. Polym. J.* 72, 726–735.
- Fraczek, J., Bolleyn, J., Vanhaecke, T., Rogiers, V., and Vinken, M. (2013). Primary hepatocyte cultures for pharmaco-toxicological studies: At the busy crossroad of various anti-dedifferentiation strategies. *Arch. Toxicol.* 87, 577–610.
- Freyer, N., Knöspel, F., Strahl, N., Amini, L., Schrade, P., Bachmann, S., Damm, G., Seehofer, D., Jacobs, F., Monshouwer, M., et al. (2016). Hepatic differentiation of human induced pluripotent stem cells in a perfused three-dimensional multicompartiment bioreactor. *Biores. Open Access* 5, 235–248.
- Gault, C.R., Obeid, L.M., and Hannun, Y.A. (2010). An overview of sphingolipid metabolism: From synthesis to breakdown. *Adv. Exp. Med. Biol.* 688, 1–23.
- Gerbail-Chaloin, S., Funakoshi, N., Caillaud, A., Gondeau, C., Champon, B., and Si-Tayeb, K. (2014). Human induced pluripotent stem cells in hepatology: beyond the proof of concept. *Am. J. Pathol.* 184, 332–347.
- Gieseck, R.L., Hannan, N.R.F., Bort, R., Hanley, N.A., Drake, R.A.L., Cameron, G.W.W., Wynn, T.A., and Vallier, L. (2014). Maturation of induced pluripotent stem cell derived hepatocytes by 3D-culture. *PLoS One* 9, e86372.
- Gissen, P., and Arias, I.M. (2015). Structural and functional hepatocyte polarity and liver disease. *J. Hepatol.* 63, 1023–1037.

- Glück, T., Rupp, H., and Alter, P. (2016). Mechanisms increasing n-3 highly unsaturated fatty acids in the heart. *Can. J. Physiol. Pharmacol.* 94, 309–323.
- Godoy, P., Hengstler, J.G., Ilkavets, I., Meyer, C., Bachmann, A., Müller, A., Tuschl, G., Mueller, S.O., and Dooley, S. (2009). Extracellular matrix modulates sensitivity of hepatocytes to fibroblastoid dedifferentiation and transforming growth factor  $\beta$ -induced apoptosis. *Hepatology* 49, 2031–2043.
- Godoy, P., Hewitt, N.J., Albrecht, U., Andersen, M.E., Ansari, N., Bhattacharya, S., Bode, J.G., Bolleyn, J., Borner, C., Böttger, J., et al. (2013). Recent advances in 2D and 3D in vitro systems using primary hepatocytes, alternative hepatocyte sources and non-parenchymal liver cells and their use in investigating mechanisms of hepatotoxicity, cell signaling and ADME. *Arch. Toxicol.* 87, 1315–1530.
- Goldman, O., Han, S., Sourrisseau, M., Dziedzic, N., Hamou, W., Corneo, B., D’Souza, S., Sato, T., Kotton, D.N., Bissig, K.D., et al. (2013). KDR identifies a conserved human and murine hepatic progenitor and instructs early liver development. *Cell Stem Cell* 12, 748–760.
- Goodwin, B., Jones, S.A., Price, R.R., Watson, M.A., McKee, D.D., Moore, L.B., Galardi, C., Wilson, J.G., Lewis, M.C., Roth, M.E., et al. (2000). A regulatory cascade of the nuclear receptors FXR, SHP-1, and LRH-1 represses bile acid biosynthesis. *Mol. Cell* 6, 517–526.
- Gordillo, M., Evans, T., and Gouon-Evans, V. (2015). Orchestrating liver development. *Development* 142, 2094–2108.
- Gouliarmou, V., Pelkonen, O., and Coecke, S. (2015). Differentiation-promoting medium additives for hepatocyte cultivation and cryopreservation. In *Protocols in in Vitro Hepatocyte Research*, M. Viken, and V. Rogiers, eds. (New York: Humana Press), pp. 143–159.
- Hannan, N.R.F., Segeritz, C.-P., Touboul, T., and Vallier, L. (2013). Production of hepatocyte-like cells from human pluripotent stem cells. *Nat. Protoc.* 8, 430–437.
- Hannun, Y.A., and Obeid, L.M. (2008). Principles of bioactive lipid signalling: lessons from sphingolipids. *Nat. Rev. Mol. Cell Biol.* 9, 139–150.
- Haramoto, Y., Tanegashima, K., Onuma, Y., Takahashi, S., Sekizaki, H., and Asashima, M. (2004). *Xenopus tropicalis* nodal-related gene 3 regulates BMP signaling: An essential role for the pro-region. *Dev. Biol.* 265, 155–168.
- Hay, D.C., Fletcher, J., Payne, C., Terrace, J.D., Gallagher, R.C.J., Snoeys, J., Black, J.R., Wojtacha, D., Samuel, K., Hannoun, Z., et al. (2008). Highly efficient differentiation of hESCs to functional hepatic endoderm requires ActivinA and Wnt3a signaling. *Proc. Natl. Acad. Sci.* 105, 12301–12306.
- Heidariyan, Z., Ghanian, M.H., Ashjari, M., Farzaneh, Z., Najarasl, M., Rezaei Larijani, M., Piryaei, A., Vosough, M., and Baharvand, H. (2018). Efficient and cost-effective generation of hepatocyte-like cells through microparticle-mediated delivery of growth factors in a 3D culture of human pluripotent stem cells. *Biomaterials* 159, 174–188.
- Heslop, J.A., Rowe, C., Walsh, J., Sison-Young, R., Jenkins, R., Kamalian, L., Kia, R., Hay, D., Jones, R.P., Malik, H.Z., et al. (2017). Mechanistic evaluation of primary human hepatocyte culture using global proteomic analysis reveals a selective dedifferentiation profile. *Arch. Toxicol.* 91, 439–452.
- Hu, C., and Li, L. (2015). In vitro culture of isolated primary hepatocytes and stem cell-derived hepatocyte-like cells for liver regeneration. *Protein Cell* 6, 562–574.

- Huang, H.-C., and Lin, J.-K. (2012). Pu-erh tea, green tea, and black tea suppresses hyperlipidemia, hyperleptinemia and fatty acid synthase through activating AMPK in rats fed a high-fructose diet. *Food Funct.* 3, 170–177.
- Huang, J., Guo, X., Li, W., and Zhang, H. (2017). Activation of Wnt/ $\beta$ -catenin signalling via GSK3 inhibitors direct differentiation of human adipose stem cells into functional hepatocytes. *Sci. Rep.* 7, doi:10.1038/srep40716.
- Hunter, M.P., Wilson, C.M., Jiang, X., Cong, R., Vasavada, H., Kaestner, K.H., and Bogue, C.W. (2007). The homeobox gene *Hhex* is essential for proper hepatoblast differentiation and bile duct morphogenesis. *Dev. Biol.* 308, 355–367.
- Ichimura, A., Hirasawa, A., Poulain-Godefroy, O., Bonnefond, A., Hara, T., Yengo, L., Kimura, I., Leloire, A., Liu, N., Iida, K., et al. (2012). Dysfunction of lipid sensor GPR120 leads to obesity in both mouse and human. *Nature* 483, 350–354.
- Ikonen, E. (2008). Cellular cholesterol trafficking and compartmentalization. *Nat. Rev. Mol. Cell Biol.* 9, 125–138.
- Irizarry, R.A., Bravo, H.C., Irizarry, R.A., Irizarry, R., Hobbs, B., Collin, F., Beazer-Barclay, Y., Antonellis, K., Scherf, U., Speed, T., et al. (2003). Exploration, normalization, and summaries of high density oligonucleotide array probe level data. *Biostatistics* 4, 249–264.
- Ishibashi, H., Nakamura, M., Komori, A., Migita, K., and Shimoda, S. (2009). Liver architecture, cell function, and disease. *Semin. Immunopathol.* 31, 399–409.
- Ishibashi, Y., Kohyama-Kogane, A., and Hirabayashi, Y. (2013). New insights on glucosylated lipids: Metabolism and functions. *Biochim. Biophys. Acta - Mol. Cell Biol. Lipids* 1831, 1475–1485.
- Jensen-Urstad, A.P.L., and Semenkovich, C.F. (2012). Fatty acid synthase and liver triglyceride metabolism: Housekeeper or messenger? *Biochim. Biophys. Acta - Mol. Cell Biol. Lipids* 1821, 747–753.
- Ji, J., Zhang, J., Huang, G., Qian, J., Wang, X., and Mei, S. (2009). Over-expressed microRNA-27a and 27b influence fat accumulation and cell proliferation during rat hepatic stellate cell activation. *FEBS Lett* 583, 759–766.
- Jiang, J., Au, M., Lu, K., Eshpeter, A., Korbitt, G., Fisk, G., and Majumdar, A.S. (2007). Generation of insulin-producing islet-like clusters from human embryonic stem cells. *Stem Cells* 25, 1940–1953.
- Kaestner, K.H. (2005). The making of the liver: Developmental competence in foregut endoderm and induction of the hepatogenic program. *Cell Cycle* 4, 1146–1148.
- Kajiwar, M., Aoi, T., Okita, K., Takahashi, R., Inoue, H., Takayama, N., Endo, H., Eto, K., Toguchida, J., Uemoto, S., et al. (2012). Donor-dependent variations in hepatic differentiation from human-induced pluripotent stem cells. *Proc. Natl. Acad. Sci.* 109, 12538–12543.
- Kakisaka, K., Cazanave, S.C., Fingas, C.D., Guicciardi, M.E., Bronk, S.F., Werneburg, N.W., Mott, J.L., and Gores, G.J. (2012). Mechanisms of lysophosphatidylcholine-induced hepatocyte lipoapoptosis. *AJP Gastrointest. Liver Physiol.* 302, G77–G84.
- Kamada, N., Kawashima, H., Sakuradani, E., Akimoto, K., Ogawa, U., and Shimizu, S. (1999). Production of 8,11-cis-eicosadienoic acid by a delta 5 and delta 12 desaturase-defective mutant derived from the arachidonic acid-producing fungus *Mortierella alpina* 1S-4. *J. Am. Oil Chem. Soc.* 76, 1269–1274.
- Kamiya, A., Kinoshita, T., Ito, Y., Matsui, T., Morikawa, Y., Senba, E., Nakashima, K., Taga, T., Yoshida, K., Kishimoto, T., et al. (1999). Fetal liver development requires a



- paracrine action of oncostatin M through the gp130 signal transducer. *EMBO J.* 18, 2127–2136.
- Kang, S.J., Park, Y. Il, Hwang, S.R., Yi, H., Tham, N., Ku, H.O., Song, J.Y., and Kang, H.G. (2017). Hepatic population derived from human pluripotent stem cells is effectively increased by selective removal of undifferentiated stem cells using YM155. *Stem Cell Res. Ther.* 8, doi: 10.1186/s13287-017-0517-2.
- Kia, R., Sison, R.L.C., Heslop, J., Kitteringham, N.R., Hanley, N., Mills, J.S., Park, B.K., and Goldring, C.E.P. (2012). Stem cell-derived hepatocytes as a predictive model for drug-induced liver injury: Are we there yet? *Br. J. Clin. Pharmacol.* 75, 885–896.
- Kim, Y., and Rajagopalan, P. (2010). 3D hepatic cultures simultaneously maintain primary hepatocyte and liver sinusoidal endothelial cell phenotypes. *PLoS One* 5, e15456.
- Kim, H.R., Roe, J.S., Lee, J.E., Cho, E.J., and Youn, H.D. (2013). P53 regulates glucose metabolism by miR-34a. *Biochem. Biophys. Res. Commun.* 437, 225–231.
- Kim, K., Zhao, R., Doi, A., Ng, K., Unternaehrer, J., Cahan, P., Hongguang, H., Loh, Y.H., Aryee, M.J., Lensch, M.W., et al. (2011). Donor cell type can influence the epigenome and differentiation potential of human induced pluripotent stem cells. *Nat. Biotechnol.* 29, 1117–1119.
- Kim, M.H., Kim, M.O., Kim, Y.H., Kim, J.S., and Han, H.J. (2009). Linoleic acid induces mouse embryonic stem cell proliferation via Ca<sup>2+</sup>/PKC, PI3K/Akt, and MAPKs. *Cell. Physiol. Biochem.* 23, 53–64.
- Kim, W.J., Okimoto, R.A., Purton, L.E., Goodwin, M., Haserlat, S.M., Dayyan, F., Sweetser, D.A., McClatchey, A.I., Bernard, O.A., Look, A.T., et al. (2008). Mutations in the neutral sphingomyelinase gene *Smpd3* implicate the ceramide pathway in human leukemias. *Blood* 111, 4716–4722.
- Krueger, W.H., Tanasijevic, B., Barber, V., Flamier, A., Gu, X., Manautou, J., and Rasmussen, T.P. (2013). Cholesterol-secreting and statin-responsive hepatocytes from human ES and iPS cells to model hepatic involvement in cardiovascular health. *PLoS One* 8, e67296.
- Kruitwagen, H.S., Oosterhoff, L.A., Vernooij, I.G.W.H., Schroll, I.M., van Wolferen, M.E., Bannink, F., Roesch, C., van Uden, L., Molenaar, M.R., Helms, J.B., et al. (2017). Long-term adult feline liver organoid cultures for disease modeling of hepatic steatosis. *Stem Cell Reports* 8, 822–830.
- Kubo, A. (2004). Development of definitive endoderm from embryonic stem cells in culture. *Development* 131, 1651–1662.
- Kvilekval, K., Lin, J., Cheng, W., and Abumrad, N. (1994). Fatty acids as determinants of triglyceride and cholesteryl ester synthesis by isolated hepatocytes: kinetics as a function of various fatty acids. *J. Lipid Res.* 35, 1786–1794.
- Lade, A.G., and Monga, S.P.S. (2011). Beta-catenin signaling in hepatic development and progenitors: Which way does the WNT blow? *Dev. Dyn.* 240, 486–500.
- Lauschke, V.M., Vorrink, S.U., Moro, S.M.L., Rezayee, F., Nordling, Å., Hendriks, D.F.G., Bell, C.C., Sison-Young, R., Park, B.K., Goldring, C.E., et al. (2016). Massive rearrangements of cellular MicroRNA signatures are key drivers of hepatocyte dedifferentiation. *Hepatology* 64, 1743–1756.
- Laviad, E.L., Albee, L., Pankova-Kholmyansky, I., Epstein, S., Park, H., Merrill, A.H., and Futerman, A.H. (2008). Characterization of ceramide synthase 2: Tissue distribution, substrate specificity, and inhibition by sphingosine 1-phosphate. *J. Biol. Chem.* 283, 5677–5684.



- Leamy, A.K., Egnatchik, R.A., and Young, J.D. (2013). Molecular mechanisms and the role of saturated fatty acids in the progression of non-alcoholic fatty liver disease. *Prog Lipid Res* 52, 165–174.
- Leung, A., Nah, S.K., Reid, W., Ebata, A., Koch, C.M., Monti, S., Genereux, J.C., Wiseman, R.L., Wolozin, B., Connors, L.H., et al. (2013). Induced pluripotent stem cell modeling of multisystemic, hereditary transthyretin amyloidosis. *Stem Cell Reports* 1, 451–463.
- Leventis, P.A., and Grinstein, S. (2010). The Distribution and Function of Phosphatidylserine in Cellular Membranes. *Annu. Rev. Biophys.* 39, 407–427.
- Levy, M., and Futerman, A.H. (2010). Mammalian ceramide synthases. *IUBMB Life* 62, 347–356.
- Li, J., Ning, G., and Duncan, S.A. (2000). Mammalian hepatocyte differentiation requires the transcription factor HNF-4. *Genes Dev.* 14, 464–474.
- Li, Z., Hailemariam, T.K., Zhou, H., Li, Y., Duckworth, D.C., Peake, D.A., Zhang, Y., Kuo, M.S., Cao, G., and Jiang, X.C. (2007). Inhibition of sphingomyelin synthase (SMS) affects intracellular sphingomyelin accumulation and plasma membrane lipid organization. *Biochim. Biophys. Acta - Mol. Cell Biol. Lipids* 1771, 1186–1194.
- Ling, J., Lewis, J., Douglas, D., Kneteman, N.M., and Vance, D.E. (2013). Characterization of lipid and lipoprotein metabolism in primary human hepatocytes. *Biochim. Biophys. Acta* 1831, 387–397.
- Liscum, L. (2008). Cholesterol Synthesis. In *Biochemistry of Lipids, Lipoproteins and Membranes*, J. Vance, and D. Vance, eds. (Amsterdam: Elsevier Science), pp. 399–421.
- Lund, R.J., Nikula, T., Rahkonen, N., Närvä, E., Baker, D., Harrison, N., Andrews, P., Otonkoski, T., and Lahesmaa, R. (2012). High-throughput karyotyping of human pluripotent stem cells. *Stem Cell Res.* 9, 192–195.
- Ma, X., Qu, X., Zhu, W., Li, Y.-S., Yuan, S., Zhang, H., Liu, J., Wang, P., Lai, C.S.E., Zanella, F., et al. (2016). Deterministically patterned biomimetic human iPSC-derived hepatic model via rapid 3D bioprinting. *Proc. Natl. Acad. Sci.* 113, 2206–2211.
- Maceyka, M., and Spiegel, S. (2014). Sphingolipid metabolites in inflammatory disease. *Nature* 510, 58–67.
- Malinen, M.M., Kanninen, L.K., Corlu, A., Isoniemi, H.M., Lou, Y.R., Yliperttula, M.L., and Urtti, A.O. (2014). Differentiation of liver progenitor cell line to functional organotypic cultures in 3D nanofibrillar cellulose and hyaluronan-gelatin hydrogels. *Biomaterials* 35, 5110–5121.
- Mallanna, S.K., and Duncan, S.A. (2013). Differentiation of hepatocytes from pluripotent stem cells. *Curr. Protoc. Stem Cell Biol.* 366, 89–99.
- Manzini, S., Viiri, L.E., Marttila, S., and Aalto-Setälä, K. (2015). A comparative view on easy to deploy non-integrating methods for patient-specific iPSC production. *Stem Cell Rev. Reports* 11, 900–908.
- Mao, C., and Obeid, L.M. (2008). Ceramidases: regulators of cellular responses mediated by ceramide, sphingosine, and sphingosine-1-phosphate. *Biochim. Biophys. Acta - Mol. Cell Biol. Lipids* 1781, 424–434.
- Marsh, D. (2007). Lateral pressure profile, spontaneous curvature frustration, and the incorporation and conformation of proteins in membranes. *Biophys. J.* 93, 3884–3899.
- Martin, S., and Parton, R.G. (2006). Lipid droplets: a unified view of a dynamic organelle. *Mol. Cell* 7, 373–378.

- Martinez Barbera, J.P., Clements, M., Thomas, P., Rodriguez, T., Meloy, D., Kioussis, D., and Beddington, R.S. (2000). The homeobox gene *Hex* is required in definitive endodermal tissues for normal forebrain, liver and thyroid formation. *Development* 127, 2433–2445.
- McClelland, R., Wauthier, E., Uronis, J., and Reid, L. (2008). Gradients in the liver's extracellular matrix chemistry from periportal to pericentral zones: influence on human hepatic progenitors. *Tissue Eng. Part A* 14, 59–70.
- Medico, E., Gentile, A., Celso, C.L., Williams, T.A., Gambarotta, G., Trusolino, L., and Comoglio, P.M. (2001). Osteopontin is an autocrine mediator of hepatocyte growth factor-induced invasive growth. *Cancer Res.* 61, 5861–5868.
- Medine, C.N., Lucendo-Villarin, B., Storck, C., Wang, F., Szkolnicka, D., Khan, F., Pernagallo, S., Black, J.R., Marriage, H.M., Ross, J.A., et al. (2013). Developing high-fidelity hepatotoxicity models from pluripotent stem cells. *Stem Cells Transl. Med.* 2, 505–509.
- Van Meer, G. (2005). Cellular lipidomics. *EMBO J.* 24, 3159–3165.
- Van Meer, G., Voelker, D.R., and Feigenson, G.W. (2008). Membrane lipids: where they are and how they behave. *Nat. Rev. Mol. Cell Biol.* 9, 112–124.
- Meex, S.J.R., Andreo, U., Sparks, J.D., and Fisher, E.A. (2011). Huh-7 or HepG2 cells: which is the better model for studying human apolipoprotein-B100 assembly and secretion? *J. Lipid Res.* 52, 152–158.
- Meikle, P.J., Wong, G., Tsorotes, D., Barlow, C.K., Weir, J.M., Christopher, M.J., MacIntosh, G.L., Goudey, B., Stern, L., Kowalczyk, A., et al. (2011). Plasma lipidomic analysis of stable and unstable coronary artery disease. *Arterioscler. Thromb. Vasc. Biol.* 31, 2723–2732.
- Merrill, A.H., Sullards, M.C., Allegood, J.C., Kelly, S., and Wang, E. (2005). Sphingolipidomics: high-throughput, structure-specific, and quantitative analysis of sphingolipids by liquid chromatography tandem mass spectrometry. *Methods* 36, 207–224.
- Mesicek, J., Lee, H., Feldman, T., Jiang, X., Skobeleva, A., Berdyshev, E. V., Haimovitz-Friedman, A., Fuks, Z., and Kolesnick, R. (2010). Ceramide synthases 2, 5, and 6 confer distinct roles in radiation-induced apoptosis in HeLa cells. *Cell. Signal.* 22, 1300–1307.
- Messner, S., Agarkova, I., Moritz, W., and Kelm, J.M. (2013). Multi-cell type human liver microtissues for hepatotoxicity testing. *Arch. Toxicol.* 87, 209–213.
- Michalopoulos, G.K., Bowen, W.C., Mule, K., and Luo, J. (2003). HGF-, EGF-, and dexamethasone-induced gene expression patterns during formation of tissue in hepatic organoid cultures. *Gene Expr.* 11, 55–75.
- Montagner, A., Rando, G., Degueurce, G., Leuenberger, N., Michalik, L., and Wahli, W. (2011). New insights into the role of PPARs. *Prostaglandins Leukot. Essent. Fat. Acids* 85, 235–243.
- Morales, A., Lee, H., Goñi, F.M., Kolesnick, R., and Fernandez-Checa, J.C. (2007). Sphingolipids and cell death. *Apoptosis* 12, 923–939.
- Muro, E., Atilla-Gokcumen, G.E., and Eggert, U.S. (2014). Lipids in cell biology: how can we understand them better? *Mol. Biol. Cell* 25, 1819–1823.
- Nagamoto, Y., Tashiro, K., Takayama, K., Ohashi, K., Kawabata, K., Sakurai, F., Tachibana, M., Hayakawa, T., Furue, M.K., and Mizuguchi, H. (2012). The promotion of hepatic maturation of human pluripotent stem cells in 3D co-culture using type I collagen and Swiss 3T3 cell sheets. *Biomaterials* 33, 4526–4534.

- Nantasanti, S., Spee, B., Kruitwagen, H.S., Chen, C., Geijsen, N., Oosterhoff, L.A., Van Wolferen, M.E., Pelaez, N., Fieten, H., Wubbolts, R.W., et al. (2015). Disease modeling and gene therapy of copper storage disease in canine hepatic organoids. *Stem Cell Reports* 5, 895–907.
- Nejak-Bowen, K., and Monga, S.P.S. (2008). Wnt/ $\beta$ -catenin signaling in hepatic organogenesis. *Organogenesis* 4, 92–99.
- Newman, A.M., and Cooper, J.B. (2010). Lab-specific gene expression signatures in pluripotent stem cells. *Cell Stem Cell* 7, 258–262.
- Ng, S., Schwartz, R.E., March, S., Galstian, A., Gural, N., Shan, J., Prabhu, M., Mota, M.M., and Bhatia, S.N. (2015). Human iPSC-derived hepatocyte-like cells support plasmodium liver-stage infection in vitro. *Stem Cell Reports* 4, 348–359.
- No, D.Y., Lee, S.A., Choi, Y.Y., Park, D.Y., Jang, J.Y., Kim, D.S., Lee, S.H., and Johnson, R. (2012). Functional 3D human primary hepatocyte spheroids made by co-culturing hepatocytes from partial hepatectomy specimens and human adipose-derived stem cells. *PLoS One* 7, e50723.
- Novák, J., Olejníčková, V., Tkáčová, N., and Santulli, G. (2015). Mechanistic role of microRNAs in coupling lipid metabolism and atherosclerosis. In *Advances in Experimental Medicine and Biology*, G. Santulli, ed. (Springer, Cham), pp. 79–100.
- Ntambi, J.M. (1999). Regulation of stearoyl-CoA desaturase by polyunsaturated fatty acids and cholesterol. *J Lipid Res* 40, 1549–1558.
- Ntambi, J.M., and Miyazaki, M. (2004). Regulation of stearoyl-CoA desaturases and role in metabolism. *Prog. Lipid Res.* 43, 91–104.
- Oda, Y., Nakajima, M., Tsuneyama, K., Takamiya, M., Aoki, Y., Fukami, T., and Yokoi, T. (2014). Retinoid X receptor  $\alpha$  in human liver is regulated by miR-34a. *Biochem. Pharmacol.* 90, 179–187.
- Oh, D.Y., Talukdar, S., Bae, E.J., Imamura, T., Morinaga, H., Fan, W.Q., Li, P., Lu, W.J., Watkins, S.M., and Olefsky, J.M. (2010). GPR120 Is an omega-3 fatty acid receptor mediating potent anti-inflammatory and insulin-sensitizing effects. *Cell* 142, 687–698.
- Ohnuki, M., Takahashi, K., and Yamanaka, S. (2009). Generation and characterization of human induced pluripotent stem cells. In *Current Protocols in Stem Cell Biology*, T. Schlaeger, ed. (John Wiley & Sons, Inc.), p. Chapter 4: Unit 4A.2.1–4A.2.25.
- Olsavsky, K.M., Page, J.L., Johnson, M.C., Zarbl, H., Strom, S.C., and Omiecinski, C.J. (2007). Gene expression profiling and differentiation assessment in primary human hepatocyte cultures, established hepatoma cell lines, and human liver tissues. *Toxicol. Appl. Pharmacol.* 222, 42–56.
- Ørom, U.A., Nielsen, F.C., and Lund, A.H. (2008). MicroRNA-10a binds the 5'UTR of ribosomal protein mRNAs and enhances their translation. *Mol. Cell* 30, 460–471.
- Park, J.W., Park, W.J., and Futerman, A.H. (2014). Ceramide synthases as potential targets for therapeutic intervention in human diseases. *Biochim. Biophys. Acta - Mol. Cell Biol. Lipids* 1841, 671–681.
- Parviz, F., Matullo, C., Garrison, W.D., Savatski, L., Adamson, J.W., Ning, G., Kaestner, K.H., Rossi, J.M., Zaret, K.S., and Duncan, S.A. (2003). Hepatocyte nuclear factor 4 alpha controls the development of a hepatic epithelium and liver morphogenesis. *Nat. Genet.* 34, 292–296.
- Peters, D.T., Henderson, C.A., Warren, C.R., Friesen, M., Xia, F., Becker, C.E., Musunuru, K., and Cowan, C.A. (2016). Asialoglycoprotein receptor 1 is a specific cell-surface marker for isolating hepatocytes derived from human pluripotent stem cells. *Development* 143, 1475–1481.

- Pomorski, T., and Menon, A.K. (2006). Lipid flippases and their biological functions. *Cell. Mol. Life Sci.* 63, 2908–2921.
- Puzio-Kuter, A.M. (2011). The role of p53 in metabolic regulation. *Genes Cancer* 2, 385–391.
- Ramasamy, T.S., Yu, J.S.L., Selden, C., Hodgson, H., and Cui, W. (2013). Application of three-dimensional culture conditions to human embryonic stem cell-derived definitive endoderm cells enhances hepatocyte differentiation and functionality. *Tissue Eng. Part A* 19, 360–367.
- Rasmussen, T.P. (2015). Genomic medicine and lipid metabolism: LDL targets and stem cell research approaches. In *Translational Cardiometabolic Genomic Medicine*, A. Rodriguez-Oquendo, ed. (Academic Press), pp. 99–118.
- Rawicz, W., Smith, B.A., McIntosh, T.J., Simon, S.A., and Evans, E. (2008). Elasticity, strength, and water permeability of bilayers that contain raft microdomain-forming lipids. *Biophys. J.* 94, 4725–4736.
- Reyes, R.K., Motiwala, T., and Jacob, S.T. (2014). Regulation of glucose metabolism in hepatocarcinogenesis by MicroRNAs. *Gene Expr.* 16, 85–92.
- Rodgers, J.T., and Puigserver, P. (2007). Fasting-dependent glucose and lipid metabolic response through hepatic sirtuin 1. *Proc. Natl. Acad. Sci. U. S. A.* 104, 12861–12866.
- Rong, X., Wang, B., Dunham, M.M., Hedde, P.N., Iklas, Wong, J.S., Gratton, E., Young, S.G., Ford, D.A., and Tontonoz, P. (2015). Lpcat3-dependent production of arachidonoyl phospholipids is a key determinant of triglyceride secretion. *Elife* 4, doi: 10.7554/eLife.06557.
- Rossi, J.M., Dunn, N.R., Hogan, B.L.M., and Zaret, K.S. (2001). Distinct mesodermal signals, including BMPs from the septum, transversum mesenchyme, are required in combination for hepatogenesis from the endoderm. *Genes Dev.* 15, 1998–2009.
- Rouhani, F., Kumasaka, N., de Brito, M.C., Bradley, A., Vallier, L., and Gaffney, D. (2014). Genetic background drives transcriptional variation in human induced pluripotent stem cells. *PLoS Genet* 10, e1004432.
- Rowe, C., Goldring, C.E.P., Kitteringham, N.R., Jenkins, R.E., Lane, B.S., Sanderson, C., Elliott, V., Platt, V., Metcalfe, P., and Park, B.K. (2010). Network analysis of primary hepatocyte dedifferentiation using a shotgun proteomics approach. *J. Proteome Res.* 9, 2658–2668.
- Ruhanen, H., Nidhina Haridas, P.A., Eskelinen, E.L., Eriksson, O., Olkkonen, V.M., and Käkälä, R. (2017). Depletion of TM6SF2 disturbs membrane lipid composition and dynamics in HuH7 hepatoma cells. *Biochim. Biophys. Acta - Mol. Cell Biol. Lipids* 1862, 676–685.
- Ruiz, S., Diep, D., Goreb, A., Panopoulos, A.D., Montserrat, N., Plongthongkum, N., Kumar, S., Fung, H.-L., Giorgetti, A., Bilic, J., et al. (2012). Identification of a specific reprogramming-associated epigenetic signature in human induced pluripotent stem cells. *Proc Natl Acad Sci U S A* 109, 16196–16201.
- Saddoughi, S.A., Song, P., and Ogretmen, B. (2008). Roles of bioactive sphingolipids in cancer biology and therapeutics. *Subcell. Biochem.* 49, 413–440.
- Sahi, J., Grepper, S., and Smith, C. (2010). Hepatocytes as a tool in drug metabolism, transport and safety evaluations in drug discovery. *Curr. Drug Discov. Technol.* 7, 188–198.
- Santangelo, L., Marchetti, A., Cicchini, C., Conigliaro, A., Conti, B., Mancone, C., Bonzo, J.A., Gonzalez, F.J., Alonzi, T., Amicone, L., et al. (2011). The stable repression of

- mesenchymal program is required for hepatocyte identity: A novel role for hepatocyte nuclear factor 4 $\alpha$ . *Hepatology* 53, 2063–2074.
- Santos, N.C., Figueira-Coelho, J., Martins-Silva, J., and Saldanha, C. (2003). Multidisciplinary utilization of dimethyl sulfoxide: Pharmacological, cellular, and molecular aspects. *Biochem. Pharmacol.* 65, 1035–1041.
- Sasaki, A., Kimura, F., Miura, M., Toshima, G., Takahashi, J., Maruya, S., Kobayashi, M., and Hata, K. (2017). Lipoprotein profiles of hepatic cell lines at various stages of differentiation. *Vitr. Cell. Dev. Biol. - Anim.* 53, 93–95.
- Schmiedel, J.M., Klemm, S.L., Zheng, Y., Sahay, A., Blüthgen, N., Marks, D.S., and Van Oudenaarden, A. (2015). MicroRNA control of protein expression noise. *Science* (80-). 348, 128–131.
- Schwartz, R.E., Trehan, K., Andrus, L., Sheahan, T.P., Ploss, A., Duncan, S.A., Rice, C.M., and Bhatia, S.N. (2012). Modeling hepatitis C virus infection using human induced pluripotent stem cells. *Proc. Natl. Acad. Sci. U. S. A.* 109, 2544–2548.
- Schwartz, R.E., Fleming, H.E., Khetani, S.R., and Bhatia, S.N. (2014). Pluripotent stem cell-derived hepatocyte-like cells. *Biotechnol. Adv.* 32, 504–513.
- Schyschka, L., Sánchez, J.J.M., Wang, Z., Burkhardt, B., Müller-Vieira, U., Zeilinger, K., Bachmann, A., Nadalin, S., Damm, G., and Nussler, A.K. (2013). Hepatic 3D cultures but not 2D cultures preserve specific transporter activity for acetaminophen-induced hepatotoxicity. *Arch. Toxicol.* 87, 1581–1593.
- Shirasaki, T., Honda, M., Shimakami, T., Horii, R., Yamashita, T., Sakai, Y., Sakai, A., Okada, H., Watanabe, R., Murakami, S., et al. (2013). MicroRNA-27a regulates lipid metabolism and inhibits hepatitis C virus replication in human hepatoma cells. *J Virol* 87, 5270–5286.
- Shomron, N., and Levy, C. (2009). MicroRNA-biogenesis and pre-mRNA splicing crosstalk. *J. Biomed. Biotechnol.* 2009, doi: 10.1155/2009/594678.
- Si-Tayeb, K., Noto, F.K., Nagaoka, M., Li, J., Battle, M.A., Duris, C., North, P.E., Dalton, S., and Duncan, S.A. (2010a). Highly efficient generation of human hepatocyte-like cells from induced pluripotent stem cells. *Hepatology* 51, 297–305.
- Si-Tayeb, K., Lemaigre, F.P., and Duncan, S.A. (2010b). Organogenesis and development of the liver. *Dev. Cell* 18, 175–189.
- Simeonov, K.P., and Uppal, H. (2014). Direct reprogramming of human fibroblasts to hepatocyte-like cells by synthetic modified mRNAs. *PLoS One* 9, e100134.
- Simons, K., and Gerl, M.J. (2010). Revitalizing membrane rafts: New tools and insights. *Nat. Rev. Mol. Cell Biol.* 11, 688–699.
- Sivertsson, L., Ek, M., Darnell, M., Edebert, I., Ingelman-Sundberg, M., and Neve, E.P.A. (2010). CYP3A4 catalytic activity is induced in confluent Huh7 hepatoma cells. *Drug Metab. Dispos.* 38, 995–1002.
- Skardal, A., Devarasetty, M., Soker, S., and Hall, A.R. (2015). In situ patterned micro 3D liver constructs for parallel toxicology testing in a fluidic device. *Biofabrication* 7, 031001.
- Sprecher, H. (2000). Metabolism of highly unsaturated n-3 and n-6 fatty acids. *Biochim. Biophys. Acta - Mol. Cell Biol. Lipids* 1486, 219–231.
- Steenbergen, R., Oti, M., ter Horst, R., Tat, W., Neufeldt, C., Belovodskiy, A., Chua, T.T., Cho, W.J., Joyce, M., Dutilh, B.E., et al. (2018). Establishing normal metabolism and differentiation in hepatocellular carcinoma cells by culturing in adult human serum. *Sci. Rep.* 8, doi: 10.1038/s41598-018-29763-2.



- Stübiger, G., Aldover-Macasaet, E., Bicker, W., Sobal, G., Willfort-Ehringer, A., Pock, K., Bochkov, V., Widhalm, K., and Belgacem, O. (2012). Targeted profiling of atherogenic phospholipids in human plasma and lipoproteins of hyperlipidemic patients using MALDI-QIT-TOF-MS/MS. *Atherosclerosis* 224, 177–186.
- Sullivan, G.J., Hay, D.C., Park, I.-H., Fletcher, J., Hannoun, Z., Payne, C.M., Dalgetty, D., Black, J.R., Ross, J.A., Samuel, K., et al. (2010). Generation of functional human hepatic endoderm from human induced pluripotent stem cells. *Hepatology* 51, 329–335.
- Swift, B., Pfeifer, N.D., and Brouwer, K.L.R. (2010). Sandwich-cultured hepatocytes: An in vitro model to evaluate hepatobiliary transporter-based drug interactions and hepatotoxicity. *Drug Metab. Rev.* 42, 446–471.
- Szkolnicka, D., Farnworth, S.L., Lucendo-Villarin, B., Storck, C., Zhou, W., Iredale, J.P., Flint, O., and Hay, D.C. (2014). Accurate prediction of drug-induced liver injury using stem cell-derived populations. *Stem Cells Transl. Med.* 3, 141–148.
- Takagi, S., Nakajima, M., Kida, K., Yamaura, Y., Fukami, T., and Yokoi, T. (2010). MicroRNAs regulate human hepatocyte nuclear factor 4alpha, modulating the expression of metabolic enzymes and cell cycle. *J. Biol. Chem.* 285, 4415–4422.
- Takahashi, K., Tanabe, K., Ohnuki, M., Narita, M., Ichisaka, T., Tomoda, K., and Yamanaka, S. (2007). Induction of pluripotent stem cells from adult human fibroblasts by defined factors. *Cell* 131, 861–872.
- Takayama, K., Inamura, M., Kawabata, K., Sugawara, M., Kikuchi, K., Higuchi, M., Nagamoto, Y., Watanabe, H., Tashiro, K., Sakurai, F., et al. (2012). Generation of metabolically functioning hepatocytes from human pluripotent stem cells by FOXA2 and HNF1 $\alpha$  transduction. *J. Hepatol.* 57, 628–636.
- Takayama, K., Kawabata, K., Nagamoto, Y., Kishimoto, K., Tashiro, K., Sakurai, F., Tachibana, M., Kanda, K., Hayakawa, T., Furue, M.K., et al. (2013). 3D spheroid culture of hESC/hiPSC-derived hepatocyte-like cells for drug toxicity testing. *Biomaterials* 34, 1781–1789.
- Takebe, T., Zhang, R.R., Koike, H., Kimura, M., Yoshizawa, E., Enomura, M., Koike, N., Sekine, K., and Taniguchi, H. (2014). Generation of a vascularized and functional human liver from an iPSC-derived organ bud transplant. *Nat. Protoc.* 9, 396–409.
- Tostões, R.M., Leite, S.B., Serra, M., Jensen, J., Björquist, P., Carrondo, M.J.T., Brito, C., and Alves, P.M. (2012). Human liver cell spheroids in extended perfusion bioreactor culture for repeated-dose drug testing. *Hepatology* 55, 1227–1236.
- Tremblay, K.D., and Zaret, K.S. (2005). Distinct populations of endoderm cells converge to generate the embryonic liver bud and ventral foregut tissues. *Dev. Biol.* 280, 87–99.
- Treyer, A., and Müsch, A. (2013). Hepatocyte polarity. *Compr. Physiol.* 3, 243–287.
- Uhl, E.W., and Warner, N.J. (2015). Mouse Models as Predictors of Human Responses: Evolutionary Medicine. *Curr. Pathobiol. Rep.* 3, 219–223.
- Vasconcellos, R., Alvarenga, É.C., Parreira, R.C., Lima, S.S., and Resende, R.R. (2016). Exploring the cell signalling in hepatocyte differentiation. *Cell. Signal.* 28, 1773–1788.
- van der Veen, J.N., Kennelly, J.P., Wan, S., Vance, J.E., Vance, D.E., and Jacobs, R.L. (2017). The critical role of phosphatidylcholine and phosphatidylethanolamine metabolism in health and disease. *Biochim. Biophys. Acta - Biomembr.* 1859, 1558–1572.
- Vellonen, K.-S., Malinen, M., Mannermaa, E., Subrizi, A., Toropainen, E., Yan-Ru, L., Kidron, H., Yliperttula, M., and Urtti, A. (2014). A critical assessment of in vitro tissue models for ADME and drug delivery. *J Control Release* 190, 94–114.

- Vincent, S.D., Dunn, N.R., Hayashi, S., Norris, D.P., and Robertson, E.J. (2003). Cell fate decisions within the mouse organizer are governed by graded Nodal signals. *Genes Dev.* 17, 1646–1662.
- Wandzioch, E., and Zaret, K.S. (2009). Dynamic signaling network for the specification of embryonic pancreas and liver progenitors. *Science* (80-. ). 324, 1707–1710.
- Wang, B., Hsu, S.H., Frankel, W., Ghoshal, K., and Jacob, S.T. (2012). Stat3-mediated activation of microRNA-23a suppresses gluconeogenesis in hepatocellular carcinoma by down-regulating Glucose-6-phosphatase and peroxisome proliferator-activated receptor gamma, coactivator 1 alpha. *Hepatology* 56, 186–197.
- Wassall, S.R., Brzustowicz, M.R., Shaikh, S.R., Cherezov, V., Caffrey, M., and Stillwell, W. (2004). Order from disorder, corralling cholesterol with chaotic lipids: The role of polyunsaturated lipids in membrane raft formation. *Chem. Phys. Lipids* 132, 79–88.
- Wells, J.M., and Melton, D.A. (1999). Vertebrate endoderm development. *Annu. Rev. Cell Dev. Biol.* 15, 393–410.
- Westerink, W.M.A., and Schoonen, W.G.E.J. (2007). Cytochrome P450 enzyme levels in HepG2 cells and cryopreserved primary human hepatocytes and their induction in HepG2 cells. *Toxicol. Vitro* 21, 1581–1591.
- Yang, Z., Cappello, T., and Wang, L. (2015). Emerging role of microRNAs in lipid metabolism. *Acta Pharm. Sin. B* 5, 145–150.
- Ye, X., Li, M., Hou, T., Gao, T., Zhu, W., and Yang, Y. (2017). Sirtuins in glucose and lipid metabolism. *Oncotarget* 8, 1845–1859.
- Ying, Q.-L., Wray, J., Nichols, J., Batlle-Morera, L., Doble, B., Woodgett, J., Cohen, P., and Smith, A. (2008). The ground state of embryonic stem cell self-renewal. *Nature* 453, 519–523.
- Younossi, Z.M., Koenig, A.B., Abdelatif, D., Fazel, Y., Henry, L., and Wymer, M. (2016). Global epidemiology of non-alcoholic fatty liver disease-Meta-analytic assessment of prevalence, incidence and outcomes. *Hepatology* 64, 73–84.
- Zaret, K.S. (2002). Regulatory phases of early liver development: Paradigms of organogenesis. *Nat. Rev. Genet.* 3, 499–512.
- Zeilinger, K., Freyer, N., Damm, G., Seehofer, D., and Knöspel, F. (2016). Cell sources for in vitro human liver cell culture models. *Exp. Biol. Med.* 241, 1684–1698.
- Zhang, M., Sun, W., Zhou, M., and Tang, Y. (2017). MicroRNA-27a regulates hepatic lipid metabolism and alleviates NAFLD via repressing FAS and SCD1. *Sci. Rep.* 7, 1–10.
- Zhong, L., Gou, J., Deng, N., Shen, H., He, T., and Zhang, B.Q. (2015). Three-dimensional Co-culture of hepatic progenitor cells and mesenchymal stem cells in vitro and in vivo. *Microsc. Res. Tech.* 78, 688–696.
- Zhou, X., Sun, P., Lucendo-Villarin, B., Angus, A.G.N., Szkolnicka, D., Cameron, K., Farnworth, S.L., Patel, A.H., and Hay, D.C. (2014). Modulating innate immunity improves hepatitis C virus infection and replication in stem cell-derived hepatocytes. *Stem Cell Reports* 3, 204–214.





## ORIGINAL PUBLICATIONS



# PUBLICATION I

## **Lipidomic profiling of patient-specific iPSC-derived hepatocyte-like cells**

Kiamehr M, Viiri L, Vihervaara T, Koistinen K, Hilvo M, Ekroos K, Käkälä R,  
Aalto-Setälä K.

Disease Models & Mechanisms. 2017; 10:1141-1153  
doi: 10.1242/dmm.030841

**Publication reprinted with the permission of the copyright holders.**



## RESOURCE ARTICLE

# Lipidomic profiling of patient-specific iPSC-derived hepatocyte-like cells

Mostafa Kiamehr<sup>1,\*‡</sup>, Leena E. Viiri<sup>1,\*</sup>, Terhi Vihervaara<sup>2</sup>, Kaisa M. Koistinen<sup>2</sup>, Mika Hilvo<sup>2</sup>, Kim Ekroos<sup>2</sup>, Reijo Käkälä<sup>3</sup> and Katriina Aalto-Setälä<sup>1,4</sup>

## ABSTRACT

Hepatocyte-like cells (HLCs) differentiated from human induced pluripotent stem cells (iPSCs) offer an alternative model to primary human hepatocytes to study lipid aberrations. However, the detailed lipid profile of HLCs is yet unknown. In the current study, functional HLCs were differentiated from iPSCs generated from dermal fibroblasts of three individuals by a three-step protocol through the definitive endoderm (DE) stage. In parallel, detailed lipidomic analyses as well as gene expression profiling of a set of lipid-metabolism-related genes were performed during the entire differentiation process from iPSCs to HLCs. Additionally, fatty acid (FA) composition of the cell culture media at different stages was determined. Our results show that major alterations in the molecular species of lipids occurring during DE and early hepatic differentiation stages mainly mirror the quality and quantity of the FAs supplied in culture medium at each stage. Polyunsaturated phospholipids and sphingolipids with a very long FA were produced in the cells at a later stage of differentiation. This work uncovers the previously unknown lipid composition of iPSC-HLCs and its alterations during the differentiation in conjunction with the expression of key lipid-associated genes. Together with biochemical, functional and gene expression measurements, the lipidomic analyses allowed us to improve our understanding of the concerted influence of the exogenous metabolite supply and cellular biosynthesis essential for iPSC-HLC differentiation and function. Importantly, the study describes in detail a cell model that can be applied in exploring, for example, the lipid metabolism involved in the development of fatty liver disease or atherosclerosis.

**KEY WORDS:** Induced pluripotent stem cell, iPSC, Hepatocyte-like cell, HLC, Differentiation, Cell model, Lipidomics, Fatty acid

## INTRODUCTION

The liver is the main metabolic and synthetic organ in the human body, carrying out more than 500 different functions. It is mainly composed of hepatocytes, which constitute approximately 60% of the cells in the liver and possess many important functions.

Hepatocytes produce the majority of circulating plasma proteins, including transporters (such as albumin and lipoproteins), protease inhibitors ( $\alpha$ 1-antitrypsin, antithrombin and  $\alpha$ 2-macroglobulin), blood coagulation factors, and modulators of immune complexes and inflammation (complement C3, C-reactive protein). Hepatocytes also control the homeostasis of energy/fuel molecules such as glucose/glycogen and fatty acids (FAs) as well as other essential compounds of lipid metabolism such as cholesterol and bile acids. Additionally, liver has a central role in lipid metabolism as it is the major site for the generation of plasma lipoproteins (Godoy et al., 2013).

The use of hepatocytes as *in vitro* models to explore different aspects of liver function and metabolism has escalated in recent years but primary human hepatocytes (PHHs), the key *in vitro* cell type involved in e.g. cholesterol metabolism, are scarce because they are obtained from organ donors. Furthermore, when in culture the PHHs quickly dedifferentiate and lose their liver functions, thus making them impractical for modelling the liver *in vivo* (Elaut et al., 2006). Human induced pluripotent stem cell (iPSC)-derived hepatocytes provide a good alternative to PHHs because iPSCs can be easily reprogrammed from dermal fibroblasts and then differentiated into hepatocyte-like cells (HLCs), which functionally resemble PHHs (Hu and Li, 2015). iPSC-HLCs can recapitulate metabolic variations observed in the population and have proved to be potent in both short- and long-term drug screening and in investigating hepatotoxicity or developing novel therapeutics (Holmgren et al., 2014; Medine et al., 2013; Szkolnicka et al., 2014). In addition, they have been utilised for studying fetal liver exposure to harmful substances (Lucendo-Villarin et al., 2017) and in identifying noncoding micro-RNAs regulating human liver damage (Szkolnicka et al., 2016; Yang et al., 2016). Furthermore, HLCs have been successfully used in developing *in vitro* models for studying hepatic diseases such as systemic amyloidosis (Leung et al., 2013), liver-stage malaria (Ng et al., 2015) and hepatitis C viral infection (Zhou et al., 2014). iPSC-HLCs could also offer a good model for investigating basic mechanisms of e.g. lipid metabolism as well as its dysregulation related to different diseases such as fatty liver disease or atherosclerosis.

Lipids are a highly diverse class of biological molecules with crucial roles in cellular energy storage (mainly in the form of triacylglycerols), structure (e.g. key components of plasma and nuclear membranes, endoplasmic reticulum and Golgi apparatus, and trafficking vesicles like endosomes and lysosomes) and signalling (as ligands that activate signal transduction pathways as well as mediators of signalling pathways) (Van Meer et al., 2008). Furthermore, *de novo* FA synthesis in the cells has a significant impact on the acquisition and maintenance of cellular pluripotency through increased mitochondrial fission (Wang et al., 2017). Mammalian cells express tens of thousands of different lipid species and use hundreds of proteins to synthesise, metabolise and

<sup>1</sup>Faculty of Medicine and Life Sciences, University of Tampere, Tampere, 33520, Finland. <sup>2</sup>Zora Biosciences, Espoo, 02150, Finland. <sup>3</sup>Department of Biosciences, University of Helsinki, Helsinki, 00014, Finland. <sup>4</sup>Heart Hospital, Tampere University Hospital, Tampere, 33520, Finland.

\*These authors contributed equally to this work

‡Author for correspondence (mostafa.kiamehr@uta.fi)

DOI: M.K., 0000-0003-1894-3237

This is an Open Access article distributed under the terms of the Creative Commons Attribution License (<http://creativecommons.org/licenses/by/3.0/>), which permits unrestricted use, distribution and reproduction in any medium provided that the original work is properly attributed.

transport them (Muro et al., 2014). Moreover, lipid defects are central to the pathogenesis of many common diseases such as non-alcoholic fatty liver disease (Ruhanen et al., 2017; Younossi et al., 2016) or atherosclerosis (Meikle et al., 2011; Stübiger et al., 2012). However, because the cellular lipidome is highly complex and very dynamic, the study of lipids and identifying the precise underlying defects has previously been hampered by analytical limitations. This has been resolved by the emergence of advanced lipidomic technologies. Lipidomics aims to precisely define and quantitate the molecular profiles of lipids present in a cell, organism or tissue (Watson, 2006; Wenk, 2005), and provides precise quantitative snapshots of the lipidomes comprising hundreds of different molecules (Llorente et al., 2013; Sales et al., 2016). This technological advancement in conjunction with computational technologies has made this field a promising area for biomedical research (Ekroos, 2012).

In this study, we produced iPSCs from patient-derived dermal fibroblasts and differentiated them into HLCs. In total, we quantified 165 molecular species of lipids, and are the first to report a comprehensive lipidomic profile of cells during the entire differentiation process from iPSCs through the definitive endoderm (DE) stage to HLCs. We assess the occurring lipidomic alterations in relation to the variable supply of different FAs measured in the cell culture media at each stage of the differentiation. Thus, we do not overlook the comprehensive effects of the essential exogenous metabolites the cells acquire from the culture medium. Additionally, we present biochemical and functional measurements and expression of sphingolipid (SL) metabolism-related genes during HLC differentiation.

## RESULTS

### Characterisation of the iPSC lines

The three iPSC lines used in this study – UTA.10100.EURCA, UTA.11104.EURCA and UTA.11304.EURCC – were characterised in detail for their pluripotency. All three iPSC lines expressed characteristic markers of pluripotency at the protein (Fig. S1A) and gene (Fig. S1B) level, and the virally transferred exogenous pluripotency genes were silenced (Fig. S1C). The pluripotency of iPSC lines was proven *in vitro* by embryoid body (EB) formation and performing PCR to show the presence of all three germ layers (Fig. S1D). The karyotypes of all three iPSC lines were normal (Fig. S2).

### Differentiation of iPSCs to HLCs through a DE stage

We used a previously described three-step protocol (Hay et al., 2008) to produce HLCs from human iPSCs (Fig. 1A). During the differentiation process, the cells underwent morphological changes: iPSCs gradually lost their typical round and dense morphology and after migration formed spiky-shaped DE cells. During the second week of differentiation, at the hepatoblast stage, cells gradually increased in size and, as they matured during the third week, formed polygonal HLCs with distinct canalicular borders (Fig. 1B). The immunocytochemical staining at day 5 showed that cells expressed only low levels of pluripotency marker OCT3/4 but were strongly positive for the DE marker SOX17 (Fig. S3A). Furthermore, flow cytometry analyses showed that 71–96% of the cells were positive for the DE marker CXCR4 at day 5 of differentiation (Fig. S3B). These results indicated that the iPSCs had efficiently differentiated into DE during the endodermal induction step of the differentiation protocol.

Consistent with the morphological changes observed during the differentiation process (Fig. 1B), changes in gene expression were

detected (Fig. S3C). The expression of *OCT3/4* was clearly downregulated by day 5, whereas the DE marker *SOX17* was highly expressed at this stage. *FOXA2*, a transcription factor involved in liver metabolism (Wolfrum et al., 2004), had a continuous expression pattern starting around day 5 and continuing until the end of differentiation. As the cells differentiated further from DE towards HLCs, they started expressing *AFP* (around day 10, which peaked around day 15–20 depending on the cell line). Expression of *ALB*, the gene for the most abundant liver protein, increased strongly around day 15 and peaked at day 20–25 (Fig. S3C). Immunocytochemical staining further confirmed the expression of hepatic proteins at day 20 of differentiation (Fig. 1C,D). Low-density lipoprotein receptor (LDL-R), asialoglycoprotein receptor (ASGR), alpha fetoprotein (AFP) as well as albumin (ALB) were all expressed in HLCs (Fig. 1C,D). HLCs stained positive for ALB in 13, 18 and 19% of the cells differentiated from UTA.10100, UTA.11104 and UTA.11304, respectively. Both AFP and ASGR stained positive in more than 90% of HLCs in all three cell lines.

### Functionality assessment of mature HLCs

To assess the functionality of the iPSC-HLCs, we performed several experiments. Because liver is the most important organ for LDL catabolism and LDL-R activity, the ability of HLCs to uptake LDL from the culture medium was evaluated. As shown in Fig. 1E, iPSC-HLCs were able to efficiently uptake LDL. The level of secreted albumin was measured from the cell culture medium at days 14, 17, 20 and 23 of differentiation, and all the iPSC-HLCs synthesised and released albumin into the culture medium with maximum secretion at day 20 (Fig. 1F).

Apolipoprotein B (*APOB*) and apolipoprotein A-I (*APOA1*) gene expression levels of the iPSC-HLCs during the differentiation were also measured as a surrogate for estimating very low-density lipoprotein (VLDL) and high-density lipoprotein (HDL) production levels of the cells. *APOB* is the main protein component of VLDL, and the product of the *APOA1* gene is the main protein component of HDLs. The expressions of both *APOB* and *APOA1* genes rose around day 10, reached their peak at day 15 and then lowered towards the levels of expression in PHHs (Fig. 1G,H). The increasing expression of these liver-specific genes further demonstrated that the iPSCs were differentiating and maturing towards functional hepatocytes.

### Lipidomic profiling of iPSC-HLCs

We performed lipidomic profiling of the cells during the entire differentiation process from iPSCs to HLCs, and observed changes in cellular lipid content and composition. Overall, more than 160 molecular species of lipids including cholesteryl esters (CEs), diacylglycerols (DAGs), phospholipids (PLs) and SLs were detected during the course of differentiation (Table S5). The cellular contents of lipid classes (per protein) were constantly altered during the differentiation. In the beginning, the protein-normalised concentrations of the majority of lipid classes decreased from day 0 to day 6, which mostly mirrors the low supply of lipids or FAs from the culture media at this stage (Fig. 2A,B). However, clear increases were observed in three classes – sphingomyelin (SM), CE and phosphatidylinositol (PI) – independent of the lower or undetectable levels of those lipids in medium B. This was followed by a drastic increase in all lipid classes from day 6 to day 12, which clearly reflected the abundant lipid and FA in medium C (supplied to the cells from ~day 7 to day 12). Thus, the amount of FAs and lipids available in the media affects the lipid

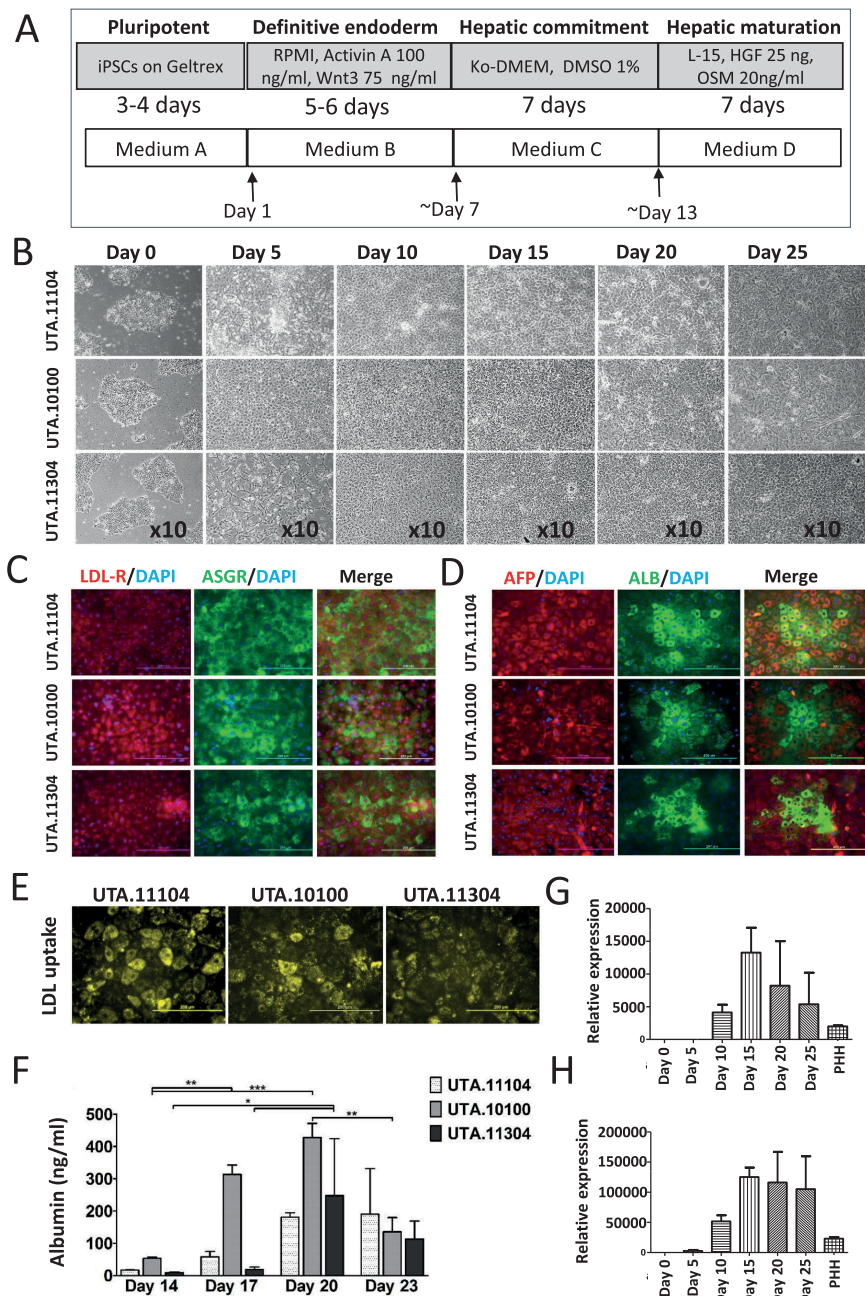


Fig. 1. See next page for legend.

composition and content of the cells. The measured concentrations of medium lipids and FAs were nicely in line with each other (Fig. 2A,B). During the hepatic maturation, from ~day 12 onwards, changes in the lipid levels were more subtle, in agreement with the

constant FA level of medium D, which was given to the cells during the hepatic maturation phase and contained on average 32.0 nmol FA/ml of medium (Fig. 2A). Principal component analysis (PCA) showed that the cellular lipid composition of iPSCs and DE stage



**Fig. 1. Hepatic differentiation of iPSCs through the definitive endoderm (DE) stage.** (A) A schematic representation of the hepatic differentiation protocol (modified from Hay et al., 2008) and cell culture media used at each stage. See text for details of the media. (B) Phase-contrast images showing sequential morphological changes from iPSCs (day 0) to DE (day 5) and finally hepatocyte-like cells (HLCs) (day 20) during differentiation. (C,D) Immunocytochemistry of the iPSC-HLCs differentiated from three patient lines (UTA.10100.EURCAs, UTA.11104.EURCAs and UTA.11304.EURCCs) at day 20 showing the expression of (C) LDL receptor (LDL-R) and asialoglycoprotein receptor (ASGR), as well as (D)  $\alpha$ -fetoprotein (AFP) and albumin (ALB). Nuclei are stained with DAPI. (E) The iPSC-HLCs were able to uptake LDL at day 20 of differentiation and (F) produce and secrete albumin during differentiation. Values are normalised per 1 million cells per 24 h. Bars represent means $\pm$ s.d. of three biological replicates. Gene expression levels of (G) apolipoprotein B (*ApoB*) and (H) apolipoprotein A1 (*ApoA1*) at different time points during the iPSC to HLC differentiation normalised to the housekeeping gene *GAPDH*, and expressed relative to day 0. Each sample was run in triplicate and bars represent means $\pm$ s.d. of three studied cell lines. iPSC, induced pluripotent stem cell; KO-DMEM, KnockOut Dulbecco's modified Eagle medium; DMSO, dimethyl sulfoxide; HGF, hepatocyte growth factor; OSM, oncostatin M; PHH, primary human hepatocyte. Scale bars: 200  $\mu$ m.

cells (days 0 and 6, respectively) clearly differs from the later time points representing hepatoblasts (day 12) and HLCs (day 16–28) (Fig. 2C). A similar PCA plot pattern was detected for the FA composition of cell culture media (Fig. 2D).

To visualise the alterations occurring in the cellular lipidome during the iPSC to HLCs differentiation in more detail, a heat map was computed using day 0 as the reference and including all the detected molecular lipids (Fig. S4A). Because the biggest alterations in the cellular lipid content and composition happened before day 12 as observed in the PCA (Fig. 2C) and appeared mostly to reflect the FA supply from the media, we computed another heat map using day 12 as the reference (Fig. S4B). From this heat map, the lipid remodelling during the hepatocyte maturation phase became more evident as the fluctuation from days 0 to 6 was excluded. We further restricted the heat map to include only molecular lipids, the concentration of which changed statistically significantly between days 12 and 28 ( $P < 0.05$ ). In the resulting heat map, 41 molecular lipids divided into two distinct clusters visible on the heat map dendrogram (Fig. 2E). The upper cluster consists of mainly SLs with very-long-chain FAs (C24–26), levels of which increased during the maturation. Lipids that decreased after day 12 are clustered in the lower part of the heat map consisting of several CE species as well as lipids containing FA 18:2 [linoleic acid (LA)]. Similar phenomena were observed in another heat map drawn separately for the 45 FAs present in specific lipid classes in the cells (Fig. S5).

We detected 16 different CE species, the most abundant during the iPSC to HLC differentiation being CE 18:1, CE 16:0 and CE 18:0 (Fig. 3A, lines), concurring with the higher level of FAs 16:0, 18:0 and 18:1 available in the medium C (Fig. 3A, columns). Interestingly, CE 18:0 concentration was low in medium C whereas CE 18:2 was detected the highest (Fig. 3A, insert). This CE 18:2 loading did not cause comparable accumulation of CE 18:2 in the cells. The majority of CEs peaked at day 12, with the exception of CE 20:1 (peak day 16) and CE 20:3, CE 22:5 and CE 22:6 (peak day 24). The decrease of several CEs and the increase of CE 22:6 are clearly visible in the heat maps, illustrating the statistically significant lipid and FA changes between days 12 and 28 (Fig. 2E, Fig. S5). It is of note that only the last medium (medium D, given to the cells from ~day 13 onwards) provided the cells abundantly with FA 22:6 (Fig. 3A).

During hepatic differentiation and maturation, we detected an overall increase in the FA chain length of SLs (Fig. 3B). The C16–18

species predominated (64%) in the beginning of differentiation but their relative abundance gradually decreased (to 44%) during the hepatocyte maturation process. At day 6, a temporary increase in the proportion of the C16–18 species was detected. Interestingly, as the differentiation progressed, the SL chain length profile approached that of PHHs, in which the very-long-chain species (C20–26) predominate (Fig. 3B).

Closer examination of the PL molecular species revealed that the largest changes occurred in polyunsaturated fatty acid (PUFA)-containing lipid species, whereas lipids comprised of saturated or monounsaturated FAs (SFA or MUFA, respectively) were more constant throughout the entire differentiation (Fig. 3C, Table S5). The polyunsaturated lipid species were essentially absent at the beginning of differentiation and increased drastically until day 12 or 16, reflecting the increasing concentration of *n*-3 and *n*-6 PUFAs in the media during differentiation, as shown in Fig. 3C for the phosphatidylcholines (PCs). On the other hand, the PCs containing FA 22:5 and 22:6 appeared later during the differentiation and at a lower concentration, consistent with their low medium concentration as well as a late and (as compared to *n*-6 PUFAs) low level supply of *n*-3 PUFAs from the medium (Fig. 3C). Lipids with different PUFA constituents mostly peaked around day 12, after which they steadily decreased following the pattern of medium FA 18:2 and 18:3 levels, which were at the highest in medium C (during ~days 7–13) and then dropped to a lower level for the rest of the differentiation (Fig. 4). The molecular species containing FA 20:3 and FA 20:4 peaked around day 12, reflecting the media rich in their C18 precursors, and then their contents remained at the fairly constant level due to the later moderate supply of FA 20:3 and 20:4 themselves (Fig. 4). The *n*-3 PUFA precursor, FA 18:3, and the successors on the metabolic pathway, FA 20:5 and 22:5, were not able to efficiently raise the levels of the 22:6-containing species, which peaked only during days 16–24, i.e. after switching to 22:6-rich medium (Fig. 4, lower row).

### Gene–lipid interaction

Levels of several ceramides with very-long-chain FAs, e.g. Cer d18:1/26:1 and Cer 18:1/26:0, increased statistically significantly during the hepatic maturation phase (Fig. 2E). Ceramide synthesis involves six different ceramide synthases (CerSs): CerS1–CerS6. The *CERS1* gene was the only highly expressed ceramidase gene at the iPSC stage and it gradually reduced to the expression levels detected in PHHs (Fig. 5A). The expression of the *CERS2* gene, by contrast, slowly increased during hepatocyte differentiation, reaching the expression level in PHHs by day 20 of differentiation (Fig. 5A). A statistically significant correlation was observed between *CERS2* expression and the very-long-chain ceramides Cer d18:1/24:0 ( $r = 0.83$ ,  $P < 0.0001$ ), Cer d18:1/23:0 ( $r = 0.78$ ,  $P < 0.001$ ) and Cer d18:1/26:0 ( $r = 0.73$ ,  $P < 0.001$ ) (Fig. 5B). A similar gene expression pattern to *CERS2* was observed for *CERS3*. *CERS4* expression varied whereas that of *CERS6* gradually increased during the differentiation, and *CERS5* was ubiquitously expressed throughout the differentiation (Fig. S6A).

Ceramides are degraded to sphingosine and free FAs by ceramidases encoded by distinct genes such as *ASAHI* and *ASAH2*. The expression of *ASAHI* increased during the differentiation (Fig. S6B). *ASAH2* expression peaked strongly at day 15 and then gradually reduced towards the levels detected in PHHs. *ASAH2b* expression was constant throughout the differentiation and at the same level as in PHHs, only peaking slightly at day 15 (Fig. S6B).

Lactosylceramide (LacCer) and glucosyl/galactosylceramide (Glc/GalCer) are members of the glycosphingolipid (GSL) family and the UDP-glucose:ceramide glucosyltransferase (*UGCG*) gene



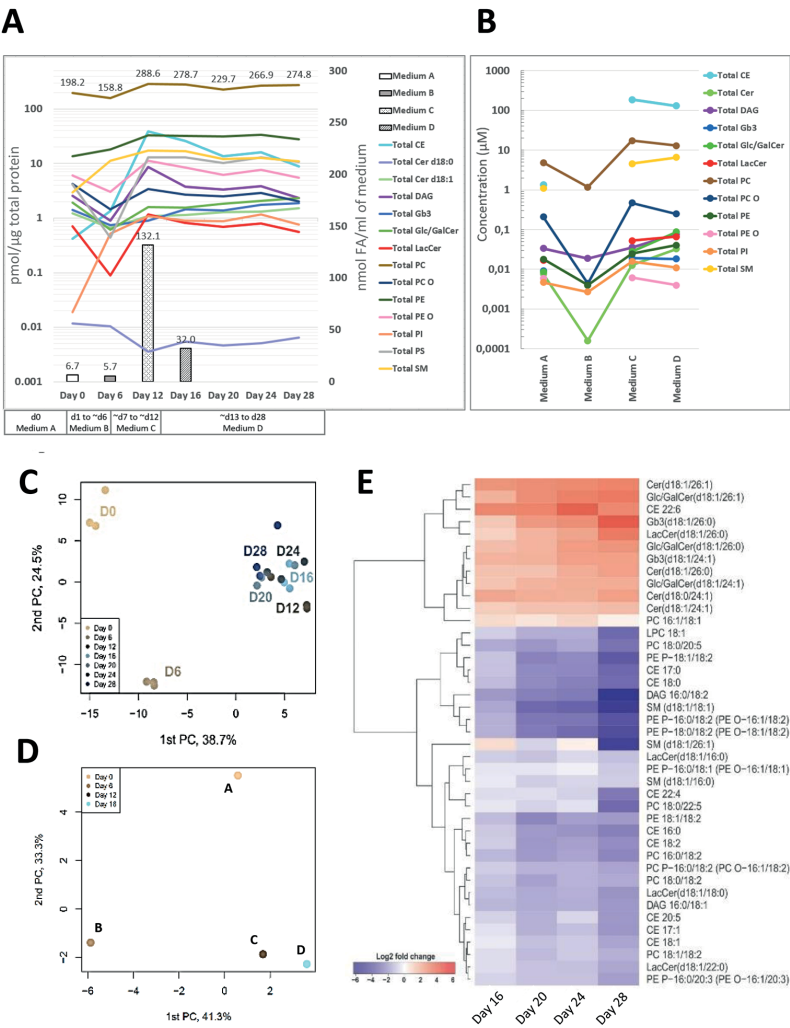


**Fig. 2. Changes in the lipidome during iPSC to hepatocyte-like cell (HLC) differentiation.** (A) Lines describe the total concentration of different lipid classes detected in the cells at seven time points during the iPSC to HLC differentiation. Bars represent the total FA concentration (nmol FA/ml of medium) of different media used during hepatic differentiation. Values at the top of bars and the top line show the total concentrations of FAs in the medium and PC in the cells, respectively. (B) Total concentration ( $\mu$ M) of different lipid classes in culture medium A, B, C and D. (C) Principal component analysis (PCA) plot showing the separation of samples based on lipid profiles. PCA analysis of the 165 molecular lipids showed that the two first principal components constitute 63.2% of the variance. (D) PCA analysis of the FA content of cell culture media used at different stages of hepatic differentiation. (E) Lipidomic heat map showing fold increase of molecular lipid species at day 16, 20, 24 and 28 of iPSC to HLC differentiation as compared to day 12. Each horizontal row represents a molecular lipid and each vertical column represents an individual time point of the differentiation. Lipid abundance ratios are coloured according to the fold changes and the colour key indicates the magnitude of log2 fold change. Data shown are the lipids for which concentration differed statistically significantly ( $P < 0.05$ ) between day 12 and day 28. iPSC, induced pluripotent stem cell; CE, cholesteryl ester; Cer, ceramide; DAG, diacylglycerol; Gb3, globotriaosylceramide; Glc/GalCer, glucosyl/galactosylceramide; LacCer, lactosylceramide; LPC, lysophosphatidylcholine; LPE, lysophosphatidylethanolamine; PC, phosphatidylcholine; PC O, alkyl-linked phosphatidylcholine; PE, phosphatidylethanolamine; PE O, alkyl-linked phosphatidylethanolamine; PI, phosphatidylinositol; PS, glycerophosphoserine; SM, sphingomyelin.

encodes the enzyme that catalyses the first glycosylation step in GSL biosynthesis. There was a statistically significant increase in four different GSLs, including LacCer d18:1/26:0 and Glc/GalCer d18:1/26:1, during the hepatic maturation phase (Fig. 2E). Compatibly, *UGCG* expression increased during the iPSC-HLC differentiation (Fig. 5A), and we observed a statistically significant correlation between *UGCG* expression and the total level of Glc/

GlcCer ( $r = 0.54$ ,  $P < 0.05$ ), particularly with Glc/GalCer d18:1/26:0 ( $r = 0.84$ ,  $P < 0.0001$ ) (Fig. S6C).

An almost fourfold increase in total SM level was detected from day 0 to day 28 of the iPSC-HLC differentiation (Fig. 2A). Specifically, an increase in the longer (C23-26) SM species was observed (Fig. S7A). SM is metabolised from ceramides by SM synthases (SMS1 and SMS2). The expression of the corresponding

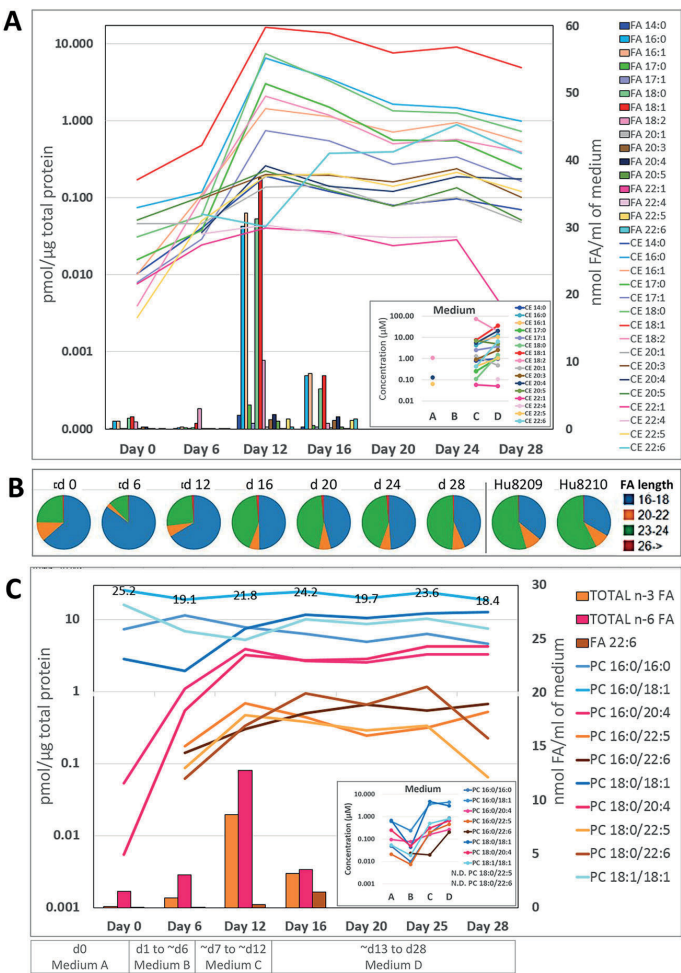


**Fig. 3. Changes in cholesterol ester (CE), polyunsaturated fatty acid (PUFA)-containing phosphatidylcholine (PC) species and the chain length of sphingolipids (SLs) during the iPSC to hepatocyte-like cell (HLC) differentiation.** (A) Lines represent the concentration (pmol/ $\mu$ g total protein) of all detected CE species at different time points of the iPSC to HLC differentiation. Concentrations are presented on a logarithmic scale. Bars represent concentration of all different FAs (nmol FA/ml of medium) detected in different cell culture media used during hepatic differentiation. The insert on the lower right shows the concentration ( $\mu$ M) of CE species detected in culture medium A, B, C and D. No CE species were detected in medium B. (B) The distribution of SLs with different FA chain lengths at different time points shows that, during hepatic differentiation and maturation, the relative abundance of C16-18 species gradually decrease, whereas C23-24 species increase. At the end of the hepatic maturation phase, the distribution closely resembles that of primary human hepatocytes (Hu8209 and Hu8210). All SLs detected were included in the calculations. (C) Lines represent the concentrations (pmol/ $\mu$ g total protein) of selected PC species at different time points. The levels of saturated/monounsaturated FA (in blue)-containing species remain rather constant, whereas levels of PUFA-containing lipid species (20:4 in red; 22:5/22:6 in orange) emerge/increase considerably at day 6 and 12. Bars represent the total n-3 FA, n-6 FA and FA 22:6 concentration (nmol FA/ml of medium) in cell culture media at each stage of differentiation. The insert on the lower right shows the concentration ( $\mu$ M) of PC species detected in culture medium A, B, C and D. PCs 18:0/22:5 and 18:0/22:6 were not detected in the media. Values at the top line show the concentration of PC 16:0/18:1 in the cells during differentiation.

genes, *SGMS1* and *SGMS2*, increased during differentiation, reaching the expression levels of PHHs by day 10 (Fig. 5A). A statistically significant correlation was detected between *SGMS2* expression and levels of very-long-chain SMs (Fig. 5C) such as d18:1/24:0 ( $r=0.82$ ,  $P<0.0001$ ), SM d18:1/24:1 ( $r=0.78$ ,  $P<0.001$ ) and SM d18:1/26:1 ( $r=0.67$ ,  $P<0.01$ ). Levels of these very-long-chain SMs increased independently of the exogenous lipid supplies during the hepatoblast phase, whereas the shorter-chain SMs such as SM d18:1/18:0 and SM d18:1/18:1 decreased at the hepatic maturation stage (Fig. 5A,B). Several different sphingomyelinase (Smase) enzymes degrade SMs. The *SMPD1* gene encodes a lysosomal acid Smase, the expression of which increased during the hepatic differentiation (Fig. 5A) along with the expression of another sphingomyelinase gene, *SMPD3* (Fig. 5C). The expression of two other Smase genes, *SMPD2* and *SMPD4*, was fairly constant through the differentiation and similar to that in PHHs (Fig. 5C).

**DISCUSSION**

In this study, we successfully produced functional HLCs from iPSCs and describe a comprehensive lipidomic fingerprint of these cells in

conjunction with biochemical and functional measurements. We quantitatively monitored a total of 165 molecular species of lipids during the course of hepatic differentiation, as well as measuring the concentrations of different lipids and FAs in the cell culture media at each stage of differentiation. The analyses of lipids and FAs in the media were complementary in characterising the supplies of the cells. After commitment of the cells to the hepatic lineage (around day 12), protein-normalised concentrations of most studied lipid classes increased. These included functionally important specific PLs and SLs but, as expected, the main building blocks of bulk membrane, PC and PE, showed less variation. At the same time, the levels of storage lipids were elevated, indicated by the increased CE totals. DAGs were also analysed because they are an important intermediary lipid class between the storage and structural lipids, and their elevated levels at day 12 indicate enhanced lipid metabolism (complex triacylglycerol molecular species were not addressed in this study). These lipidome alterations mirror the large increase in medium FA levels and improved supply of PUFAs to the cells. Simultaneously, the cells grew in size and approached hepatocyte cell morphology. Along with the influence of

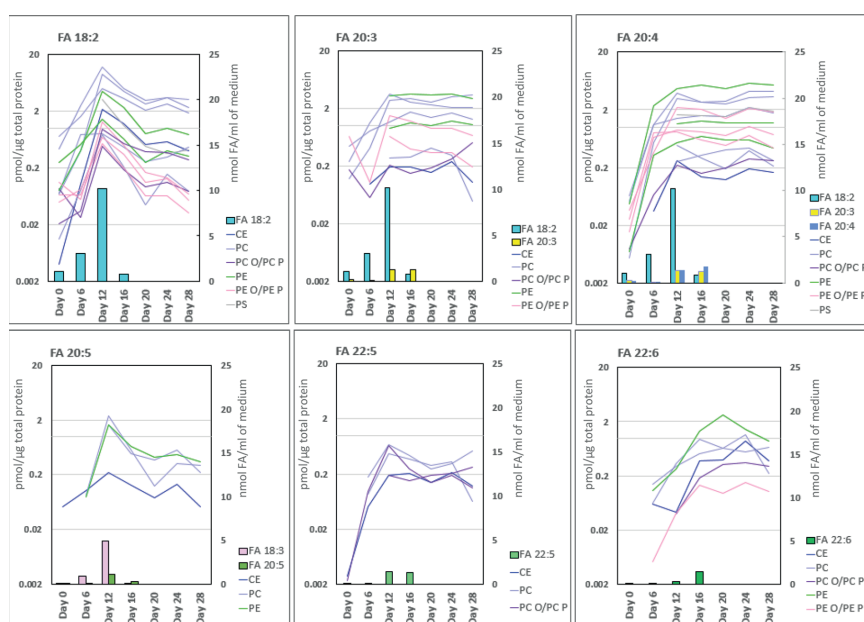


**Fig. 4. The levels of polyunsaturated fatty acid (PUFA)-containing lipids during iPSC to HLC differentiation.** Lines in the graphs show concentrations (pmol/μg total protein; logarithmic scale on the left) of lipids containing the given PUFA moiety at different time points. Each line represents the lipid species with the specific PUFA in a particular lipid class; line colour refers to lipid class (colour key depicted on the right). The bars represent the concentration of FA 18:2, 20:3, 20:4, 18:3, 20:5, 22:5 and 22:6 (nmol FA/ml of medium, scale on the right) in the cell culture media during hepatic differentiation. CE, cholesteryl ester; PC, phosphatidylcholine; PC O/PC P, ether-linked PC; PE, phosphatidylethanolamine; PE O/PE P, ether-linked PE; PS, phosphatidylserine; FA, fatty acid.

exogenous supplies, we also found endogenous cellular responses: specific SL-metabolism-related genes correlated with distinct SL species levels, which showed that, during the differentiation, changes in gene expression levels were reflected in the levels of specific lipid species at a given time point.

Cholesterol biosynthesis is one of the important functions of hepatic cells. Interestingly, the three most abundant storage forms of CEs detected during the differentiation of iPSCs to HLCs, i.e. CE 18:1, CE 16:0 and CE 18:0, have previously been shown to be among the most abundant CEs in the human liver (Nestel and Couzens, 1966). Despite the level of CE 18:2 being very high in media C and D, when analysing cellular CE levels, this species was not among the highest species but the essential 18:2n-6 [linoleic acid (LA)] was apparently incorporated into structural PLs, priming these PUFAs for signalling. This gives confidence that lipid metabolism of this cell model resembles that of genuine hepatocytes. Most CE species were at their highest levels at day 12 and then, along with decreasing medium CE and FA levels, CEs in the cells decreased during hepatocyte maturation. Compared to medium A and B, medium C (provided to the cells from ~day 7 to ~day 13) contained a very high total concentration of FAs, exceeding the sufficient amount for a cell's consumption. This is also consistent with our observation of lipid droplet (LD) formation during the second week of differentiation (results not shown), suggesting that the excess amount of FAs provided in medium C are stored as LDs in the cells. LDs are the main reservoir for neutral lipids in the cells and can be used for metabolism, membrane synthesis (PLs and cholesterol) and steroid synthesis (Martin and Parton, 2006).

SLs form a class of lipids defined by their C18 amino-alcohol backbones, which are synthesised in the ER from non-SL precursors. Modification of this basic structure gives rise to the vast family of SLs such as ceramides, SMs and GSLs, which are structural components of biological membranes and bioactive molecules participating in diverse cellular activities such as cell division, differentiation, gene expression and apoptosis (Gault et al., 2010). SLs also participate in cell signalling and modulate inflammation (Hannun and Obeid, 2008; Maceyka and Spiegel, 2014). Furthermore, increasing evidence shows that SLs contribute to the pathogenesis of metabolic diseases including atherosclerosis (Borodicz et al., 2015; Haus et al., 2009; Hornemann and Worgall, 2013) and that SL metabolism is affected by dyslipidemia (Holland and Summers, 2008). Because the liver is heavily involved in lipid metabolism, hepatocytes offer a good cell model for studying the basic mechanisms of lipid metabolism and its dysregulation.

The precursor of all SLs is ceramide, which primarily consists of a sphingoid long-chain base (sphingosine) and one FA chain, the length of which typically ranges from C14 to C26, the ceramide species with FAs 16:0, 24:0 and 24:1 being predominant in most mammalian tissues. Ceramide synthesis is a complex process and orchestrated by six mammalian CerSs, each of which produces ceramides with distinct FA chain lengths (Cingolani et al., 2016; Levy and Futerman, 2010; Park et al., 2014). The expression pattern of CerS is cell specific, which is reflected in the different SL acyl chain composition in a given tissue (Levy and Futerman, 2010). CerS2, the dominant CerS isoform found in the liver, utilises C20-C26 acyl-CoA species as substrate and is one of the major CerSs responsible for the synthesis of long-chain ceramide species

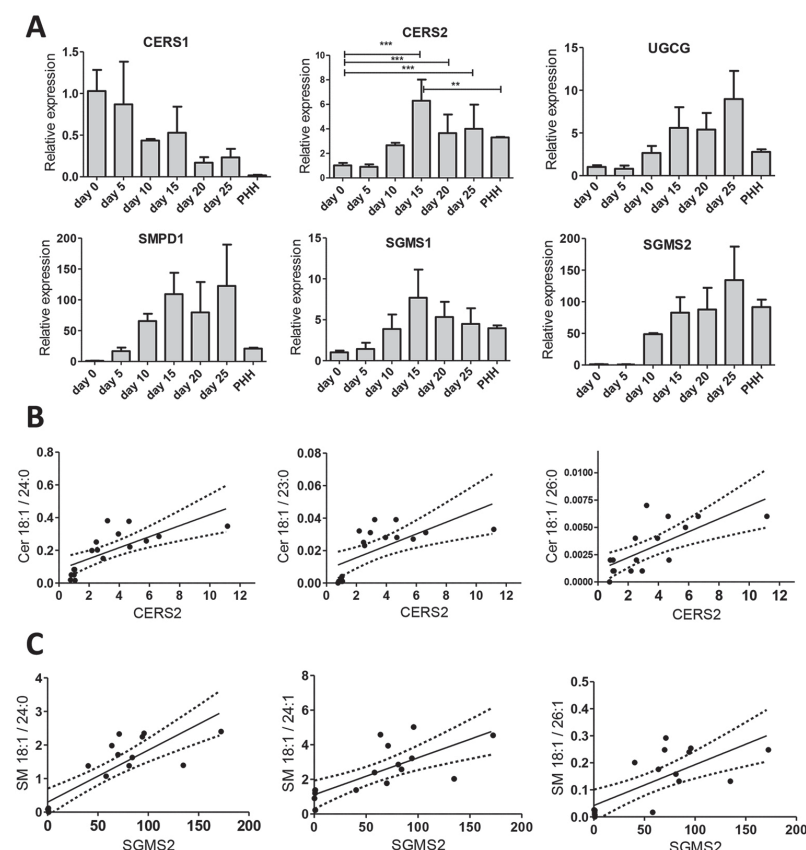


**Fig. 5. Expression levels of sphingolipid (SL) metabolism-related genes during hepatic differentiation and in primary human hepatocytes (PHHs).** (A) The expression of *CERS1*, *CERS2*, *UGCG*, *SMPD1*, *SGMS1* and *SGMS2* during hepatic differentiation from iPSCs at day 0, 5, 10, 15, 20 and 25 as well as in PHHs. The expression of each gene was normalised to the endogenous control gene, *GAPDH*, and presented relative to day 0 (iPSCs). Each sample was run in triplicate and bars represent means  $\pm$  s.d. of three studied cell lines or two PHH donors. \*\* $P \leq 0.01$ ; \*\*\* $P \leq 0.001$ . (B) The expression of *CERS2* correlates positively with Cer d18:1/24:0 (Spearman  $r = 0.83$ ,  $P < 0.0001$ ), Cer d18:1/23:0 ( $r = 0.78$ ,  $P < 0.001$ ) and Cer d18:1/26:0 ( $r = 0.73$ ,  $P < 0.001$ ). (C) *SGMS2* expression correlates positively with levels of SM d18:1/24:0 ( $r = 0.85$ ,  $P < 0.0001$ ), SM d18:1/24:1 ( $r = 0.78$ ,  $P < 0.001$ ) and d18:1/26:1 ( $r = 0.67$ ,  $P < 0.01$ ). Cer, ceramide; CERS, ceramide synthase; SGMS, sphingomyelin synthase; SMPD, sphingomyelin phosphodiesterase; UGCG, UDP-glucose ceramide glucosyltransferase; SM, sphingomyelin.

(C20–C26) (Laviad et al., 2008). In our study, the concentration of several very-long-chain (C22 to C26) SLs increased statistically significantly between days 12 and 28, which indicates an increase in CerS2 activity as the cells matured towards functional HLCs. This was supported by a clear and statistically significant increase of *CERS2* gene expression during iPSC–HLC differentiation. Furthermore, a statistically significant positive correlation between *CERS2* expression and very-long-chain ceramides (e.g. Cer d18:1/24:0) was found. The very-long-chain ceramides produced by CerS2 are essential for liver function (Park et al., 2014); thus, the increase in their levels acts as evidence of hepatocyte functionality. Admittedly, we have not measured CerS2 enzyme activities but only the level of *CERS2* gene expression. Still, both the increased *CERS2* gene expression as well as the increase in long-chain ceramides and other long-chain SLs showed that the stepwise hepatic differentiation protocol produced iPSC–HLCs with a lipid phenotype resembling that of PHHs. Ceramide can be degraded to sphingosine and free FA by ceramidases (Mao and Obeid, 2008). Acid ceramidase (encoded by the *ASAH1* gene) most efficiently hydrolyses ceramide with medium-chain FA components (C12 to C14), whereas the neutral ceramidase (*ASAH2*) prefers long-chain to very-long-chain components (C16 to >C24) (Gault et al., 2010). In the current study, expression of *ASAH1* and *ASAH2b* was rather constant, whereas, concurrent with the increase in very-long-chain ceramide, the expression of *ASAH2* peaked at day 15 and then

gradually decreased towards levels in PHHs. These findings suggest that there is a balance between ceramide production by CerS and degradation by ceramidases during differentiation, which could partly explain why ceramide levels stay constant towards the end of the differentiation. The C26 FAs were not detected in any of the culture media and the C26 species of ceramides and SLs (synthesised from their precursor) were still found in the cells, with increasing amounts towards the end of the differentiation process. Thus, the levels and molecular species composition of ceramide and the successor SLs seemed to be endogenously regulated.

Total SM levels increased during iPSC–HLC differentiation. We showed that the corresponding genes for SM synthases – *SGMS1* and *SGMS2* – were expressed in the iPSC–HLCs throughout the differentiation at levels approaching those in PHHs. It has previously been shown that both *SGMS1* and *SGMS2* positively correlate with levels of cellular SM (Li et al., 2007). Our study supports this because the expression of *SGMS1* and *SGMS2* correlated well with several molecular SM species, especially the long-chain ones (C23 to C26). Furthermore, during the DE differentiation stage, a sharp increase in total level of SM was observed, whereas PC and ceramide decreased. SM synthases use ceramide and PC as substrates to produce SM (Liu et al., 2009), offering an explanation for the transient decreases of ceramide and PC in the beginning of the hepatic differentiation. However, this still requires further studies owing to the



very complex and dynamic nature of the cellular lipidome, and strong influence of the culture media. Because SM is the most abundant SL in human cells, its coordinated breakdown is an essential part of membrane homeostasis. It occurs by the Smase family and results in the production of ceramide and free phosphocholine. The *SMPD1* gene encodes a lysosomal acid Smase, whereas *SMPD2*, *SMPD3* and *SMPD4* are neutral Smases localised to different cellular compartments (Kim et al., 2008). *SMPD2* is located in ER, and *SMPD4* in both ER and Golgi. The expression of *SMPD1* increased during the hepatic differentiation as early as at DE stage, suggesting that lysosomal degradation of SM might be crucial for differentiation, maturation or functional structure of the HLCs because ceramide, as one of the products of SM catabolism, is considered crucial to the above-mentioned vital cellular processes, as are its derivatives (Delgado et al., 2006; Gault et al., 2010). Pharmacological inhibition of SM *de novo* synthesis decreases not only SM levels but also ceramide and sphingosine (Liu et al., 2009). This clearly emphasises that the metabolic conversions among the SLs in the cell are tightly interconnected. In line with this, we observed a similar gene expression pattern between *SMPD1*, *ASAHI* and *UGCG* during the entire hepatic differentiation.

GSLs are complex carbohydrate-containing SLs and characteristic components of plasma membranes, residing specifically in the membrane microdomains called lipid rafts. GSL metabolism and composition are altered during the proliferation and differentiation of various types of cells (Iwabuchi et al., 2010). LacCer is a precursor in the biosynthesis of complex GSLs, and known to activate a signal transduction pathway leading to cell proliferation. In our study, LacCer d18:1/26:0 as well as three different very-long-chain Glc/GalCer increased during hepatic maturation. There was also a trend of increased expression of *UGCG* (responsible for glycosylation) during the iPSC-HLC differentiation, correlating with the levels of Glc/GalCer. This suggests that active UGCG enzyme function is vital in hepatic maturation because its GSL products are essential players in cell growth, development and differentiation, and mediate cell adhesion and modulate signal transduction (Gault et al., 2010).

We detected an overall increase in the FA chain lengths in the studied SL classes during the differentiation. This might suggest induction of membrane lateral heterogeneity with more lipid rafts incorporating SLs with longer chain lengths as the cells differentiate towards HLCs. The lipid rafts are regarded as small (from 10 to 200 nm) specialised regions of plasma membrane enriched in cholesterol and SLs with very-long and saturated acyl chains. The lipid rafts are more ordered and slightly thicker lipid domains than the surrounding bulk membrane, which contains unsaturated PL molecules. In line with this, we found significant increase in very-long and saturated SLs (24:0 and 26:0) (Fig. S5), as well as high levels of unsaturated PLs provided by medium C from day 7 (Fig. 3C). Signalling and cell-adhesion molecules are localised in lipid rafts, implicating that these domains may form platforms for signal transduction and cell adhesion. Complex SLs are needed in the lipid rafts for example for cell–cell contact and efficient membrane trafficking (Wassall et al., 2004). However, besides cholesterol and SLs, the emergence of the raft domains from bulk membrane also involves unsaturated PLs.

Enrichment of *n*-3 PUFA in the plasma membrane alters the lateral organisation of lipids. Polyunsaturated PLs, especially those with highly unsaturated *n*-3 PUFAs, are sterically incompatible with cholesterol and lipids with long saturated acyl chains, and thus the incorporation of these PUFAs into the membrane PLs forces the raft lipids out of the bulk membrane, inducing raft formation (Wassall

and Stillwell, 2009). However, supplementing cells in excess with highly unsaturated FAs, consequently inserted into the membranes, may disturb raft integrity (Turk and Chapkin, 2013). By regulating the sizes and properties of the raft versus non-raft domains, the *n*-3 PUFAs regulate raft-mediated downstream signalling, transcriptional activation and cytokine secretion (Turk and Chapkin, 2013). We detected a strong increase in PUFA-containing PL species during hepatic differentiation. In addition to driving raft formation, the polyunsaturated PLs affect bulk membrane properties, such as fluidity, flexibility and permeability (Rawicz et al., 2008). The changing of these properties affects membrane vesicle formation and thereby lipid and protein trafficking, which needs to be efficient as the cells grow, differentiate and make more membranes (Van Meer et al., 2008). Very recently, Ghini and co-workers showed that supplementing culture medium with 22:6n-3 [docosahexaenoic acid (DHA)] affected both the lipidome and metabolome of HepG2 hepatoma cells. Owing to the supplement, the total contents of cholesterol, SFAs and MUFAs decreased, whereas the PUFA and TAG contents of the cells increased (Ghini et al., 2017). In our study, 22:6n-3 was present at a very low level in media A, B and C, and present mainly in medium D, used during the late hepatic maturation. The precursors of 22:6n-3 (e.g. 18:3n-3), given to the differentiating cells at an earlier phase, did not immediately give rise to 22:6n-3, which is likely owing to the required multistep synthetic pathway. Compared to the synthesis of 20:4n-6 from its precursor 18:2n-6, the metabolism of 22:6n-3 from 18:3n-3 requires two additional chain elongations and a desaturation in the ER followed by a peroxisomal chain-shortening step, the process thus requiring more time and being less efficient than the synthesis of 20:4n-6 (Tigistu-Sahle et al., 2017). The HLCs, however, were able to produce some 22:6n-3 from its precursors, as can be seen from the rising levels of e.g. 22:6-containing PC-P (plasmalogen) during hepatic maturation. Incorporating 22:6n-3 into PS is crucial to activate protein kinase C pathways (Aires et al., 2007; Giorgione et al., 1995) and, apparently, this type of signalling is actively recruited only at late stages of the differentiation.

PC is the major component of eukaryotic cell membranes and the major PL component of all plasma lipoprotein classes (Cole et al., 2012), and is currently the only known PL class to be required for lipoprotein assembly and secretion (Castro-Gómez et al., 2015). PC molecules contain a range of FA chains with varying lengths and double-bond positions (Yamashita et al., 1997). We saw a more drastic increase (at ~day 12) of PC species containing FA 20:4, the precursor of which is an essential FA (18:2n-6), than PCs containing other PUFAs. This can partly be explained by the concurrent strong rise of *n*-6 PUFAs in the medium. When the cells get enough 18:2n-6 from the medium, they are able to synthesise all the other members of the *n*-6 PUFA family (Russo, 2009). However, cellular remodelling processes prefer producing PC species with 20:4n-6 in the *sn*-2 position of the molecule: such PC species are the preferred substrates for cytosolic phospholipase A2 type IV (PLA2IV), cleaving 20:4n-6 for synthesis of eicosanoids, which modulate immune responses, cell growth and differentiation (Astudillo et al., 2012; Fujishima et al., 1999). Apparently, the capacity of the differentiating cells to produce these lipid mediators arises along with the appearance of 20:4n-6-containing PC species.

It is especially interesting that, in our cells, *APOB* expression peaked and LD were observed at 2 weeks, soon after the maturing HLCs reached their highest levels of 20:4n-6-containing PC. It was recently revealed that defects in proteins such as *Lpcat3* and *Tm6sf2*, needed for efficient incorporation of 20:4n-6 into ER

membranes, reduce TAG secretion from hepatic cells (Rong et al., 2015; Ruhanen et al., 2017). Thus, it appears that the 20:4n-6-containing PC species are crucial for the assembly and excretion of TAG-containing mature lipoprotein particles, and are likely needed for the proper function of our cell model, the HLCs. Because these specific PC species regulate both immune functions and lipid metabolism of the cells, it is understandable that, when the levels of these 20:4-containing PCs first increased in the 18:2n-6-rich medium, they did not peak very high (as happened for many 18:2-containing lipids) but remained at a constant level to the end of the experiment, independent of the latest switch of the medium. The levels of 20:4n-6-containing PCs were apparently efficiently regulated to avoid excessive eicosanoid signalling and to adjust the rate of lipid secretion from the cells.

Taken together, we show how the lipidome of stem cells is remodelled in response to supplies available in the cell culture media and as a result of changing lipid-gene expression as the cells differentiate and mature towards functional HLCs. The lipidome and expression of lipid-related genes in HLCs resemble those of the PHHs, and the HLCs display the expected morphology and cellular functions of a functional hepatocyte. The observed elevations in the production of very-long-chain SLs and PUFA-containing PLs during hepatic maturation clearly show that cells efficiently take up FAs from the media, incorporate them and modify simple lipids into more complex ones, which in turn can change the membrane architecture, causing the alterations in cellular functions.

## Conclusions

Here, we show an efficient differentiation of iPSCs to HLCs and demonstrate their functionality determined by their cellular lipidomic fingerprint in conjunction with biochemical and functional measurements and lipid-metabolism-focused gene expression. To our knowledge, this is the first time a lipidomic profile has been acquired of stem cells during the course of their maturation into functional HLCs. We anticipate that the described approach will open up new avenues in lipid-focused stem-cell biology and medicine as it provides detailed maps of the underlying lipid content and metabolism of a cell at a given time point, taking into account the cell culture environment and FA components available in the culture media. This provides a novel tool in utilising the lipidome to follow cell differentiation and maturation and how this is affected under different conditions or stimuli. Thus, we expect that the stem-cell lipidomic fingerprinting through HLC differentiation will facilitate the production of target cells that more closely resemble the primary human hepatocytes, helping to improve our understanding of many hepatocyte-related diseases and their treatments.

## MATERIALS AND METHODS

### iPSC culture

iPSC lines were maintained at 37°C in 5% CO<sub>2</sub> on mitotically inactivated mouse embryonic fibroblasts (MEFs; Applied StemCell, cat. no. ASF-1223). Cells were treated with KnockOut Dulbecco's modified Eagle medium (KO-DMEM) supplemented with 20% KnockOut Serum Replacement (Ko-SR), 2 mM GlutaMAX, 0.1 mM 2-mercaptoethanol (2-ME) (all from Gibco), 1% nonessential amino acids (NEAA) and 50 U/ml penicillin/streptomycin (both from LONZA). Medium was supplemented with 4 ng/ml human basic fibroblast growth factor (bFGF; R&D System). To generate HLCs, iPSCs were adapted to feeder-free condition on pre-coated plates with Geltrex (Gibco®, 1:100 dilution) in mTeSR medium (=medium A) before hepatic differentiation. Cell lines were checked for mycoplasma contamination.

### iPSC reprogramming

Three iPSC lines (UTA.10100.EURCAs, UTA.11104.EURCAs and UTA.11304.EURCCs) were used in this study. The lines were derived directly from the fibroblast of three individual patients. The study was approved by the Ethical Committee of Pirkanmaa Hospital District (R12123) and written consent was obtained from all fibroblast donors. The collected fibroblasts were induced to pluripotency using the Sendai reprogramming kit (OCT4, SOX2, KLF4, C-MYC; CytoTune; Life Technologies) based on the protocol described by Takahashi et al. (2007). Cell lines were induced according to the manufacturer's instructions and cultured on MEF feeders until characterisation.

### iPSC characterisation

All the iPSC lines were characterised in detail as described before (Manzini et al., 2015). In short, we used PCR to study the expression of endogenous pluripotency genes (*NANOG*, *REX1*, *OCT3/4*, *SOX2* and *c-MYC*) and the absence of virally imported exogenes (*OCT4*, *SOX2*, *c-MYC* and *KLF4*). Immunocytochemistry was performed to study the protein expression of pluripotency markers (Nanog, OCT-3/4, SOX2, SSEA-4, TRA 1-60 and TRA 1-81) (Table S1). The normal karyotype of the iPSC lines was confirmed by performing genome-wide screening for gross chromosomal abnormalities with KaryoLite BoBs (product number 4501–0010, Perkin Elmer) in the Finnish Microarray and Sequencing Centre, as described elsewhere (Lund et al., 2012).

The pluripotency of the iPSCs was verified *in vitro* by the formation of embryoid bodies (EBs) from which RNA was extracted and reverse transcription performed as described previously (Manzini et al., 2015). The expression of marker genes characteristic of endoderm (*SOX17* or *AFP*), mesoderm (*KDR* or *ACTC1*) or ectoderm (nestin or *musashi*) were studied from EBs by PCR and *GAPDH* was used as an endogenous control. The primer sequences for pluripotency genes and virally imported exogenes as well as for marker genes of the three germ layers are presented in Table S2.

### Hepatic differentiation

Hepatic differentiation was performed according to the protocol developed by Hay et al. (2008). After the colonies became 60–70% confluent, differentiation was initiated by culturing the cells in RPMI1640+GlutaMAX medium (Gibco) supplemented with 100 ng/ml Activin A (R&D Systems), 75 ng/ml Wnt3, 1 mM sodium butyrate (NaB) on the first day and 0.5 mM from day 2, and 2% B27 (Gibco) (=medium B) for 5–6 days to DE stage. Hepatic differentiation was initiated by switching the medium to KO-DMEM+20% Knockout Serum Replacement, 1 mM GlutaMAX, 1% NEAA, 0.1% 2-ME and 1% dimethyl sulfoxide (DMSO) (=medium C) for 7 days. From this point cells were cultured in Leibovitz's L-15 medium (Invitrogen), supplemented with 8.3% fetal bovine serum (FBS) (Biosera), 8.3% tryptose phosphate broth (Sigma-Aldrich), 10 μM hydrocortisone 21-hemisuccinate, 1 mM insulin (both from Sigma-Aldrich), 2 M GlutaMAX, 25 ng/ml hepatocyte growth factor (HGF) and 20 ng/ml oncostatin M (R&D Systems) (=medium D) (Fig. 1A).

### Hepatic characterisation

#### Flow cytometry

DE cells were detached at day 5 by a 7- to 8-min incubation with Gentle Cell Dissociation Reagent (StemCell Technologies) at 37°C and then suspended in 3% FBS before being stained by CXCR4 conjugated antibody (R&D Systems) for 15 min at room temperature (RT). The percentage of CXCR4-positive cells were assessed using a BD Accuri C6 cytometer.

#### Real-time quantitative PCR (RT-qPCR) analyses

RNA samples were collected at days 0, 5, 10, 15, 20 and 25 using the RNeasy kit (Qiagen, cat. no. 74106). cDNAs were generated using the High Capacity cDNA Reverse Transcription kit (Applied Biosystems, USA) according to the manufacturer's instructions in the presence of RNase inhibitor. The PCR reaction was performed by using Power SYBR Green PCR Master Mix (Life Technologies, cat. no. 1408470) and the cDNA was multiplied using the Applied Biosystems 7300 Real-time Sequence

Detection system.  $C_T$  values were determined using 7300 SDS software (Applied Biosystems) and relative quantification was calculated by the  $2^{-\Delta\Delta CT}$  method (Livak and Schmittgen, 2001). The primer sequences are presented in Table S3.

The expression of 18 genes involved in lipoprotein formation or SL metabolism was studied by RT-qPCR with the Biomark HD system (Fluidigm Corp., San Francisco, USA) and using TaqMan assays. cDNA was prepared and pre-amplified according to the manufacturer's instructions, as were the RT-qPCR reactions. TaqMan assays (Life Technologies) used in the RT-qPCR are presented in Table S4. The levels of mRNA expression were normalised to the endogenous control gene, *GAPDH*, and expressed as relative expression compared to the undifferentiated iPSCs (at day 0). Each sample was run in triplicate.

### Immunocytochemistry

Cultured cells were fixed in 4% paraformaldehyde (PFA) for 20 min at RT. Permeabilization and blocking was performed at the same time by 10% normal donkey serum (NDS), 0.1% Triton-X 100 and 1% bovine serum albumin (BSA) for 45 min. Cells were incubated overnight with primary antibodies (Table S1) in the above solution with reduced NDS to 1%. Antigens were visualised using Alexa Fluor 488- and 568-conjugated secondary antibodies (Table S1). Finally, the cells were mounted with Vectashield (Vector Laboratories Inc., Burlingame, CA, USA) containing 40,6-diamidino-2-phenylindole (DAPI) for the nuclei staining and imaged with an Olympus IX51 phase-contrast microscope equipped with fluorescence optics and an Olympus DP30BW camera (Olympus Corporation, Hamburg, Germany).

### Functionality of the differentiated iPSC-HLCs

The ability of the iPSC-HLCs to both uptake LDL and secrete albumin was studied using the LDL Uptake Assay kit (Cayman Chemicals, USA) and Human Albumin ELISA Quantitation set (Bethyl Laboratories, USA), respectively, according to the manufacturers' instructions. Secreted albumin was measured from 24-h conditioned medium and normalised to the cell number.

### Lipidomic profiling of cells and FA analyses of cell culture media

#### Lipid sample preparation and extraction

Lipids [CEs, SLs, glycerophospholipids (GPL) and polar glycerolipids] were extracted at days 0, 6, 12, 16, 20, 24 and 28 of differentiation from PBS-resuspended cells by a modified Folch lipid extraction, using chloroform [high-performance liquid chromatography (HPLC) grade], methanol and acetic acid [both liquid-chromatography–mass-spectrometry (LC-MS) grade] for liquid–liquid extraction (Ståhlman et al., 2009), which was performed on 96-well plates employing a Hamilton Microlab Star system (Hamilton Robotics AB, Kista, Sweden). All solvents were purchased from Sigma-Aldrich. Samples were spiked with known amounts of lipid-class-specific non-endogenous synthetic internal standards. After lipid extraction, samples were reconstituted in chloroform:methanol (1:2, v/v) and synthetic external standards were post-extract spiked to the extracts (Heiskanen et al., 2013). Quality control samples (QCs) were prepared along with the actual samples for all lipidomic analyses to monitor the extraction and MS performance. In addition, calibration lines were prepared to determine the linear dynamic range of the MS analyses. QCs and calibration lines were prepared in fresh frozen plasma (FFP) samples (Veripalvelu, Finland).

### Mass spectrometric analyses and data processing

In shotgun lipidomics, lipid extracts were analysed on a hybrid triple quadrupole/linear ion trap mass spectrometer (QTRAP 5500) equipped with a robotic nanoflow ion source (NanoMate, Advion Biosciences Inc., Ithaca, NJ, USA) as described (Heiskanen et al., 2013). Molecular lipids were analysed in both positive and negative ion modes using either multiple precursor ion or neutral loss scans (Ekroos et al., 2002, 2003). The molecular species of lipids were identified and quantified in absolute [CE; PC; phosphatidylethanolamine (PE); phosphatidylserine (PS); lysophosphatidylcholine (LPC); lysophosphatidylethanolamine (LPE); DAG; SM] or semi-absolute [PI; alkyl-linked phosphatidylcholine (PC-

O); alkanyl-linked phosphatidylcholine (PC-P); alkyl-linked PE (PE-O); alkanyl-linked PE (PE-P)] amounts (Ejsing et al., 2006) by normalising to their respective synthetic internal standard and the sample amount. SLs were analysed as described before (Merrill et al., 2005), using an Acquity BEH C18, 2.1×50 mm column with a particle size of 1.7  $\mu$ m (Waters, Milford, MA, USA). A 25 min gradient using 10 mM ammonium acetate in water with 0.1% formic acid (mobile phase A) and 10 mM ammonium acetate in acetonitrile:2-propanol (4:3, v/v) containing 0.1% formic acid (mobile phase B). SLs were analysed on a hybrid triple quadrupole/linear ion trap mass spectrometer (4000/5500 QTRAP) equipped with an ultra-high-pressure liquid chromatography (UHPLC) system (CTC HTC PAL autosampler and Rheos Allegro pump or Shimadzu Nexera X2) using a multiple reaction monitoring (MRM)-based method in negative ion mode.

Molecular lipids were normalised to the total protein concentration in the cell samples. Total protein concentrations were determined using the Micro BCA Protein Assay kit (Thermo Scientific Pierce Protein Research Products) according to the manufacturer's instructions. Data processing was performed by MultiQuant, LipidProfiler/LipidView (AB Sciex) softwares and SAS.

### FA analysis

FA composition and concentrations in the cell culture media (medium A, B, C and D, see above for details) used at iPSC stage and at different stages of hepatocyte differentiation were analysed by gas chromatography. First, the lipid residues of nitrogen-dried media were subjected to transmethylation in 1% methanolic  $H_2SO_4$  at a temperature of 96°C and under nitrogen atmosphere for 120 min, according to the recommendations of Christie (1993). The FA methyl esters (FAMES) formed were recovered with hexane and their quantitative analysis was performed using a Shimadzu GC-2010 Plus gas chromatograph with flame-ionization detector (GC-FID). The FAME structures were identified by Shimadzu GCMSQP2010 Ultra with mass selective detector (GC-MSD). Both GC equipments were equipped with ZB-wax capillary columns (30 m, 0.25 mm ID, 0.25  $\mu$ m film, Phenomenex, USA). When calculating the composition, the FID responses were corrected according to the theoretical response factors (Ackman, 2007) and, when calculating the concentrations in medium, the FAME 13:0 (not present in the samples) was used as an internal standard. In the Results, the FAs were marked by using the abbreviations: [carbon number]:[number of double bonds] n-[position of the first double bond calculated from the methyl end] (e.g. 22:6n-3).

### Statistical analyses

#### Gene expression data

GraphPad Prism version 5.02 software was used for the data analysis. The standard deviation (s.d.) was calculated from the average of three independent samples. Statistical analyses comparing gene expression levels in more than two groups was performed with one-way ANOVA and  $P < 0.05$  was considered statistically significant.

#### Lipidomic data

Statistical analyses for lipidomic data was performed with R (version x64 3.2.1). Zero values in the data were imputed with a value corresponding to half of the minimum value of the corresponding lipid across all the samples. PCA was performed for the log<sub>2</sub>-transformed data applying centering and scaling. Heat maps were generated with gplots package by calculating the mean log<sub>2</sub> fold change to samples at day 0 or 12.

#### Correlation analyses

Correlation analyses (Spearman) were performed to study whether the expression of SL metabolism genes pairs with relevant lipid parameters and how strong the potential correlation is.

#### Acknowledgements

The authors acknowledge Markus Happonen, Henna Lappi and Merja Lehtinen for general technical support. Tony Futerman is acknowledged for fruitful discussions about lipidomics.

## Competing interests

T.V., K.M.K. and M.H. are employed by Zora Biosciences, Espoo, Finland. K.E. is currently employed by Lipidomics Consulting, Espoo, Finland. Other authors declare no conflict of interest.

## Author contributions

Conceptualization: M.K., K.E., R.K., K.A.-S.; Methodology: M.K., L.E.V., T.V., K.M.K., K.E., R.K.; Software: M.K., L.E.V., T.V., K.M.K., M.H.; Validation: M.K., L.E.V., T.V., K.M.K., M.H., K.E., R.K.; Formal analysis: M.K., L.E.V., T.V., K.M.K., M.H., K.E., R.K.; Investigation: M.K., L.E.V., T.V., M.H., K.E., R.K.; Resources: K.A.-S.; Writing - original draft: M.K., L.E.V.; Writing - review & editing: M.K., L.E.V., T.V., K.E., R.K., K.A.-S.; Visualization: M.K., L.E.V., M.H.; Supervision: K.A.-S.; Project administration: K.A.-S.; Funding acquisition: K.A.-S.

## Funding

The research leading to these results has received funding from the European Union Seventh Framework Programme [FP7-2007-2013] under two grant agreements, HEALTH-F2-2013-602222 'Targeting novel lipid pathways for treatment of cardiovascular disease' (Athero-Flux), and HEALTH.2012-3057392 'Personalized diagnostics and treatment for high risk coronary artery disease' (RiskyCAD), as well as Instrumentarium Science Foundation (Instrumentarium Tiedesäätiö).

## Supplementary information

Supplementary information available online at <http://dmm.biologists.org/lookup/doi/10.1242/dmm.030841.supplemental>

## References

- Ackman, R.** (2007). *Application of Gas-Liquid Chromatography to Lipid Separation and Analysis*. In *Fatty Acids in Foods and their Health Implications*, Third Edition (ed. C. K. Chow), pp. 47-65. New York: Marcel Dekker, Inc.
- Aires, V., Hichami, A., Filomenko, R., Ple, A., Rebe, C., Bettaieb, A. and Khan, N. A.** (2007). Docosahexaenoic acid induces increases in [Ca<sup>2+</sup>]<sub>i</sub> via inositol 1,4,5-triphosphate production and activates protein kinase C $\gamma$  and - $\delta$  via phosphatidylserine binding site: implication in apoptosis in U937 cells. *Mol. Pharmacol.* **72**, 1545-1556.
- Astudillo, A. M., Balcama, D., Balboa, M. A. and Balsinde, J.** (2012). Dynamics of arachidonic acid mobilization by inflammatory cells. *Biochim. Biophys. Acta Mol. Cell Biol. Lipids* **1821**, 249-256.
- Borodicz, S., Czarasta, K., Kuch, M. and Cudnoch-Jedrzejewska, A.** (2015). Sphingolipids in cardiovascular diseases and metabolic disorders. *Lipids Health Dis.* **14**, 1-8.
- Castro-Gómez, P., García-Serrano, A., Visioli, F. and Fontecha, J.** (2015). Relevance of dietary glycerophospholipids and sphingolipids to human health. *Prostaglandins Leukot. Essent. Fat. Acids* **101**, 41-51.
- Christie, W. W.** (1993). Preparation of ester derivatives of fatty acids for chromatographic analysis. In *Advances in Lipid Methodology* (ed. W. W., Christie), pp. 69-111. Dundee, Scotland: Oily Press.
- Cingolani, F., Futerman, A. H. and Casas, J.** (2016). Ceramide synthases in biomedical research. *Chem. Phys. Lipids* **197**, 25-32.
- Cole, L. K., Vance, J. E. and Vance, D. E.** (2012). Phosphatidylcholine biosynthesis and lipoprotein metabolism. *Biochim. Biophys. Acta Mol. Cell Biol. Lipids* **1821**, 754-761.
- Delgado, A., Casas, J., Liebaria, A., Abad, J. L. and Fabrias, G.** (2006). Inhibitors of sphingolipid metabolism enzymes. *Biochim. Biophys. Acta Biomembr.* **1758**, 1957-1977.
- Ejsing, C. S., Duchoslav, E., Sampaio, J., Simons, K., Bonner, R., Thiele, C., Ekroos, K. and Shevchenko, A.** (2006). Automated identification and quantification of glycerophospholipid molecular species by multiple precursor ion scanning. *Anal. Chem.* **78**, 6202-6214.
- Ekroos, K.** (2012). Lipidomics perspective: from molecular lipidomics to validated clinical diagnostics. In *Lipidomics Technologies and Applications* (ed. K. Ekroos), pp. 1-16. Weinheim, Germany: Wiley-VCH Verlag GmbH & Co. KGaA.
- Ekroos, K., Chernushevich, I. V., Simons, K. and Shevchenko, A.** (2002). Quantitative profiling of phospholipids by multiple precursor ion scanning on a hybrid quadrupole time-of-flight mass spectrometer. *Anal. Chem.* **74**, 941-949.
- Ekroos, K., Ejsing, C. S., Bahr, U., Karas, M., Simons, K. and Shevchenko, A.** (2003). Charting molecular composition of phosphatidylcholines by fatty acid scanning and ion trap MS3 fragmentation. *J. Lipid Res.* **44**, 2181-2192.
- Elaut, G., Henkens, T., Papeleu, P., Snykers, S., Vinken, M., Vanhaecke, T. and Rogiers, V.** (2006). Molecular mechanisms underlying the differentiation process of isolated hepatocytes and their cultures. *Curr. Drug Metab.* **7**, 629-660.
- Fujishima, H., Sanchez Mejia, R. O., Bingham, C. O., III, Lam, B. K., Sapirstein, A., Bonventre, J. V., Austen, K. F. and Arm, J. P.** (1999). Cytosolic phospholipase A2 is essential for both the immediate and the delayed phases of eicosanoid generation in mouse bone marrow-derived mast cells. *Proc. Natl. Acad. Sci. USA* **96**, 4803-4807.
- Gault, C. R., Obeid, L. M. and Hannun, Y. A.** (2010). An overview of sphingolipid metabolism: From synthesis to breakdown. *Adv. Exp. Med. Biol.* **688**, 1-23.
- Ghini, V., Di Nunzio, M., Tenori, L., Valli, V., Danesi, F., Capozzi, F., Luchinat, C. and Bordoni, A.** (2017). Evidence of a DHA signature in the lipidome and metabolome of human hepatocytes. *Int. J. Mol. Sci.* **18**, 1-19.
- Giorgetti, J., Epand, R. M., Buda, C. and Farkas, T.** (1995). Role of phospholipids containing docosahexaenoyl chains in modulating the activity of protein kinase C. *Proc. Natl. Acad. Sci. USA* **92**, 9767-9770.
- Godoy, P., Hewitt, N. J., Albrecht, U., Andersen, M. E., Ansari, N., Bhattacharya, S., Bode, J. G., Bolleyn, J., Borner, C., Böttger, J. et al.** (2013). Recent advances in 2D and 3D in vitro systems using primary hepatocytes, alternative hepatocyte sources and non-parenchymal liver cells and their use in investigating mechanisms of hepatotoxicity, cell signaling and ADME. *Arch. Toxicol.* **87**, 1315-1530.
- Hannun, Y. A. and Obeid, L. M.** (2008). Principles of bioactive lipid signalling: lessons from sphingolipids. *Nat. Rev. Mol. Cell Biol.* **9**, 139-150.
- Haus, J. M., Kashyap, S. R., Kasumov, T., Zhang, R., Kelly, K. R., Defronzo, R. A. and Kirwan, J. P.** (2009). Plasma ceramides are elevated in obese subjects with type 2 diabetes and correlate with the severity of insulin resistance. *Diabetes* **58**, 337-343.
- Hay, D. C., Fletcher, J., Payne, C., Terrace, J. D., Gallagher, R. C. J., Snoeys, J., Black, J. R., Wojtacha, D., Samuel, K., Hannoun, Z. et al.** (2008). Highly efficient differentiation of hESCs to functional hepatic endoderm requires ActivinA and Wnt3a signaling. *Proc. Natl. Acad. Sci. USA* **105**, 12301-12306.
- Heiskanen, L. A., Suoniemi, M., Ta, H. X., Tarasov, K. and Ekroos, K.** (2013). Long-term performance and stability of molecular shotgun lipidomic analysis of human plasma samples. **85**, 8757-8763.
- Holland, W. L. and Summers, S. A.** (2008). Sphingolipids, insulin resistance, and metabolic disease: new insights from in vivo manipulation of sphingolipid metabolism. *Endocr. Rev.* **29**, 381-402.
- Holmgren, G., Sjögren, A.-K., Barragan, I., Sabirsh, A., Sartipy, P., Synnergren, J., Björquist, P., Ingelman-Sundberg, M., Andersson, T. B. and Edsbacke, J.** (2014). Long-term chronic toxicity testing using human pluripotent stem cell-derived hepatocytes. *Drug Metab. Dispos.* **42**, 1401-1406.
- Hornemann, T. and Worgall, T. S.** (2013). Sphingolipids and atherosclerosis. *Atherosclerosis* **226**, 16-28.
- Hu, C. and Li, L.** (2015). In vitro culture of isolated primary hepatocytes and stem cell-derived hepatocyte-like cells for liver regeneration. *Protein Cell* **6**, 562-574.
- Iwabuchi, K., Nakayama, H., Iwahara, C. and Takamori, K.** (2010). Significance of glycosphingolipid fatty acid chain length on membrane microdomain-mediated signal transduction. *FEBS Lett.* **584**, 1642-1652.
- Kim, W. J., Okimoto, R. A., Purton, L. E., Goodwin, M., Haserlat, S. M., Dayyani, F., Sweetser, D. A., McClatchey, A. I., Bernard, O. A., Look, A. T. et al.** (2008). Mutations in the neutral sphingomyelinase gene *Smpd3* implicate the ceramide pathway in human leukemias. *Blood* **111**, 4716-4722.
- Laviad, E. L., Albee, L., Pankova-Kholmyansky, I., Epstein, S., Park, H., Merrill, A. H. and Futerman, A. H.** (2008). Characterization of ceramide synthase 2: Tissue distribution, substrate specificity, and inhibition by sphingosine 1-phosphate. *J. Biol. Chem.* **283**, 5677-5684.
- Leung, A., Nah, S. K., Reid, W., Ebata, A., Koch, C. M., Monti, S., Genereux, J. C., Wiseman, R. L., Wolozin, B., Connors, L. H. et al.** (2013). Induced pluripotent stem cell modeling of multisystemic, hereditary transthyretin amyloidosis. *Stem Cell Rep.* **1**, 451-463.
- Levy, M. and Futerman, A. H.** (2010). Mammalian ceramide synthases. *IUBMB Life* **62**, 347-356.
- Li, Z., Hailemariam, T. K., Zhou, H., Li, Y., Duckworth, D. C., Peake, D. A., Zhang, Y., Kuo, M.-S., Cao, G. and Jiang, X.-C.** (2007). Inhibition of sphingomyelin synthase (SMS) affects intracellular sphingomyelin accumulation and plasma membrane lipid organization. *Biochim. Biophys. Acta Mol. Cell Biol. Lipids* **1771**, 1186-1194.
- Liu, J., Zhang, H., Li, Z., Hailemariam, T. K., Chakraborty, M., Jiang, K., Qiu, D., Bui, H. H., Peake, D. A., Kuo, M.-S. et al.** (2009). Sphingomyelin synthase 2 is one of the determinants for plasma and liver sphingomyelin levels in mice. *Arterioscler. Thromb. Vasc. Biol.* **29**, 850-856.
- Livak, K. J. and Schmittgen, T. D.** (2001). Analysis of relative gene expression data using real-time quantitative PCR and the 2<sup>-</sup> $\Delta\Delta$ CT method. *Methods* **25**, 402-408.
- Llorente, A., Skotland, T., Sylvänte, T., Kauhainen, D., Róg, T., Orlowski, A., Vattulainen, I., Ekroos, K. and Sandvig, K.** (2013). Molecular lipidomics of exosomes released by PC-3 prostate cancer cells. *Biochim. Biophys. Acta Mol. Cell Biol. Lipids* **1831**, 1302-1309.
- Lucendo-Villarin, B., Filis, P., Swortwood, M. J., Huestis, M. A., Meseguer-Ripollés, J., Cameron, K., Iredale, J. P., O'Shaughnessy, P. J., Fowler, P. A. and Hay, D. C.** (2017). Modelling foetal exposure to maternal smoking using hepatoblasts from pluripotent stem cells. *Arch. Toxicol.* **91**, 1-11.
- Lund, R. J., Nikula, T., Rakkonen, N., Närä, E., Baker, D., Harrison, N., Andrews, P., Otonkoski, T. and Laheesmaa, R.** (2012). High-throughput karyotyping of human pluripotent stem cells. *Stem Cell Res.* **9**, 192-195.
- Maceyka, M. and Spiegel, S.** (2014). Sphingolipid metabolites in inflammatory disease. *Nature* **510**, 58-67.



- Manzini, S., Viiri, L. E., Marttila, S. and Aalto-Setälä, K. (2015). A comparative view on easy to deploy non-integrating methods for patient-specific iPSC production. *Stem Cell Rev. Rep.* **11**, 900-908.
- Mao, C. and Obeid, L. M. (2008). Ceramidases: regulators of cellular responses mediated by ceramide, sphingosine, and sphingosine-1-phosphate. *Biochim. Biophys. Acta Mol. Cell Biol. Lipids* **1781**, 424-434.
- Martin, S. and Parton, R. G. (2006). Lipid droplets: a unified view of a dynamic organelle. *Mol. Cell* **7**, 373-378.
- Medine, C. N., Lucendo-Villarin, B., Storck, C., Wang, F., Szkolnicka, D., Khan, F., Pernagallo, S., Black, J. R., Marriage, H. M., Ross, J. A. et al. (2013). Developing high-fidelity hepatotoxicity models from pluripotent stem cells. *Stem Cells Transl. Med.* **2**, 505-509.
- Meikle, P. J., Wong, G., Tzoroties, D., Barlow, C. K., Weir, J. M., Christopher, M. J., MacIntosh, G. L., Goudey, B., Stern, L., Kowalczyk, A. et al. (2011). Plasma lipidomic analysis of stable and unstable coronary artery disease. *Arterioscler. Thromb. Vasc. Biol.* **31**, 2723-2732.
- Merrill, A. H., Jr, Sullards, M. C., Allegood, J. C., Kelly, S. and Wang, E. (2005). Sphingolipidomics: high-throughput, structure-specific, and quantitative analysis of sphingolipids by liquid chromatography tandem mass spectrometry. *Methods* **36**, 207-224.
- Muro, E., Atilla-Gokcumen, G. E. and Eggert, U. S. (2014). Lipids in cell biology: how can we understand them better? *Mol. Biol. Cell* **25**, 1819-1823.
- Nestel, P. J. and Couzens, E. A. (1966). Turnover of individual cholesterol esters in human liver and plasma. *J. Clin. Invest.* **45**, 1234-1240.
- Ng, S., Schwartz, R. E., March, S., Gaistian, A., Gural, N., Shan, J., Prabhu, M., Mota, M. M. and Bhatia, S. N. (2015). Human iPSC-derived hepatocyte-like cells support plasmodium liver-stage infection in vitro. *Stem Cell Rep.* **4**, 348-359.
- Park, J.-W., Park, W.-J. and Futerman, A. H. (2014). Ceramide synthases as potential targets for therapeutic intervention in human diseases. *Biochim. Biophys. Acta Mol. Cell Biol. Lipids* **1841**, 671-681.
- Rawicz, W., Smith, B. A., McIntosh, T. J., Simon, S. A. and Evans, E. (2008). Elasticity, strength, and water permeability of bilayers that contain raft microdomain-forming lipids. *Biophys. J.* **94**, 4725-4736.
- Rong, X., Wang, B., Dunham, M. M., Hedde, P. N., Wong, J. S., Gratton, E., Young, S. G., Ford, D. A. and Tontonoz, P. (2015). Lpcat3-dependent production of arachidonoyl phospholipids is a key determinant of triglyceride secretion. *Elife* **4**, 1-23.
- Ruhanen, H., Nidhina Haridas, P. A., Eskelinen, E.-L., Eriksson, O., Olkkonen, V. M. and Kälälä, R. (2017). Depletion of TM6SF2 disturbs membrane lipid composition and dynamics in HuH7 hepatoma cells. *Biochim. Biophys. Acta Mol. Cell Biol. Lipids* **1862**, 676-685.
- Russo, G. L. (2009). Dietary n-6 and n-3 polyunsaturated fatty acids: from biochemistry to clinical implications in cardiovascular prevention. *Biochem. Pharmacol.* **77**, 937-946.
- Sales, S., Graessler, J., Ciucci, S., Al-Atrib, R., Vihervaara, T., Schuhmann, K., Kauhanen, D., Sysi-Aho, M., Bornstein, S. R., Bickel, M. et al. (2016). Gender, contraceptives and individual metabolic predisposition shape a healthy plasma lipidome. *Sci. Rep.* **6**, 27710.
- Ståhlman, M., Ejlsing, C. S., Tarasov, K., Perman, J., Borén, J. and Ekroos, K. (2009). High-throughput shotgun lipidomics by quadrupole time-of-flight mass spectrometry. *J. Chromatogr. B Anal. Technol. Biomed. Life Sci.* **877**, 2664-2672.
- Stübiger, G., Aldover-Macasaet, E., Bicker, W., Sobal, G., Willfort-Ehringer, A., Pock, K., Bochkov, V., Widhalm, K. and Belgacem, O. (2012). Targeted profiling of atherogenic phospholipids in human plasma and lipoproteins of hyperlipidemic patients using MALDI-QIT-TOF-MS/MS. *Atherosclerosis* **224**, 177-186.
- Szkolnicka, D., Farnworth, S. L., Lucendo-Villarin, B., Storck, C., Zhou, W., Iredale, J. P., Flint, O. and Hay, D. C. (2014). Accurate prediction of drug-induced liver injury using stem cell-derived populations. *Stem Cells Transl. Med.* **3**, 141-148.
- Szkolnicka, D., Lucendo-Villarin, B., Moore, J. K., Simpson, K. J., Forbes, S. J. and Hay, D. C. (2016). Reducing hepatocyte injury and necrosis in response to paracetamol using noncoding RNAs. *Stem Cells Transl. Med.* **5**, 764-772.
- Takahashi, K., Tanabe, K., Ohnuki, M., Narita, M., Ichisaka, T., Tomoda, K. and Yamanaka, S. (2007). Induction of pluripotent stem cells from adult human fibroblasts by defined factors. *Cell* **131**, 861-872.
- Tigistu-Sahle, F., Lampinen, M., Kilpinen, L., Holopainen, M., Lehenkari, P., Laitinen, S. and Kälälä, R. (2017). Metabolism and phospholipid assembly of polyunsaturated fatty acids in human bone marrow mesenchymal stromal cells. *J. Lipid Res.* **58**, 92-110.
- Turk, H. F. and Chapkin, R. S. (2013). Membrane lipid raft organization is uniquely modified by n-3 polyunsaturated fatty acids. *Prostaglandins Leukot. Essent. Fat. Acids* **88**, 43-47.
- Van Meer, G., Voelker, D. R. and Feigenson, G. W. (2008). Membrane lipids: where they are and how they behave. *Nat. Rev. Mol. Cell Biol.* **9**, 112-124.
- Wang, L., Zhang, T., Wang, L., Cai, Y., Zhong, X., He, X., Hu, L., Tian, S., Wu, M., Hui, L. et al. (2017). Fatty acid synthesis is critical for stem cell pluripotency via promoting mitochondrial fission. *EMBO J.* **36**, 1330-1347.
- Wassall, S. R. and Stillwell, W. (2009). Polyunsaturated fatty acid-cholesterol interactions: domain formation in membranes. *Biochim. Biophys. Acta Biomembr.* **1788**, 24-32.
- Wassall, S. R., Brzustowicz, M. R., Shaikh, S. R., Cherezov, V., Caffrey, M. and Stillwell, W. (2004). Order from disorder, corraling cholesterol with chaotic lipids: The role of polyunsaturated lipids in membrane raft formation. *Chem. Phys. Lipids* **132**, 79-88.
- Watson, A. D. (2006). Thematic review series: systems biology approaches to metabolic and cardiovascular disorders. Lipidomics: a global approach to lipid analysis in biological systems. *J. Lipid Res.* **47**, 2101-2111.
- Wenk, M. R. (2005). The emerging field of lipidomics. *Nat. Rev. Drug Discov.* **4**, 594-610.
- Wolfrum, C., Asilmaz, E., Luca, E., Friedman, J. M. and Stoffel, M. (2004). Foxa2 regulates lipid metabolism and ketogenesis in the liver during fasting and in diabetes. *Nature* **432**, 1027-1032.
- Yamashita, A., Sugiura, T. and Waku, K. (1997). Acyltransferases and transacylases involved in fatty acid remodeling of phospholipids and metabolism of bioactive lipids in mammalian cells. *J. Biochem.* **122**, 1-16.
- Yang, D., Yuan, Q., Balakrishnan, A., Bantel, H., Klusmann, J.-H., Manns, M. P., Ott, M., Cantz, T. and Sharma, A. D. (2016). MicroRNA-125b-5p mimic inhibits acute liver failure. *Nat. Commun.* **7**, 11916.
- Younossi, Z. M., Koenig, A. B., Abdelatif, D., Fazel, Y., Henry, L. and Wymer, M. (2016). Global epidemiology of non-alcoholic fatty liver disease-Meta-analytic assessment of prevalence, incidence, and outcomes. *Hepatology* **64**, 73-84.
- Zhou, X., Sun, P., Lucendo-Villarin, B., Angus, A. G. N., Szkolnicka, D., Cameron, K., Farnworth, S. L., Patel, A. H. and Hay, D. C. (2014). Modulating innate immunity improves hepatitis C virus infection and replication in stem cell-derived hepatocytes. *Stem Cell Rep.* **3**, 204-214.



## PUBLICATION

### II

**hiPSC-derived hepatocytes closely mimic the lipid profile of primary hepatocytes: A future personalised cell model for studying the lipid metabolism of the liver.**


Kiammehr M, Alexanova A, Viiri L, Heiskanen L, Vihervaara T, Kauhanen D, Ekroos K, Laaksonen R, Käkälä R, Aalto-Setälä K.

Journal of Cellular Physiology. 2018  
<https://doi.org/10.1002/jcp.27131>

**Publication reprinted with the permission of the copyright holders.**



# hiPSC-derived hepatocytes closely mimic the lipid profile of primary hepatocytes: A future personalised cell model for studying the lipid metabolism of the liver

Mostafa Kiamehr<sup>1</sup>  | Anna Alexanova<sup>1</sup> | Leena E. Viiri<sup>1</sup> | Laura Heiskanen<sup>2</sup> | Terhi Vihervaara<sup>2</sup> | Dimple Kauhanen<sup>2</sup> | Kim Ekroos<sup>5</sup> | Reijo Laaksonen<sup>1,2</sup> | Reijo Käkälä<sup>3</sup> | Katriina Aalto-Setälä<sup>1,4</sup>

<sup>1</sup>Faculty of Medicine and Life Sciences, University of Tampere, Tampere, Finland

<sup>2</sup>Zora Biosciences, Espoo, Finland

<sup>3</sup>Faculty of Biology and Environmental Sciences, University of Helsinki, Helsinki, Finland

<sup>4</sup>Heart Hospital, Tampere University Hospital, Tampere, Finland

<sup>5</sup>Lipidomics Consulting Ltd, Espoo, Finland

## Correspondence

Mostafa Kiamehr, Faculty of Medicine and Life Sciences, University of Tampere, Tampere, Finland.

Email: mostafa.kiamehr@uta.fi

## Funding information

Finnish Cardiovascular Foundation; Instrumentarium Tiedesäätiö; FP7 Health, Grant/Award Numbers: F2-2013-602222, 2012-3057392

## Abstract

Hepatocyte-like cells (HLCs) differentiated from human-induced pluripotent stem cells offer an alternative platform to primary human hepatocytes (PHHs) for studying the lipid metabolism of the liver. However, despite their great potential, the lipid profile of HLCs has not yet been characterized. Here, we comprehensively studied the lipid profile and fatty acid (FA) metabolism of HLCs and compared them with the current standard hepatocyte models: HepG2 cells and PHHs. We differentiated HLCs by five commonly used methods from three cell lines and thoroughly characterized them by gene and protein expression. HLCs generated by each method were assessed for their functionality and the ability to synthesize, elongate, and desaturate FAs. In addition, lipid and FA profiles of HLCs were investigated by both mass spectrometry and gas chromatography and then compared with the profiles of PHHs and HepG2 cells. HLCs resembled PHHs by expressing hepatic markers: secreting albumin, lipoprotein particles, and urea, and demonstrating similarities in their lipid and FA profile. Unlike HepG2 cells, HLCs contained low levels of lysophospholipids similar to the content of PHHs. Furthermore, HLCs were able to efficiently use the exogenous FAs available in their medium and simultaneously modify simple lipids into more complex ones to fulfill their needs. In addition, we propose that increasing the polyunsaturated FA supply of the culture medium may positively affect the lipid profile and functionality of HLCs. In conclusion, our data showed that HLCs provide a functional and relevant model to investigate human lipid homeostasis at both molecular and cellular levels.

## KEYWORDS

fatty acid (FA), gas chromatography, hepatocyte-like cell (HLC), HepG2, human-induced pluripotent stem cell (hiPSC), lipidomics, mass spectrometry (MS), primary human hepatocyte (PHH)

**Abbreviations:** APOA1, apolipoprotein A-I gene; APOB, apolipoprotein B gene; ASGR, asialoglycoprotein receptor; BMP4, bone morphogenic protein 4; CE, cholesteryl ester; Cer, ceramide; DAG, diacylglycerol; DE, definitive endoderm; EGF, epidermal growth factor; ELOVL, fatty acid elongase; FA, fatty acid; FADS, fatty acid desaturase; FASN, fatty acid synthase; Gb3, globotriaosylceramide; GCK, Glucokinase; Glc/GalCer, glucosyl/galactosylceramide; GSL, glycosphingolipid; HGF, hepatocyte growth factor; hiPSC, human induced pluripotent stem cell; HLC, hepatocyte-like cell; hLTR, Human Liver Total RNA; LacCer, lactosylceramide; LPC, lysophosphatidylcholine; LPE, lysophosphatidylethanolamine; LPI, lysophosphatidylinositol; LPL, lysophospholipid; M1, Method 1; M2, Method 2; M3, Method 3; M4, Method 4; M5, Method 5; MUFA, monounsaturated fatty acid; PC, phosphatidylcholine; PE, phosphatidylethanolamine; PHH, primary human hepatocyte; PI, phosphatidylinositol; PL, phospholipid; PUFA, polyunsaturated fatty acid; SFA, saturated fatty acid; SL, sphingolipid; SM, sphingomyelin; TAG, triacylglycerol; UGCG, UDP-glucose ceramide glucosyltransferase.

## 1 | INTRODUCTION

The liver plays an important role in the regulation of many physiological functions of the body, including lipid and carbohydrate metabolism, glycolytic/urea metabolism, plasma protein synthesis, and the detoxification of a wide variety of molecules (Si-Tayeb et al., 2010). Hepatocytes, which comprise about 70% of the liver's mass, originate from the anterior portion of the definitive endoderm (DE), one of the three embryonic layers (Blouin, Bolender, & Weibel, 1977). Hepatocytes handle many crucial metabolic functions of the liver, including the synthesis of lipoproteins, triacylglycerols (TAGs), cholesterol, and phospholipids (PLs; Gordillo, Evans, & Gouon-Evans, 2015).

Primary human hepatocytes (PHHs) are currently considered the "gold standard" in cell modeling for studying, for example, liver physiology, toxicity, and lipid homeostasis. Typically, PHHs are obtained from cadaveric donors, but they are scarce and functionally heterogeneous, and it is hard to maintain them in a culture. When cultured, PHHs lose functionality relatively fast, and their liver-specific features progressively deteriorate, which particularly hampers long-term studies (Elaut et al., 2006; Godoy et al., 2013). To address these limitations, various human hepatoma cell lines, including HepG2 and Huh7, have been used due to their ease of handling, unlimited life span, and stable phenotype. Nevertheless, they do not faithfully mirror the metabolic activities of healthy liver cells. In fact, the expression levels and profiles of genes involved in liver-specific functions are poorly presented in these systems (Olsavsky et al., 2007). As a result, hepatoma cell lines have failed to predict the numerous adverse hepatotoxic side effects of new drugs (Castell, Jover, Martínez-Jiménez, & Gómez-Lechón, 2006). Alternatively, animal models, such as rats and mice, or animal primary hepatocytes have been widely used to study lipid metabolism and lipoprotein production in the liver (Kvilekval, Lin, Cheng, & Abumrad, 1994). However, the information gained from murine cells is not fully translatable to humans, and there are significant differences in lipid metabolism between the species. Animal models are also expensive and unsuitable for large-scale screening. Furthermore, due to growing ethical concerns, there is an urgent need to reduce the use of rodents and other animal models in research.

Human-induced pluripotent stem cells (hiPSCs) provide an unlimited supply of tissue-specific differentiated cell types for disease modeling and cell therapy. Hepatocytes differentiated from pluripotent stem cells circumvent the problem of the limited availability of cells faced when working with PHHs. They show very similar characteristics to PHHs; for instance, they secrete albumin as well as urea, and to some extent express drug transporters and cytochrome P450 enzymes (Kia et al., 2012). Unlike rodent hepatocytes and some human hepatoma cells, these hepatocyte-like cells (HLCs) are sensitive to hepatitis C virus infection and support viral replication similar to PHHs (Schwartz et al., 2012). Patient-specific iPSC lines provide us with an advantageous system of HLCs from patients of different genetic backgrounds, a prerequisite for the development of personalised medicine.

The generation of hiPSC-derived HLCs (hiPSC-HLCs) in large quantities enables their use in modeling inborn errors of hepatic metabolism, understanding the molecular basis of liver cell differentiation, studying disease mechanisms, and facilitating drug discovery and safety. HLCs have already proven to be of great value in developing novel therapeutics (Medine et al., 2013; Szkolnicka et al., 2014) and identifying the noncoding micro-RNAs regulating human liver damage (Szkolnicka et al., 2016; Yang et al., 2016). HLCs have also been successfully used as *in vitro* cell culture systems, for example, to recapitulate the pathophysiology of familial hypercholesterolemia (Cayo et al., 2012) and human cholesterol homeostasis (Krueger et al., 2013). Lipid defects are central to the pathogenesis of many common diseases, such as atherosclerosis (Meikle et al., 2011; Stübiger et al., 2012) and nonalcoholic fatty liver disease (Ruhanen et al., 2017; Younossi et al., 2016). Therefore, hiPSC-HLCs offer a great platform for investigating the basic mechanisms of lipid metabolism and its dysregulation in a patient-specific manner. However, to date, no detailed studies have yet been performed on the lipid profile and fatty acid (FA) metabolism of HLCs. To better use HLCs as a cell model to study the role of molecular lipids in liver diseases, it is essential to know their lipid profile in relation to actual human adult liver tissue and to the currently used cell models, namely PHHs and hepatoma cell lines.

Hepatic differentiation methods have greatly improved over the last decade, enabling the efficient generation of high quality HLCs from pluripotent stem cells (Cameron et al., 2015; Hannan, Segeritz, Touboul, & Vallier, 2013; Hay et al., 2008; Kajiwarra et al., 2012; Si-Tayeb et al., 2010). Nevertheless, the experimental details and some differentiation factors differ between the current protocols, which might affect the phenotype of the HLCs. To reproduce the physiological conditions of the human liver, it is crucial to generate functional HLCs that are as similar as possible to PHHs. In this study, we describe five protocols for generating HLCs from hiPSCs and comprehensively compare the morphology, genetics, biochemistry, and functional traits of the HLCs produced. In addition, we compare the HLCs with the two most common cell models currently used—PHHs and HepG2 cells—as well as human liver tissue. Most importantly, the lipid profiles of HLCs, PHHs, and HepG2 cells are analyzed by both mass spectrometry (MS) and gas chromatography, and the similarities and main differences between the cell types are discussed in light of selected key genes involved in FA metabolism. Finally, the lipid profile of HLCs is fully characterized, and the potential and limitations of HLCs as a model for studying lipid metabolism are evaluated.

## 2 | MATERIAL AND METHODS

### 2.1 | Ethical issues

The study and patient recruitment have been approved by the Ethics Committee of Tampere University Hospital (approval number: R12123). All participants providing skin biopsies were adults more

than 18 years old who had signed an informed consent form after receiving both oral and written descriptions of the study.

## 2.2 | hiPSC reprogramming and cell culture

Three hiPSC lines (UTA.10100.EURCAs, UTA.11104.EURCAs, and UTA.11304.EURCCs) were generated directly from the fibroblasts of three individuals. Pluripotency was induced with the Sendai reprogramming kit (OCT4, SOX2, KLF4, C-MYC; CytoTune; Life Technologies, USA) based on the protocol described by Ohnuki, Takahashi, Yamanaka, (2009) and Takahashi & Yamanaka, (2006). hiPSCs were then maintained as described before (Kiamehr et al., 2017). Details of the hiPSC cell culture are also described in the Supporting Information.

## 2.3 | Hepatic differentiation

In all methods except Method 4 (M4), hiPSCs were transferred from mouse embryonic fibroblasts to Geltrex™ (USA; Cat: A14133-01, 1:50 dilution), kept in mTeSR1™ medium, and adapted to the changed culture conditions for a few passages before commencing the differentiation. In M4, hiPSCs were adapted on Laminin 521 (BioLamina, Lot: 80104) first, and the differentiation was completed on Laminin mix 111/521-coated plates (3:1 ratio, 10 µg/ml). The hiPSCs used in all methods were at passage 20 or higher before commencing the differentiation. Three lines were differentiated using each method, except Method 5 (M5), which was applied to two cell lines. Figure 1 shows a schematic view of all five methods used in the study. Details of the five differentiation methods are described in detail in the Supporting Information.

## 2.4 | PHHs and HepG2 cells

Cryopreserved PHHs (Cat. No. HMCPIs, Lot. HU8210, USA) were purchased from Gibco®, and hepatocellular carcinoma cells (HepG2, ATCC-HB-8065, Lot. No. 59947519) were purchased from ATCC™. Both cells were plated according to the manufacturer's instructions. PHHs were cultured in William's E medium (A1217601, Gibco, USA) supplemented with cocktail B (Gibco, CM 4000) and dexamethasone, whereas the HepG2 cells were cultured in Dulbecco's modified Eagle medium supplemented with 10% FBS.

## 2.5 | RT-polymerase chain reaction

RNA extraction and polymerase chain reaction (PCR) for pluripotency markers (OCT4, NANOG, SOX2, and SSEA4) were performed as published before (Manzini, Viiri, Marttila, & Aalto-Setälä, 2015).

## 2.6 | Quantitative PCR (qPCR) analysis

RNA samples were collected at the hiPSC, DE, and HLC stages, and RNA was extracted using an RNeasy kit (Qiagen, Germany, Cat. No. 74106). Complementary DNA (cDNA) was generated using a high

	Pluripotent	Definitive endoderm	Hepatic specification	Hepatic maturation
<b>Method 1</b>	iPSCs on Geltrex 3-4 days	Act. A, CHIR 99021, NaB 2 days	RPMI, BMP4, bFGF, B27 3 days	HCM (no EGF), HGF, OSM Up to day 20
<b>Method 2</b>	iPSCs on Geltrex 3-4 days	Act. A, Wnt3, NaB 5-6 days	Ko-DMEM, Ko-SR, βME, NEAA, DMSO 7 days	L-15, HGF, OSM Up to day 20
<b>Method 3</b>	Seeding single iPSCs on Geltrex	Act. A, Wnt3, NaB 1 day	Ko-DMEM, Ko-SR, βME, NEAA, DMSO 7 days	HCM, HGF, OSM Up to day 20
<b>Method 4</b>	Seeding single iPSCs on Laminin 521/111	Act. A, Wnt3, NaB 1 day	Ko-DMEM, Ko-SR, βME, NEAA, DMSO 7 days	HCM, HGF, OSM Up to day 20
<b>Method 5</b>	iPSCs on Geltrex for 24 hrs	STEMdiff™ DE Kit 4 days	Ko-DMEM, Ko-SR, βME, NEAA, DMSO 7 days	HCM, HGF, OSM Up to day 20

**FIGURE 1** A schematic representation of the five hepatic differentiation protocols used for generating hepatocyte-like cells (HLCs). Differentiation in Method 1 and Method 2 (M1 and M2) were started with hiPSC colonies, in Method 3 and Method 4 (M3 and M4) with dissociated iPSC single cells, and in Method 5 (M5) with 24 hrs post-cultured hiPSCs. Plates in Method 4 (M4) were coated with a mix of Laminin 111/521 (3:1 ratio) instead of the Geltrex™ used in the remainder of the methods. hiPSC: human-induced pluripotent stem cell [Color figure can be viewed at [wileyonlinelibrary.com](http://wileyonlinelibrary.com)]

capacity cDNA Reverse Transcription kit (Applied Biosystems) according to the manufacturer's instructions in the presence of an RNase inhibitor. cDNA was multiplied either by the Power SYBR Green PCR Master Mix (Life Technology, Cat. No. 1408470, Austin, TX) and gene-specific primers (OCT4, SOX17, FOXA2, AFP, ALB) or by the TaqMan Universal Master Mix (Applied Biosystems, 4304437, Austin, TX) and gene-specific TaqMan probes (APOA1, APOB, FADS1, FADS2, ELOVL2, ELOVL5, FASN) using the BioRad CFX384 Real-Time PCR Detection System. Values were normalized to GAPDH, which was used as an endogenous control, and relative quantification was calculated by the  $\Delta\Delta CT$  method (Livak & Schmittgen, 2001). PHH was used as the reference sample.

First Choice® Human Liver Total RNA (hLTR, Cat. No. AM7960), purchased from Ambion®, was used as an extra control. The results from qPCR were compared for the HLCs and the three reference samples (PHHs, hLTR, and HepG2 cells).

## 2.7 | Immunostaining

Cells were fixed, stained, and visualized as described before (Kiamehr et al., 2017). Details are also provided in the Supporting Information.

The percentage of ALB-positive cells and binuclear HLCs were calculated manually by counting HLCs in 3–5 stained areas and calculating the average.

## 2.8 | low-density lipoprotein uptake

The ability of the cells to uptake low-density lipoprotein (LDL) was evaluated by incubating the HLCs with labeled LDL (Cell-based assay kit, Cayman, USA, Cat. No. 10011125) for 4 hr, after which the cells were imaged by fluorescent microscopy.

## 2.9 | FACS analysis

To analyze the number of CXCR4-positive cells, endodermal cells were detached with Versene (Gibco®, UK), suspended in 3%–5% bovine serum albumin buffer, stained with a PE-conjugated CXCR4 antibody (R&D Systems FAB173P, Minneapolis, 10 µl for 10<sup>6</sup> cells) for 15 min at RT, washed three times, and analyzed using the Accuri™ C6 device (BD Biosciences).

## 2.10 | Albumin, urea, and TAG secretion

At the late stage of hepatic differentiation, HLCs were evaluated for their functionality. The albumin, urea, and TAG content of the conditioned medium were determined, respectively, with the Human Albumin ELISA Quantitation kit (Bethyl Laboratory), the Quanti-Chrom™ Urea Assay Kit (BioAssay Systems, USA), and the Triglyceride Quantification Kit (BioVision Inc., Cat. No. K622-100, USA) according to the manufacturers' instructions. The values were normalized to cell numbers. The results were then compared with the data from the PHHs and HepG2 cells, which were cultured in parallel with the HLCs.

## 2.11 | Lipid mass spectrometry

### 2.11.1 | Lipid sample preparation and extraction

Lipids (sphingolipids [SL], cholesterol, glycerolipids, and glycerophospholipids) were extracted from the HLCs by Hamilton Robotics AB and studied by shotgun lipidomics. The detailed procedure is described by Kiamehr et al., (2017).

### 2.11.2 | Mass spectrometric analyses and data processing

In the shotgun lipidomics (cholesteryl ester [CE], diacylglycerol [DAG], sphingomyelin [SM], lysophosphatidylcholine [LPC], lysophosphatidylethanolamine [LPE], lysophosphatidylserine, lysophosphatidylglycerol, and lysophosphatidylinositol [LPI]), lipid extracts were analyzed on a hybrid triple quadrupole/linear ion trap mass spectrometer (QTRAP 5500) equipped with a robotic nanoflow ion source (NanoMate, Advion Biosciences Inc., Ithaca, NJ) as described by Heiskanen, Suoniemi, Ta, Tarasov, & Ekroos, (2013). Molecular lipids were analyzed in positive ion mode using lipid class-specific

precursor ion or neutral loss scans (Ekroos, Chernushevich, Simons, & Shevchenko, 2002; Ekroos et al., 2003).

Sphingolipids (ceramide [Cer], glucosyl/galactosylceramide [Glc/GalCer], lactosylceramide [LacCer], and globotriaosylceramide [Gb3]) and molecular PLs (phosphatidylcholines [PC], phosphatidylethanolamines [PE], and phosphatidylinositols [PI]) were analyzed with a targeted approach using ultra-high-pressure liquid chromatography-mass spectrometry (UHPLC-MS; Merrill, Sullards, Allegood, Kelly, & Wang, 2005). An analytical Acquity BEH C18, 2.1 × 50 mm column with a particle size of 1.7 µm (Waters, Milford, MA) heated to 60°C was used. Mobile phases consisted of 10 mM ammonium acetate in water with 0.1% formic acid (solvent A) and 10 mM ammonium acetate in acetonitrile/isopropanol (4:3, v/v) containing 0.1% formic acid (solvent B). The flow rate was set to 500 µl/min. Sphingolipids were separated with a 15 min linear gradient from 75% B to 100% B, while molecular PLs were analyzed using a 10 min gradient from 75% B to 80% B. Both sphingolipids and PLs were analyzed on a hybrid triple quadrupole/linear ion trap mass spectrometer (5500 QTRAP) equipped with an UHPLC system (CTC HTC PAL autosampler and Rheos Allegro pump or Shimadzu Nexera X2) using a multiple reaction monitoring based method in positive ion mode for sphingolipids and negative ion mode for molecular PLs. Curtain gas was set at 25; the ion spray voltage was set at 5000 V in positive ion mode and −4500 V in negative ion mode, and the ion source was heated to 400°C in positive mode and to 300°C in negative ion mode. The collision energy was optimized for each lipid class. Identified lipids were quantified by normalizing against their respective internal standard (Ejsing et al., 2006) and total protein concentrations in the cell sample. Total protein concentrations were determined using the Micro BCA™ Protein Assay Kit (Thermo Scientific Pierce Protein Research Products) according to the manufacturer's instructions. Data processing was performed by MultiQuant, LipidView (AB Sciex) software and SAS.

## 2.12 | FA gas chromatography

To confirm our observations from the MS analysis of molecular lipids and to investigate the effect of the medium on the FA profile of the cells, the FA composition of HLCs, PHHs, and HepG2 cells and their media was analyzed by gas chromatography as described in detail by Kiamehr et al., (2017). Briefly, the acyl chains in the cell pellet lipids or the lipid residues of the nitrogen-dried media were converted to FA methyl esters (FAMES) in a transesterification reaction with 1% methanolic H<sub>2</sub>SO<sub>4</sub>. The quantitative analysis of the FAMES, which were extracted into hexane, was performed using a Shimadzu GC-2010 Plus gas chromatograph with a flame-ionization detector, and the FAME structures were identified by Shimadzu GCMSQP2010 Ultra with a mass selective detector. In both systems, the components of the FAME mixtures were separated in ZB-wax capillary columns (30 m, 0.25 mm ID, 0.25 µm film; Phenomenex). The calculations of the FA compositions and concentrations followed standard procedures (Kiamehr et al., 2017), and the FAs were marked by using the abbreviations: [carbon number]:[number of



double bonds] n-[position of the first double bond calculated from the methyl end] (e.g., 22:6n-3).

### 2.13 | Statistical analysis

GraphPad Prism version 5.02 software was used for the data analysis. Data are presented as means  $\pm$  standard deviation with *n* representing the number of independent experiments. The results were compared using one-way analysis of variance, followed by Bonferroni's multiple-comparison test. A *p* value < 0.05 was considered statistically significant.

## 3 | RESULTS

### 3.1 | Cell morphology during hepatic differentiation

In all methods, dramatic morphological changes were observed, particularly during the first few days of DE differentiation. In all methods except M5, migrating DE cells possessed a spiky morphology, whereas in M5, migrating cells were instead more round or square-shaped (Supporting Information Figure S1a). In addition, the amount of cell death in M5 was considerably lower than in the other methods. No morphological differences were observed between the DE cells treated with CHIR 99021 (Method 1, M1) or Wnt3 (Methods 2–4, M2–4). Initiating differentiation with single cells in M3 and M4 did not yield a higher efficiency of DE formation compared with M1 and M2, which were started with colonies (Supporting Information Figures S1a and S3). However, we did observe cells with a DE morphology appearing one or even two days earlier in methods initiated with single cells compared with methods initiated with colonies (Supporting Information Figure S1a). At the hepatic specification stage, cells treated with basic fibroblast growth factor, bone morphogenic protein 4 (BMP4), and hepatocyte growth factor (HGF; M1) clearly had a different morphology compared with the cells treated with DMSO (M2–5; Supporting Information Figure S1b), which might imply different pathways toward hepatoblasts in those protocols.

Binucleation is a feature of adult hepatocytes and generally considered a sign of terminal differentiation (Miyaoaka & Miyajima, 2013). We found 29% of the PHHs and on average 10% of the HLCs to be binuclear (Figures 1b and 2a). The HLCs differentiated by M4 showed the closest binuclearity (16%) to the PHHs. No individual cell line was shown to be more potent in generating binuclear cells.

### 3.2 | Characterization of DE and HLCs at the protein level

hiPSCs expressed OCT4 protein, which was lost during the DE stage, while the expression of DE markers SOX17 and FOXA2 was upregulated (Supporting Information Figure S2a). The efficiency of the DE differentiation, estimated by measuring the CXCR4 expression by flow cytometry, did not differ across M1, M2, and M3

(Supporting Information Figure S2b). In M4 and M5, the amount of CXCR4-positive cells was lower than in the other methods.

The immature hepatic marker AFP was expressed in hepatic progenitor cells and remained expressed until the later stages in all five methods (Figure 2a). In addition, ALB, LDL receptor (LDL-R), and asialoglycoprotein receptor (ASGR) were all expressed in mature HLCs (Figure 2a and Supporting Information Figure S5). The average of the ALB-positive cells in M1 to M5 was 9.8%, 16.6%, 20.8%, 37.7%, and 31.5%, respectively, and the percentage in M4 was significantly higher than in M1, M2, and M3, but not in M5 (Figure 2b). More than 90% of M2- to M5-HLCs were positive for ASGR (data not shown).

### 3.3 | Gene regulation

As expected, OCT4 was highly expressed at the iPSC stage, whereas at the DE stage, OCT4 was dramatically downregulated in most of the cell lines, and SOX17 and FOXA2 were highly expressed (Supporting Information Figure S6). Further differentiation toward HLCs resulted in significant downregulation of SOX17, whereas FOXA2 remained upregulated during the rest of the differentiation and maturation of the HLCs (Figure 2c and Supporting Information Figure S7). The HLCs expressed SOX17 at the same levels as hLTR. The level of FOXA2 in the HLCs was comparable to those in the reference samples PHH, hLTR, and HepG2. AFP was upregulated during the early and late hepatic differentiation stages, indicating the immature characteristic of the HLCs. The expression of AFP in the M2-HLCs was statistically significantly higher than in the M1-HLCs. ALB was dramatically upregulated in mature HLCs, up to  $2 \times 10^5$ -fold compared with that in the hiPSCs, and its levels remained close but below those found in the PHHs. The expression of ALB in the M5-HLCs was significantly higher than in the M1-HLCs ( $p < 0.01$ ) and M3-HLCs ( $p < 0.05$ ). The levels of ALB expression were comparable between the HepG2 and the PHHs; however, ALB expression was about 19-fold higher in the hLTR when compared with the PHHs.

### 3.4 | Hepatic maturation and functionality

The liver is responsible for producing serum albumin. Therefore, we evaluated the ability of HLCs to secrete albumin into the conditioned medium. All HLCs were able to secrete albumin (Figure 2d). Albumin secretion by UTA.11304 differentiated by M3 was about fourfold higher compared with the same cell line differentiated by M1 or M2, and twofold higher compared with M4 (data not shown), but no other statistically significant differences were observed between the differentiation protocols. However, PHHs secreted significantly larger amounts of albumin than the HLCs or even the HepG2 cells.

The level of secreted urea by the cell lines differentiated by M3 and M4 was considerably higher compared with same lines differentiated by M1, M2, and M5 and relatively closer to the amount of urea secreted by the PHHs (Figure 2d). In fact, the level of urea secreted by the HLCs differentiated by M1, M2, and M5 was comparable to the HepG2 cells, which secreted 6.5-fold less urea than the PHHs.

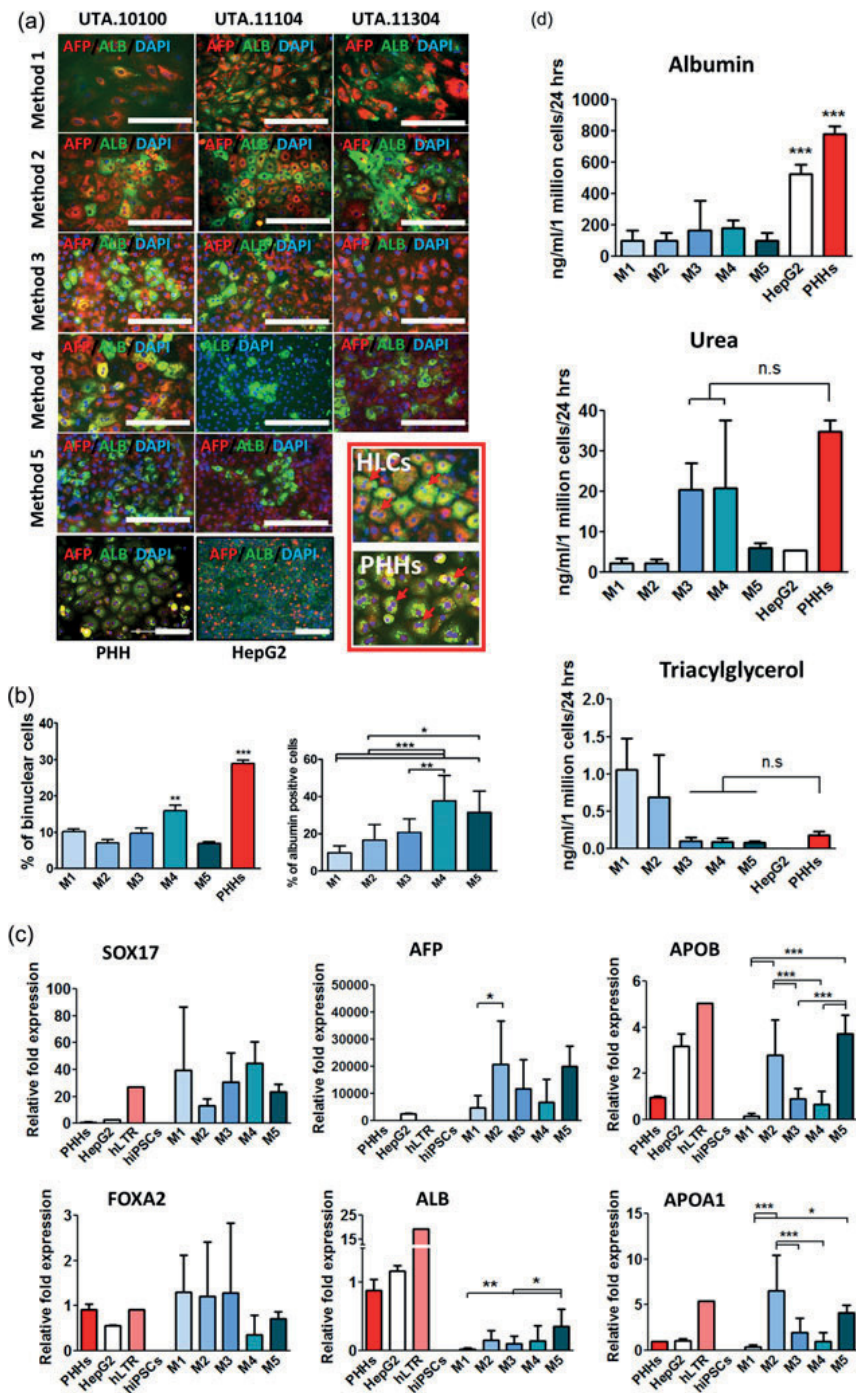


FIGURE 2 Continued.

TAG secretion in the cell lines differentiated by M3, M4, and M5 was at similar levels as in the PHHs (Figure 2d). However, cell lines differentiated by M1 and M2 secreted, on average, 5.9- and 3.8-fold more TAG than the PHHs. We were not able to detect secreted TAG in the HepG2 culture medium due to medium interference.

Apolipoprotein A-I (APOA1) encodes for apoA, which is the main protein component of high-density lipoproteins (HDL). The product of apolipoprotein B (APOB) is the main protein component of very-low-density lipoprotein (VLDL) and LDL. The expression of both APOA1 and APOB in the HLCs was comparable to the HepG2 cells, PHHs, and hLTR, which further indicated the functionality of the HLCs (Figure 2c). Interestingly, both APOA1 and APOB were expressed almost 5.5-fold more in hLTR compared with the PHHs.

All the cell lines were able to uptake the labeled LDL from the culture medium (Supporting Information Figure S5). This was confirmed by staining the LDL-R by monoclonal antibody (Supporting Information Figure S4).

### 3.5 | Lipid profiles of HLCs differentiated by different methods

The HLCs differentiated by M3, M4, and M5 showed superior functionality as for TAG and urea secretion when compared with M1 and M2. In addition, the M5-HLCs expressed higher ALB compared with the HLCs differentiated by M1 and M3. Therefore, we selected the HLCs differentiated by M3, M4, and M5, analyzed their lipid profile by MS, and compared their lipid profile. In addition, the lipid contents of their unconditioned media were studied to investigate the influence of culture media lipids and their FAs on the cells. Overall, 15 major lipid classes—including CE, DAG, PC, LPC, PI, LPI, PE, LPE, SM, Cer, LacCer, Glc/GalCer, and Gb3—were investigated, and altogether more than 150 molecular species were detected and studied (Supporting Information Tables S2 and S3).

The lipid profile of the HLCs differentiated by M3, M4, and M5 closely resembled each other (Figures ). In fact, only the levels of three PC species (PC 16:1–20:4, PC 17:0–18:1, and PC 17:0–20:4) were slightly, but statistically significantly, lower in M4 (Figure 3, marked by blue arrows) compared with the other methods. No other significant differences were found in any of the molecular species between the methods. When comparing the total levels of lipid classes, only Cer was found at significantly lower concentrations in

the cells produced by M5 compared with those produced by M4 (Figure 5b). However, at the molecular species level, none of the Cer species differed significantly between M4 and M5 (Figure 5a and Supporting Information Table S2).

### 3.6 | Lipid profiles of HLCs, PHHs, and HepG2 cells

Next, we compare the lipidomes of the HLCs with the PHHs and HepG2 cells and describe our findings for each lipid class separately. In addition, we highlight the differences and similarities between the PHHs and HepG2 cells.

#### 3.6.1 | Phospholipids

In the HLCs, the molecular species of PC, PE, and PI containing saturated FAs (SFAs) and monounsaturated FAs (MUFAs) were mostly similar to those in the PHHs, with the exceptions of PC 18:1/18:1 ( $p < 0.05$ ), PC 17:0–18:1 ( $p < 0.001$ ), and PE 18:0–18:1 ( $p < 0.05$ ), which were statistically significantly higher in the HLCs (Figure 3, marked by red arrows). When the PHHs were compared with the HepG2 cells, a large number of species showed statistically significant differences, particularly the species containing 14:0, 16:0, and 18:1 FAs. In PC and PE, the molecular species containing polyunsaturated FAs (PUFAs) were present in significantly higher concentrations in the PHHs compared with both the HLCs and HepG2 cells. This difference was especially pronounced for the species containing an SFA coupled with FA 18:2 or its derivative 20:4 (e.g., 16:0–18:2, 18:0–18:2, 16:0–18:2, and 18:0–20:4). The HepG2 cells, however, contained more of the species where an MUFA was coupled to a PUFA (or another MUFA). The total levels of PC and PI classes were similar among all three compared cell types. Total PE was, however, detected at lower levels in the HLCs compared with the PHHs (statistically significant in M4 and M5 vs the PHHs). This was mostly due to the higher levels of PE 18:0–18:2 and PE 18:0–20:4 in the PHHs. The concentration of PC, PE, and PI in the HLC and PHH media was either zero or negligible, while the HepG2 medium contained high amounts of PC (12.9  $\mu\text{M}$ ) but only minimal amounts of PE and PI (Supporting Information Figure S7 and Table S3). The profile and concentration of molecular lysophospholipids (LPLs)—such as LPC, LPE, and LPI—in the HLCs were very close to those of the PHHs (Figure 3a). Consequently, the total LPL levels of the HLCs

**FIGURE 2** Characterization and functionality of hiPSC-derived hepatocyte-like cells (hiPSC-HLCs) differentiated from three cell lines by five methods and their comparison to primary human hepatocytes (PHHs), HepG2 cells, and human liver total RNA (hLTR). (a) Immunostaining of cells for AFP (red) and ALB (green). Nuclei are stained with DAPI (blue). The red inset on the lower right shows the comparison of the morphology and binuclearity (red arrows) of M5-HLCs and PHHs. The scale bar represents 200  $\mu\text{m}$  for the HLCs and 100  $\mu\text{m}$  for the PHHs and HepG2 cells. (b) The graph on the left shows the average percentage of binuclear HLCs in each method and their comparison to PHHs. The graph on the right shows the average percentage of ALB-positive HLCs in each method. Each bar represents the mean  $\pm$  SD of the manual counts from the immunostaining image analysis of at least five areas. (c) Real-time qPCR analysis of the *SOX17*, *FOXA2*, *AFP*, *ALB*, *APOA1*, and *APOB* genes at the hiPSC and hepatic stage and their comparison to the reference samples. Each sample was run in triplicate and the bars represent the mean  $\pm$  SD of three biological replicates from three individual cell lines. The gene expression data were normalized to the housekeeping gene *GAPDH* and are presented relative to the PHHs. (d) Biochemical analysis of the conditioned media from the HLCs for albumin, urea, and triacylglycerol. Values are normalized as 1 million cells per 24 hr. The bars represent the mean  $\pm$  SD of three biological replicates of the three cell lines. \* $p < 0.05$ , \*\* $p < 0.01$ , \*\*\* $p < 0.001$ . DAPI: 6-diamidino-2-phenylindole; n.s.: not significant; qPCR: quantitative PCR; SD: standard deviation [Color figure can be viewed at [wileyonlinelibrary.com](http://wileyonlinelibrary.com)]

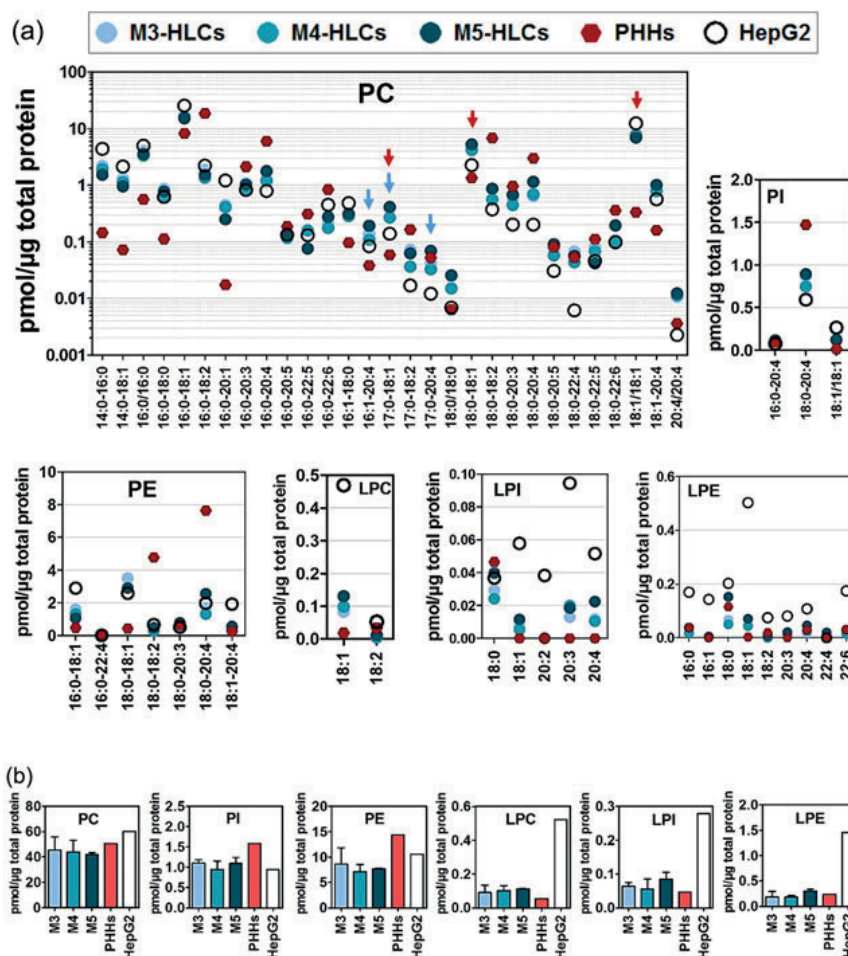


**FIGURE 3** Lipidomic analysis of phospholipids (PLs) and lysophospholipids (LPLs) in the HLCs differentiated by M3, M4, and M5, and their comparison to PHH and HepG2 cell lipids. (a) Protein-normalized concentration of molecular species detected in each class of PLs (Phosphatidylcholine [PC], phosphatidylinositol [PI], and phosphatidylethanolamine [PE]) as well as LPLs (lysophosphatidylcholine [LPC], lysophosphatidylinositol [LPI], and lysophosphatidylethanolamine [LPE]). The arrows refer to species that were found to be statistically significantly different between HLCs in M3, M4, and M5 (blue arrows) or between the HLCs and PHHs (red arrows) by one-way analysis of variance. (b) Total concentrations of PLs and LPLs calculated from the sum of all the molecular species in those specific classes. Each sample was run in triplicate and the bars represent the mean  $\pm$  standard deviation of the studied cell lines [Color figure can be viewed at [wileyonlinelibrary.com](http://wileyonlinelibrary.com)]

and PHHs were also similar (Figure 3b). The HepG2 cells, however, contained considerably higher levels of LPL as total levels and strikingly high levels of the molecular lyso-species, with the 18:1 acyl residue in each LPL class (Figure 3 and Supporting Information Table S2).

### 3.6.2 | Neutral lipids

CE concentration was the highest in the HepG2 cells, intermediate in the HLCs, and the lowest in the PHHs. The CE species profile of the HLCs and HepG2 cells was different because 16 CE species showed statistically significantly higher concentrations in the HepG2 cells

(Figure 4). When interpreting these differences, the effect of medium CE concentration was considered. The HepG2 medium contained 154  $\mu$ M of CE, whereas the CE concentrations were negligible in the HLC and PHH media (Supporting Information Figure S7 and Table S3).

Similar to PLs, the HLCs contained higher levels of DAG species with FA 18:1 when compared with the PHHs. However, the level of major DAG species 16:0-18:1 detected in the HLCs was clearly closer to that detected in the PHHs compared with what was found in the HepG2 cells. The PHHs, on the other hand, contained higher levels of DAG species with FA 18:2 (the minor species DAG 18:1-18:2 being an exception with its equally low levels in the HLCs,



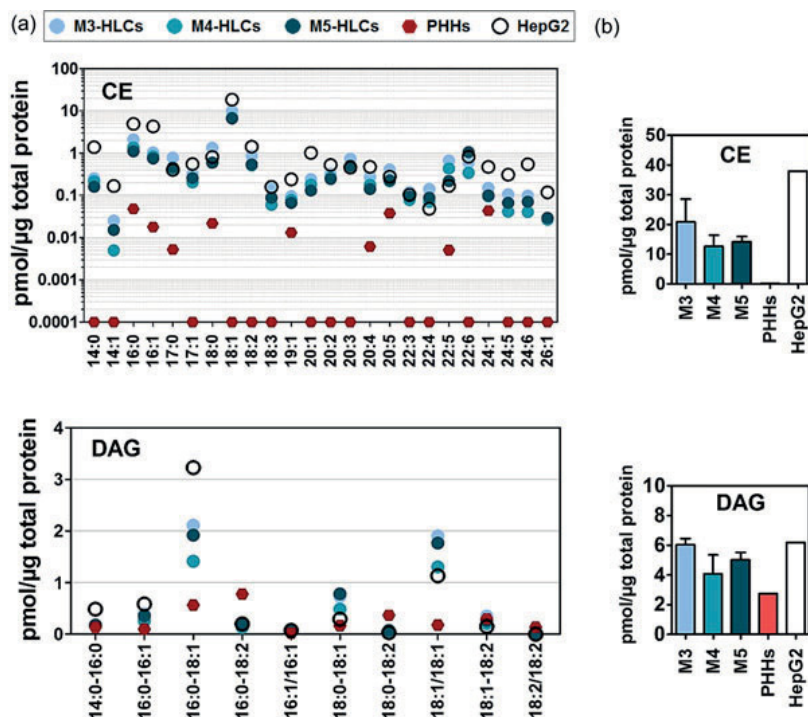


**FIGURE 4** Lipidomic analysis of cholesteryl ester (CE) and diacylglycerol (DAG) in the HLCs differentiated by M3, M4, and M5, and their comparison to PHH and HepG2 cell lipids. (a) Protein-normalized concentration of molecular species detected for the CE and DAG lipid class. (b) Total concentrations of CE and DAG calculated from the sum of all the molecular species in those specific classes. Each sample was run in triplicate and the bars represent the mean  $\pm$  standard deviation of the studied cell lines [Color figure can be viewed at [wileyonlinelibrary.com](http://wileyonlinelibrary.com)]

PHHs, and HepG2 cells). As also observed in PC, the DAG species with relatively short chain FAs (e.g., 14:0, 16:0, and 16:1) were detected at higher concentrations in the HepG2 cells than in the HLCs and PHHs (Figure 4A).

### 3.6.3 | Sphingolipids

Despite higher total SM concentration, HLCs mimicked the SM profile of PHHs and HepG2 cells, except that SM d18:1/15:0 and SM d18:1/16:1 were present at statistically significantly higher concentrations in the HepG2 cells (Figure 5a). Both the HLCs and HepG2 cells contained significantly higher levels of SM d18:1/16:0 compared with the PHHs. The level of SM in the HLC and PHH media was undetectable, whereas the HepG2 medium contained 6.5  $\mu$ M of SM (Supporting Information Figure S7 and Table S3).

In terms of the overall SL profile, the HepG2 cells situated between the PHHs and HLCs. In fact, lipid class data showed that the HLCs contained lower levels of Cer but higher levels of LacCer, Glc/GalCer, and Gb3 (members of glycosphingolipid [GSL] family) compared with the PHHs (Figure 5b). Closer examination showed that Cers and, particularly, the saturated species with long- and very-long-chain FAs (e.g., Cer d18:0/22:0 and Cer d18:1/24:0) were higher in the PHHs (Figure 5a), in fact, the Cer species profile of the HLCs

resembled more that of the HepG2 cells. On the other hand, the HLCs contained more GSLs—especially the species d18:1/16:0, d18:1/24:0, and d18:1/24:1—and the differences were the most pronounced in the Glc/GalCer class. The HepG2 medium contained trace amounts of SLs, and the concentration of SLs in the HLC and PHH media was either negligible or undetectable (Supporting Information Figure S7 and Table S3).

### 3.7 | FA analysis

The HLCs contained 15 mol% PUFAs versus 29 mol% and 10.5 mol% in the PHHs and HepG2 cells, respectively (Figure 6a). The FA 18:2n-6 was, in proportion, the highest PUFA detected in the PHHs (14 mol%); it was also the highest PUFA detected in the PHH medium (89 mol%; Figure 6b and Supporting Information Table S3). Both the HLCs and HepG2 cells had a low supply of 18:2n-6 in their media and, hence, lower relative levels of 18:2n-6 in their cellular FA profile. Interestingly, the HLCs seemed to be able to compensate for the shortage of supply better than the HepG2 cells, and the levels of 20:4n-6, a bioactive metabolite of 18:2n-6, were only 1.4-fold lower in the HLCs compared with the PHHs, indicating an active biosynthesis of 20:4n-6 from its precursor in the HLCs.

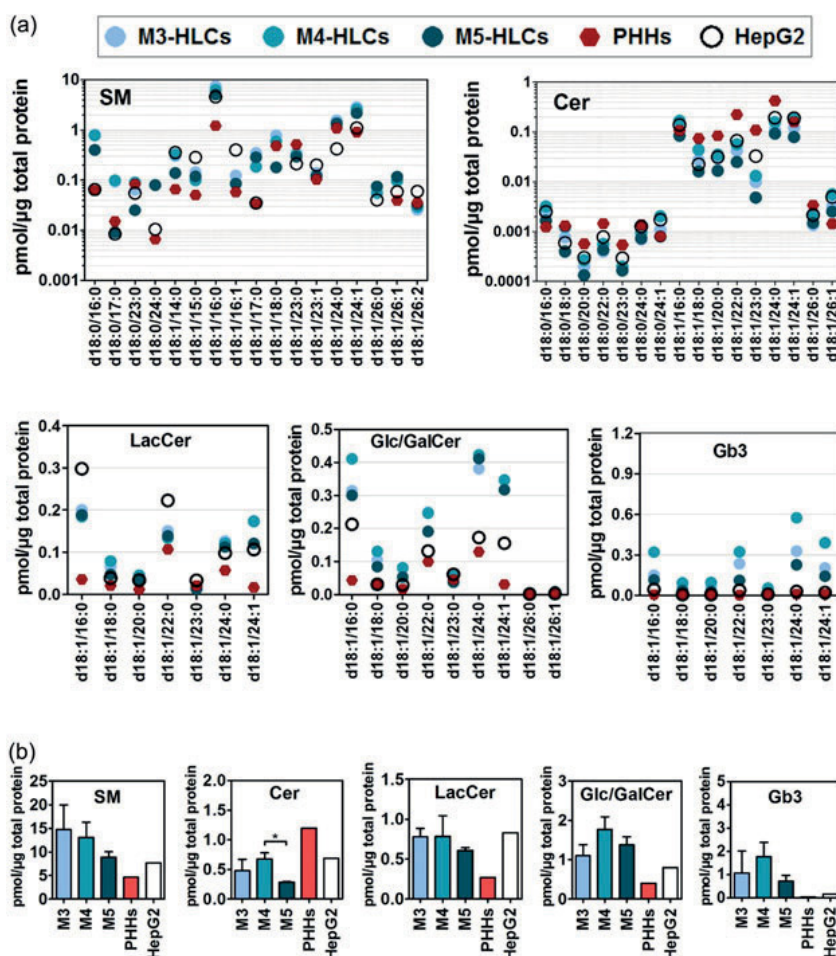


**FIGURE 5** Lipidomic analysis of sphingolipids (SLs) in the HLCs differentiated by M3, M4, and M5, and their comparison to the PHHs and HepG2 cells. (a) Protein-normalized concentration of molecular species detected for the sphingomyelin (SM), ceramide (Cer), glucosyl/galactosylceramide (Glc/GalCer), lactosylceramide (LacCer), and globotriaosylceramide (Gb3) lipid classes. (b) Total concentrations of SLs calculated from the sum of all the molecular species in those specific classes. Each sample was run in triplicate and the bars represent the mean  $\pm$  standard deviation of the studied cell lines. \* $p \leq 0.05$  [Color figure can be viewed at [wileyonlinelibrary.com](http://wileyonlinelibrary.com)]

The total levels of MUFAs in the HLCs (43 mol%) were higher than in the PHHs (25 mol%), but they were still lower than in the HepG2 cells (52 mol%) (Figure 6a). FA 18:1n-9 (with its 31 mol% of all FAs) was the major MUFA in the HLCs, a reflection of the high concentration of 18:1n-9 in their medium. FA 16:1n-7 (an SCD  $\Delta 9$ -desaturation product of 16:0) had the lowest values in the HLCs (0.6-fold the PHH level) and the highest values in the HepG2 cells (1.4-fold the PHH level). Consequently, the relative concentration of 18:1n-7 (an fatty acid elongase (ELOVL)5/6 chain elongation product of 16:1n-7) was the highest in the HepG2 cells (14 mol%) and lower in HLCs and PHHs (4 mol% and 2 mol%, respectively). This implies that the high 18:1n-7 is a specific feature of HepG2 cells, marking a clear distinction from the HLCs and PHHs, which appeared similar in having 18:1n-9 as their main MUFA component.

The total SFAs in the HLCs, PHHs, and HepG2 cells were 40 mol%, 46 mol%, and 37 mol%, respectively (Figure 6a). Relative to the PHHs, the lower SFAs in the HLCs were attributable to the slightly lower proportion of all major individual FAs (14:0, 16:0, and 18:0). The lower amount of total SFAs in the HepG2 cells, however, was mainly due to the considerably lower percentage of 18:0 compared with the PHHs (2.2-fold less).

### 3.8 | Gene expression of key enzymes in FA metabolism

To further investigate the metabolism of FAs in the HLCs, PHHs, and HepG2 cells, we studied the expression of five key genes involved in the synthesis pathways of FA by qPCR. Lipogenesis is highly affected

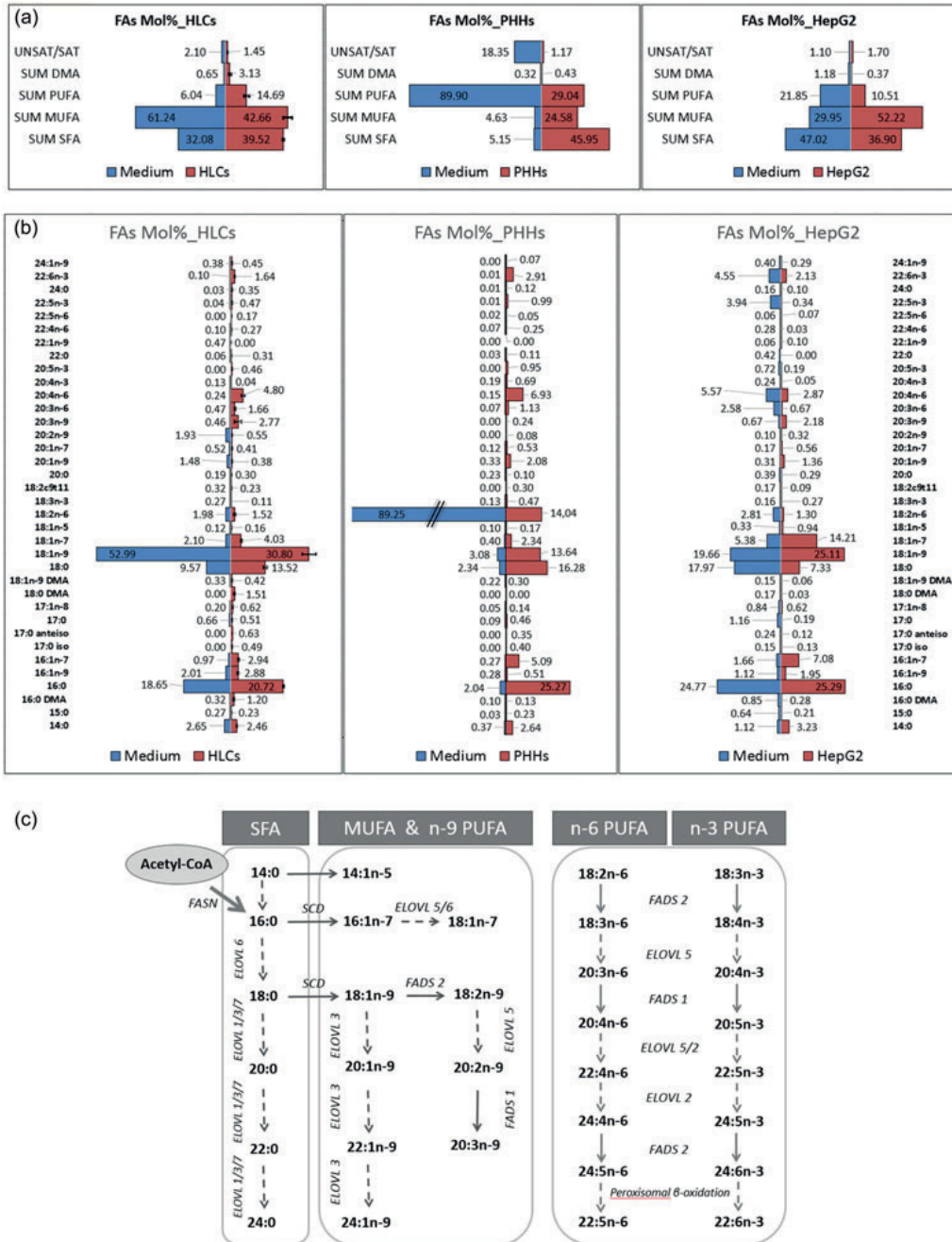


**FIGURE 6** Fatty acid (FA) analysis (mole% in total FAs) of the M3-HLCs, PHHs, and HepG2 cells versus their media. (a) Total proportions of saturated fatty acids (SFAs), monounsaturated fatty acids (MUFAs), polyunsaturated fatty acids (PUFAs), and dimethyl acetals (DMAs), derived from plasmalogen PL alkenyl chains in the studied cell types and their media. The ratio of total unsaturated FAs (UNFAs) to total SFAs is shown on the top bar. (b) Mirrored bar chart presenting the FA profiles in the M3-HLCs, PHHs, and HepG2 cells (red bars) in comparison to their media (blue bars). Each bar represents the mole% of the detected FAs. Error bars in the HLCs are calculated from the mean  $\pm$  standard deviation of three biological replicates. (c) Schematic image of the metabolic pathways of SFAs, MUFAs, and PUFAs, including the responsible genes (FASN, SCD, ELOVL, FADS). The figure is adapted from the work by Glück et al., (2016). HLC: hepatocyte-like cell; PHH: primary human hepatocyte; PL: phospholipid [Color figure can be viewed at [wileyonlinelibrary.com](http://wileyonlinelibrary.com)]

by glucose homeostasis in the liver. Therefore, the expression of Glucokinase (encoded by *GCK*), the key enzyme involved in glycolysis, was also studied. The results revealed that *FA synthase (FASN)*, a key gene in de novo FA synthesis, was expressed in the HLCs mostly at similar levels as in the PHHs (Figure 7a). The *FASN* expression level of the HepG2 cells was higher than that of the PHHs. The expression of *GCK* in HLCs was at similar levels as in the PHHs (Figure 7b). Comparing the methods, M3-HLCs and M4-HLCs expressed *GCK* at statistically significantly higher levels than M1-HLCs. *FA desaturase 1 (FADS1)* was expressed at a statistically significantly lower level in all the HLCs ( $p < 0.001$ ) when compared with the PHHs, but at similar levels as in hLTR and the HepG2 cells. In the HepG2 cells, hLTR, and almost half of the HLCs, *FADS2* was expressed at lower levels than in the PHHs. In the other half of the studied HLCs, the expression of *FADS2* was similar to that in the PHHs (Figure 7a). In addition to the *FADSs*, *FA elongases ELOVL2* and *ELOVL5*, working in sequence with the desaturases, are essential for the metabolism of long-chain and highly unsaturated FAs (Figure 6c). *ELOVL2* was expressed in most of

the HLC lines at similar levels to the PHHs, but some lines produced by M2, M3, and M5 showed statistically significantly higher expression levels (Figure 7a). The expression of *ELOVL2* was statistically significantly higher in the HepG2 cells than in the PHHs. *ELOVL5*, on the other hand, was expressed at roughly similar levels in all analyzed cells types (PHHs, HepG2 cells, hLTR, and HLCs).

## 4 | DISCUSSION

hiPSC-HLCs are a promising cell culture platform for studying lipid homeostasis and its aberrations related to metabolic syndromes manifested, for example, in atherosclerosis and fatty liver disease. In the current study, we successfully generated functional HLCs from hiPSCs using five hepatic differentiation protocols. We then compared these HLCs comprehensively for gene and protein expression, lipid composition, and functional traits. Similar comparisons were also made with the two common hepatic cell models,

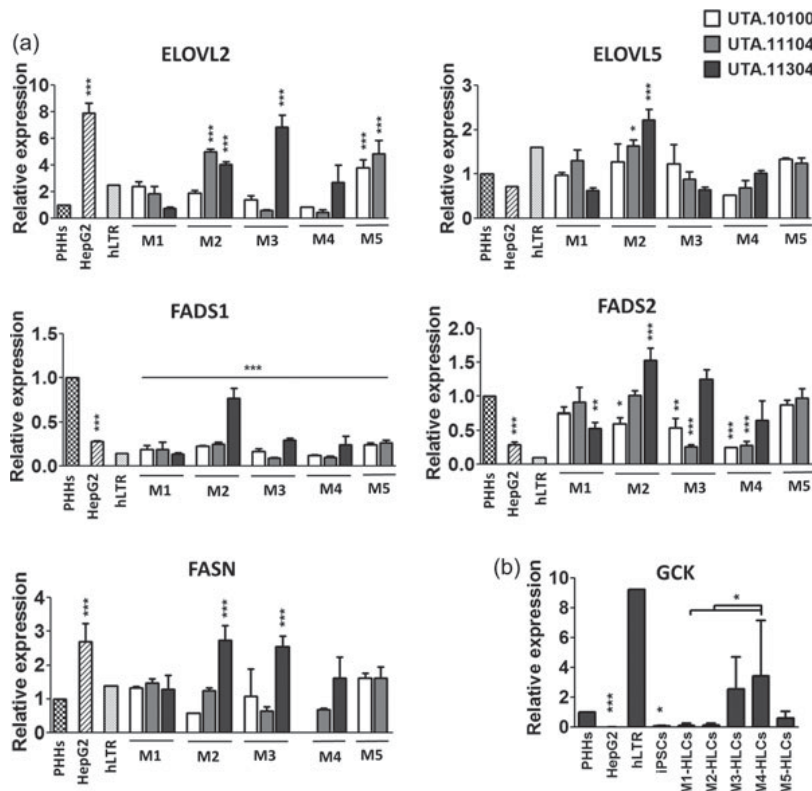


**FIGURE 7** Expression levels of genes involved in the metabolism of fatty acids (FAs) (a) and glucose (b). (a) Real-time qPCR analysis of *ELOVL2*, *ELOVL5*, *FADS1*, *FADS2*, and *FASN* in the HLCs (differentiated by five methods), PHHs, HepG2 cells, and human liver total RNA (hLTR). (b) Real-time qPCR analysis of *GCK* in HLCs (differentiated by five methods), PHHs, HepG2 cells, hiPSCs, and human liver total RNA (hLTR). The expression of each gene was normalized to the endogenous control gene *GAPDH* and is presented relative to the PHHs. Each sample was run in triplicate, and the bars in the HLCs represent the mean  $\pm$  standard deviation of three biological replicates. PHHs were used as reference group to calculate the statistical significance. \* $p < 0.05$ , \*\* $p < 0.01$ , \*\*\* $p < 0.001$ . HLC: hepatocyte-like cell; PHH: primary human hepatocyte; qPCR: quantitative PCR



PHHs and HepG2 cells. All five differentiation protocols produced HLCs capable of expressing *ALB*, uptaking LDL, and secreting albumin, urea, and TAG. The lipid profiles of the HLCs, PHHs, and HepG2 cells were analyzed by both MS and gas chromatography. In addition, the effects of FA supply from the culture media on the cells' lipid profile were examined. In this study, we performed, to our knowledge, the most thorough characterization of the metabolic traits of HLCs and investigated their potential as a new cell model for lipid studies in parallel with PHHs and HepG2 cells.

#### 4.1 | Hepatic differentiation

Most protocols for differentiating HLCs from pluripotent stem cells follow a three-step differentiation through the DE phase, continuing to the hepatoblast stage, and finally to mature HLCs. Various growth factors and cytokines known to be necessary for liver development are used through these procedures (Cameron et al., 2015; Chen et al., 2012; Gerbal-Chaloin et al., 2014; Hannan et al., 2013; Hu & Li, 2015; Mallanna & Duncan, 2013; Schwartz, Fleming, Khetani, & Bhatia, 2014; Si-Tayeb et al., 2010; Sullivan et al., 2010; Takayama et al., 2012). We observed that at the DE stage, the initial density of the hiPSCs played a more critical role than the type of DE inducer (e.g., CHIR 99021 or Wnt3). In fact, high initial cell density in M1, M2, and M5 leads to remaining undifferentiated colonies, whereas in M3 and M4, this results in the formation of new dense and undifferentiated areas. On the other hand, very low initial cell density could lead to highly sparse cells and consequently unsuccessful differentiation. Hence, it is fundamental to find the optimal cell density for each cell line in each method.

At the hepatoblast stage, cells in M1 were supplemented with FGF2 and BMP4, mimicking the stimuli present during liver development (Rasmussen, 2015). However, in other methods, DMSO was used instead of FGF2 and BMP4. DMSO has histone deacetylase inhibitor activity and significantly increases the expression levels of BMP2 and BMP4 while decreasing the expression levels of stem cell markers, such as Oct4 (Behbahan et al., 2011; Choi et al., 2015; Czysz, Minger, & Thomas, 2015; Santos, Figueira-Coelho, Martins-Silva, & Saldanha, 2003). At Day 10, the cells in M1 had clear borders; they had also formed sinusoidal canaliculi-like structures (Supporting Information Figure S1b). However, at the end of the hepatoblast stage and the beginning of the maturation stage, the cells in M2, M3, M4, and M5 also eventually gained sinusoidal canaliculi-like structures (Supporting Information Figure S3). In addition, small lipid droplets were clearly visible in the cells in the culture medium containing DMSO, which could be due to excess of FA supplies in that medium (Kiamehr et al., 2017).

For the maturation of hepatocytes, HGF and oncostatin M were used. Epidermal growth factor (EGF) was present only in M3, M4, and M5. It has been shown that HGF and EGF—two tyrosine kinase receptor ligands—together decrease the expression of several genes involved in the metabolism of FAs (Michalopoulos, Bowen, Mulè, & Luo, 2003). In our study, EGF seemed to affect urea and TAG secretion but not the albumin secretion of the HLCs. In fact, M3-, M4-, and M5-HLCs secreted both urea and TAG similarly to the

PHHs, but clearly different from the levels secreted by the M1- and M2-HLCs (Figure 2D).

It has been proposed that the unnatural microenvironment provided by current culture systems is partly responsible for the immature features of HLCs (Godoy et al., 2015), and that coating the culture plates with a mixture of Laminin 521/111 could further promote HLC maturation (Cameron et al., 2015). Hence, in M4 we replaced the Geltrex coating with Laminin 521/111. Even though we did not observe this coating to improve functionality, it increased the number of ALB-positive cells by 82% and the binuclearity of HLCs by 65% compared with those in M3. In the adult liver, 15%–30% of hepatocytes are binuclear, and binucleation is usually considered a sign of terminal differentiation in hepatocytes, even though binuclear hepatocytes are still able to divide (Miyaoaka & Miyajima, 2013). One study suggested that polyploid cells are more resistant to stressful conditions (Anatskaya & Vinogradov, 2007). However, the effect of size and number of nuclei on the hepatocyte function is an intriguing question yet to be answered.

It is well established that the levels of lipoproteins in the serum have a clear correlation with the risk of atherosclerosis (Moss, 1991). It has been shown that HLCs produce, secrete, and uptake cholesterol *in vitro* and that they robustly express apoprotein genes, for example, *APOA1*, *APOA2*, *APOB*, *APOC*, and *APOE* (Rasmussen, 2015). HLCs also respond to statin treatment *in vitro* by reducing the amount of secreted cholesterol (Krueger et al., 2013). Here, we confirmed that HLCs are capable of uptaking labeled LDL (Supporting Information Figure S5) as well as expressing *APOA1* and *APOB* at similar levels compared with PHHs (Figure 2c), which is in line with findings in other studies (Godoy et al., 2015). *APOA1* and *APOB* gene expression levels were studied as a surrogate for estimating the HDL and LDL production levels of HLCs.

Overall, the HLCs differentiated by M3, M4, and M5 showed superior characteristics for studying the liver function and lipid metabolism compared with the HLCs differentiated by M1 and M2. The M3-, M4-, and M5-HLCs secreted TAG at similar levels as the PHHs. In addition, the M3- and M4-HLCs secreted urea at levels closer to the PHHs when compared with the HLCs differentiated by other methods. M4 and M5 produced the most albumin-positive HLCs, and the M4-HLCs showed the highest binuclearity compared with the HLCs differentiated by the other methods. Furthermore, we observed that the cell lines differentiated by M5 showed the least variation. This could be attributed to the application of the STEMdiff™ DE kit at the DE stage, which resulted in uniform DE differentiation. Because the DE stage is the key phase in hepatic differentiation, evenly differentiated DE cells could result in more uniform hepatic differentiation, reducing possible variation between cell lines. Nevertheless, it should be considered that the Laminin coating applied in M4 and the STEMdiff™ DE kit used in M5 adds to the overall costs of the differentiation and makes these methods more expensive than, for example, M3.

#### 4.2 | Lipid profiling

PUFAs and their bioactive derivatives play important roles during cell proliferation and differentiation (Bieberich, 2012; Kim, Kim, Kim,

Kim, & Han, 2009). It has previously been shown that the addition of certain FAs, such as docosahexaenoic acid (22:6 n-3) or eicosapentaenoic acid (20:5 n-3), to the media could promote neuronal differentiation in neuronal stem/progenitor cells through the regulation of the cell cycle (Katakura et al., 2013). Furthermore, a definite mixture of FAs induces adipocyte-like differentiation of osteosarcoma cells through the activation of peroxisome proliferator-activated receptors (Diascro et al., 1998). It is known that the endogenous capacity of cultured cells to modify PUFAs for their needs can partially compensate for suboptimal supply from the microenvironment and culture medium (Zhang, Kothapalli, & Brenna, 2016). A simplified schematic figure of the metabolic pathways of SFAs, MUFAs, and PUFAs and the genes involved is presented in Figure 6c. PHHs possess an excellent capacity to metabolize diet-derived PUFAs (Sprecher, 2000). Most of our HLC lines expressed the key enzymes in the metabolism of FAs at similar levels to the PHHs. The HepG2 cells, however, varied significantly in most of the studied enzymes compared with the PHHs. This indicates that HLCs are superior cell models for studying the FA metabolism of the liver compared with HepG2 cells.

Our analysis revealed that PHHs contain a considerably larger proportion of PUFAs compared with HLCs and HepG2 cells. The high percentage of 18:2n-6 in the PHHs reflects the very rich supply of 18:2n-6 from the medium, part of which was apparently converted to 20:4n-6 by the cells using the FADS2, ELOVL5, and FADS1 enzymes. Even though the 18:2n-6 level in the HLCs medium was very low, these cells were able to efficiently produce 20:4n-6, suggesting the proper expression of FADS2, ELOV5, and FADS1. Interestingly, the main n-3 PUFA, 22:6n-3, was also detected in the HLCs with levels only 1.8-fold lower than in the PHHs, despite only trace amounts of n-3PUFAs in their medium. This result means that either the n-3PUFAs of HLCs originate from previous conditions (hepatoblast stage), or alternatively, these cells selectively and efficiently take up and incorporate 22:6n-3 into their lipids. The HepG2 cells received 22 mol% PUFAs from their medium, whereas the HLCs received only 6 mol%. In addition, the HepG2 medium was rich in the total FA content. Despite this, the relative levels of PUFAs in the HepG2 cells remained low (11 mol%) compared with the levels in the PHHs (29 mol%) and HLCs (15 mol%). The overloading of the HepG2 cells with the medium lipids and the consequent high content of neutral lipids (harboring fewer PUFAs than the structural PL) of the cells may have resulted in a relatively PUFA-poor FA composition in their total lipids.

In deficient states, endogenous synthesis of the 20:3n-9 from 18:1n-9 occurs (Kamada et al., 1999). It is of note that the HLCs and HepG2 cells both contained 2–3 mol% of n-9 PUFAs (20:2n-9 + 20:3n-9), which means that the cells suffered from essential PUFA deficiency. The large supply of 18:2n-6 in the PHH medium, however, prevented them from producing any significant amounts of n-9 PUFAs. PUFAs have been shown to be important in the maturation and functionality of HLCs (Kiamehr et al., 2017). Therefore, we propose that providing HLCs with a PUFA-rich medium may help to produce HLCs with a lipid profile even closer

to PHHs. A high supply of PUFA to PHHs inhibits their endogenous MUFA synthesis from SFAs (Ntambi, 1999). Likewise, in our study, the total MUFA in the PHHs remained low compared to the HLCs and HepG2 cells. The lower the PUFA totals, the higher the MUFA totals were at the expense of the SFAs.

Hepatocytes can uptake FAs from the cell culture medium. Simultaneously, hepatocytes are able to produce FAs by hydrolyzing glucose to pyruvate, which links glycolysis to lipogenesis where pyruvate is used to synthesize FAs through de novo lipogenesis (Rui, 2014). Glucokinase (encoded by GCK gene) is central to the glucose homeostasis and is the key enzyme involved in the first step of glycolysis. Changes in hepatocyte GCK expression represent an adaptive action to impaired glucose/lipid metabolism to maintain glucose homeostasis (Massa, Gagliardino, & Francini, 2011). In our study, there were no significant differences in the expression of GCK between the HLCs and the PHHs. However, the HepG2 cells expressed GCK at statistically significantly lower levels than the PHHs, which is in line with previous findings at protein level (Wiśniewski, Vildhede, Norén, & Artursson, 2016). FASN is a major determinant of the capacity of a tissue to synthesize FAs de novo, and palmitate (16:0) is its primary product (Figure 6c; Jensen-Urstad & Semenkovich, 2012). Again, most HLC lines expressed FASN equally to the PHHs, whereas the HepG2 cells had clearly higher expression levels. The high expression of FASN in the HepG2 cells has also been observed earlier (Huang & Lin, 2012). The relative activities of SCD and ELOVL dictate whether the metabolism of 16:0 follows the route 16:0–16:1n-7–18:1n-7 or the route 16:0–18:0–18:1n-9 (Glück, Rupp, & Alter, 2016). In the former route, the SCD activity is higher than the ELOVL activity, and in the latter route, the ELOVL activity is higher than the SCD activity. Clearly, among the cells analyzed, the route forming 18:1n-7 was the most active in the HepG2 cells. This feature differentiates the HLCs and HepG2 cells and shows that the MUFA-producing pathway in HLCs resembles that found in PHHs. The elevated cellular contents of 16:1n-7 and high SCD activity appear to promote de novo lipogenesis, which could partially explain the large neutral lipid stores of the HepG2 cells (Hodson & Fielding, 2013).

### 4.3 | FAs mirrored in molecular species

We observed that the PL species profile of cells was highly affected by the culture medium. The PHHs' lipid profile reflected the high medium supply of 18:2n-6, which after uptake was metabolized to 20:4n-6 and incorporated into the PLs. Consequently, the PLs composed of 16:0–18:2, 18:0–18:2, 16:0–20:4, and 18:0–20:4 were abundant in the PHHs. The much lower supply of 18:2n-6 to the HLCs and HepG2 cells kept the levels of the above-mentioned PL species low. However, the HLCs could still actively synthesize 20:4 and couple this PUFA with SFAs and MUFAs. To compensate for the overall PUFA deficiency, the HepG2 cells produced more MUFAs (observed in high levels of 18:1n-7), which is reflected in species such as 16:0–18:1 and 18:1/18:1. The HLCs instead compensated for the

PUFA shortage by uptaking 18:1n-9, which was abundant in their medium.

In general, the HLCs and HepG2 cells contained lower concentrations of Cer and higher concentrations of LacCer, Glc/GalCer, and Gb3 when compared with the PHHs. Cer synthesis is a complex process orchestrated by six CerSs (CerS1–CerS6), each of which synthesizes Cers with distinct FA chain lengths (Cingolani, Futerman, & Casas, 2016). Cer has important structural and signaling roles (Gault, Obeid, & Hannun, 2010). It has been shown that at time of cellular stress, the generation of C16:0-ceramide via CerS5 is proapoptotic, whereas synthesis of C24:0-ceramides via CerS2 is prosurvival (Mesicek et al., 2010), and the balance between these long- and very-long-chain Cers is critical for cellular homeostasis. In our study, similar levels of d18:1/16:0 were observed in all three cell types, but the PHHs had significantly higher levels of d18:1/24:0 (Figure 5a). Transferring the PHHs from a physiological environment to an artificial 2D system could be stressful for them. Therefore, it is intriguing to speculate whether the survival or antiapoptosis mechanism is turned on in PHHs. On the other hand, HepG2 cells might suppress the apoptotic Cer signal by converting Cer to complex GSLs, leading to lowered levels of Cer in HepG2 cells. Overall, the interpretation of the observed Cer profile of the studied cell types is very complicated and demands further studies.

The UDP-glucose ceramide glucosyltransferase (UGCG) gene encodes the enzyme UDP-glucose Cer glucosyltransferase, which catalyzes the first glycosylation step in the biosynthesis of GSLs. The product of this reaction is glucosylceramide, which is the core structure of many GSLs, including Glc/GalCer (Tokuda et al., 2013). We have previously reported a higher expression of UGCG in HLCs compared with PHHs (Kiamehr et al., 2017), which correlates well with our lipidomics findings of high Glc/GalCer in HLCs. In the C24 species of every sphingolipid class, the ratio of the 24:0 species to the 24:1 species was higher in the PHHs than in the HLCs or HepG2 cells. This may reflect the dominance of 24:1n-9 over 24:0 in both the HLC and HepG2 media and the reversed ratio of these trace MUFAs in the PHH medium.

The PHHs were cultured in a low FA medium. As a result, the PHHs contained low levels of CE in their cellular lipid profile. Unlike the PHH cells, the HepG2 cells—which were grown in FA-rich medium—accumulated a large amount of the neutral storage lipids CE and TAG, the latter being represented via its hydrolysis product DAG. As is normal for cultured cells, the highest CE species was 18:1, followed by 16:0 and 16:1, and there were also traces of various other species. In line with the CE profile, the HepG2 cells contained large amounts of DAG, chiefly 16:0–18:1 and 18:1/18:1. The HLCs also showed an accumulation of neutral lipids (although milder than in the HepG2 cells), which is likely due to their treatment with an FA-rich medium at the hepatoblast stage (Day 6 to Day 12; Kiamehr et al., 2017). Therefore, our work reveals the need to revise the generally overlooked FA content of culture media and to tailor it according to the HLCs' needs. In addition, we propose that increasing the supply of PUFA in the culture medium may positively affect the lipid profile and functionality of the HLCs.

To our knowledge, this is the first comparative study that considers the effects of various stimuli from different protocols on the differentiation and phenotype of HLCs. We are also the first to show the detailed lipid profile of HLCs and to evaluate their ability to metabolize FAs. Taken together, HLCs differentiated from hiPSCs provide the advantage of direct studies of cellular and molecular mechanisms that regulate lipid homeostasis in the liver. They also facilitate a novel platform for the discovery, optimization, and study of the modes of action of molecules modulating key lipids. This platform would allow the functional assessment of the impact of genetic variations in developing metabolic diseases, such as atherosclerosis.

## 5 | CONCLUSIONS

HLCs mimicked the lipid profile of PHHs very well and, thus, showed to be a better liver cell model than HepG2 cells, especially in terms of their low LPL content. HLCs were capable of metabolizing FAs to produce C20–22 highly unsaturated FAs to fulfill the complex biological functions mediated by those FAs. By improving the PUFA supply in the medium, we can produce HLCs, which can serve as a powerful and functional cell model to study patient-specific mechanisms in lipid aberrations leading to pathological states, such as atherosclerosis or fatty liver disease.

## ACKNOWLEDGEMENTS

This research received funding from the European Commission's Seventh Framework Programme [FP7–2007–2013] under two grant agreements, HEALTH.2012–3057392 “Personalized diagnostics and treatment for high risk coronary artery disease” (RiskCAD), and HEALTH-F2–2013–602222 “Targeting novel lipid pathways for treatment of cardiovascular disease” (Athero-Flux). Research funding was also received from Instrumentarium Science Foundation (Instrumentarium Tiedesäätiö) and the Finnish Cardiovascular Foundation. The authors would like to thank Markus Haponen, Henna Lappi, and Merja Lehtinen for their technical support. Jyrki Siivola, Maki Kotaka, Mauro Scaravilli, Ebrahim Afyounian, and Eric Dufour are acknowledged for their valuable help and advice in performing the experiments and analyzing the results. The authors would like to thank Professor Kenji Osafune for providing the great opportunity to visit his laboratory in CiRA, Kyoto University, Japan. The authors gratefully acknowledge the Tampere facility of iPS Cells and Flow Cytometry for their services.

## CONFLICTS OF INTEREST

The authors declare no conflicts of interest in this study.

## ORCID

Mostafa Kiamehr  <http://orcid.org/0000-0003-1894-3237>

## REFERENCES

- Anatskaya, O. V., & Vinogradov, A. E. (2007). Genome multiplication as adaptation to tissue survival: Evidence from gene expression in mammalian heart and liver. *Genomics*, 89(1), 70–80. <http://doi.org/10.1016/j.ygeno.2006.08.014>
- Behbahan, I. S., Duan, Y., Lam, A., Khoobyari, S., Ma, X., Ahuja, T. P., & Zern, M. A. (2011). New approaches in the differentiation of human embryonic stem cells and induced pluripotent stem cells toward hepatocytes. *Stem Cell Reviews*, 7(3), 748–759. <https://doi.org/10.1007/s12015-010-9216-4>
- Bieberich, E. (2012). It's a lipid's world: Bioactive lipid metabolism and signaling in neural stem cell differentiation. *Neurochemical Research*, 37, 1208–1229. <https://doi.org/10.1007/s11064-011-0698-5>
- Blouin, A., Bolender, R. P., & Weibel, E. R. (1977). Distribution of organelles and membranes between hepatocytes and nonhepatocytes in the rat liver parenchyma. A stereological study. *The Journal of Cell Biology*, 72(2), 441–455.
- Cameron, K., Tan, R., Schmidt-Heck, W., Campos, G., Lyall, M. J., Wang, Y., ... Hay, D. C. (2015). Recombinant laminins drive the differentiation and self-organization of hESC-derived hepatocytes. *Stem Cell Reports*, 5(6), 1250–1262.
- Castell, J. V., Jover, R., Martínez-Jiménez, C. P., & Gómez-Lechón, M. J. (2006). Hepatocyte cell lines: Their use, scope and limitations in drug metabolism studies. *Expert Opinion on Drug Metabolism & Toxicology*, 2(2), 183–212. <https://doi.org/10.1517/17425255.2.2.183>
- Cayo, M. A., Cai, J., Delaforest, A., Noto, F. K., Nagaoka, M., Clark, B. S., ... Duncan, S. A. (2012). JD induced pluripotent stem cell-derived hepatocytes faithfully recapitulate the pathophysiology of familial hypercholesterolemia. *Hepatology*, 56(6), 2163–2171. <https://doi.org/10.1002/hep.25871>
- Chen, Y. F., Tseng, C. Y., Wang, H. W., Kuo, H. C., Yang, V. W., & Lee, O. K. (2012). Rapid generation of mature hepatocyte-like cells from human induced pluripotent stem cells by an efficient three-step protocol. *Hepatology*, 55(4), 1193–1203. <https://doi.org/10.1002/hep.24790>
- Choi, S. C., Choi, J. H., Cui, L. H., Seo, H. R., Kim, J. H., Park, C. Y., ... Lim, D. S. (2015). Mixl1 and Flk1 are key players of Wnt/TGF- $\beta$  signaling during DMSO-induced mesodermal specification in P19 cells. *Journal of Cellular Physiology*, 230(8), 1807–1821.
- Cingolani, F., Futerma, A. H., & Casas, J. (2016). Ceramide synthases in biomedical research. *Chemistry and Physics of Lipids*, 197, 25–32. <https://doi.org/10.1016/j.chemphyslip.2015.07.026>
- Czys, K., Minger, S., & Thomas, N. (2015). DMSO efficiently down regulates pluripotency genes in human embryonic stem cells during definitive endoderm derivation and increases the proficiency of hepatic differentiation. *PLoS One*, 10(2), e0117689. <https://doi.org/10.1371/journal.pone.0117689>
- Diascro, D. D., Vogel, R. L., Johnson, T. E., Witherup, K. M., Pitznerberger, S. M., Rutledge, S. J., ... Schmidt, A. (1998). High fatty acid content in rabbit serum is responsible for the differentiation of osteoblasts into adipocyte-like cells. *Journal of Bone and Mineral Research*, 13(1), 96–106. <https://doi.org/10.1359/jbmr.1998.13.1.96>
- Ejlsing, C. S., Duchoslav, E., Sampaio, J., Simons, K., Bonner, R., Thiele, C., ... Shevchenko, A. (2006). Automated identification and quantification of glycerophospholipid molecular species by multiple precursor ion scanning. *Analytical Chemistry*, 78(17), 6202–6214. <https://doi.org/10.1021/ac060545x>
- Ekroos, K., Chernushevich, I. V., Simons, K., & Shevchenko, A. (2002). Quantitative profiling of phospholipids by multiple precursor ion scanning on a hybrid quadrupole time-of-flight mass spectrometer. *Analytical Chemistry*, 74(5), 941–949. <https://doi.org/10.1021/ac015655c>
- Ekroos, K., Ejlsing, C. S., Bahr, U., Karas, M., Simons, K., & Shevchenko, A. (2003). Charting molecular composition of phosphatidylcholines by fatty acid scanning and ion trap MS3 fragmentation. *The Journal of Lipid Research*, 44(11), 2181–2192. <http://doi.org/10.1194/jlr.D300020-JLR200>
- Elaut, G., Henkens, T., Papeleu, P., Snykers, S., Vinken, M., Vanhaecke, T., & Rogiers, V. (2006). Molecular mechanisms underlying the dedifferentiation process of isolated hepatocytes and their cultures. *Current Drug Metabolism*, 7(6), 629–660. <http://doi.org/10.2174/138920006778017759>
- Gault, C. R., Obeid, L. M., & Hannun, Y. A. (2010). An overview of sphingolipid metabolism: From synthesis to breakdown. *Advances in Experimental Medicine and Biology*, 1–23. [https://doi.org/10.1007/978-1-4419-6741-1\\_1](https://doi.org/10.1007/978-1-4419-6741-1_1)
- Gerbal-Chaloin, S., Funakoshi, N., Caillaud, A., Gondeau, C., Champon, B., & Si-Tayeb, K. (2014). Human induced pluripotent stem cells in hepatology: Beyond the proof of concept. *The American Journal of Pathology*, 184(2), 332–347. <https://doi.org/10.1016/j.ajpath.2013.09.026>
- Glück, T., Rupp, H., & Alter, P. (2016). Mechanisms increasing n-3 highly unsaturated fatty acids in the heart. *Canadian Journal of Physiology and Pharmacology*, 94(3), 309–323. <https://doi.org/10.1139/cjpp-2015-0300>
- Godoy, P., Hewitt, N. J., Albrecht, U., Andersen, M. E., Ansari, N., Bhattacharya, S., ... Hengstler, J. G. (2013). Recent advances in 2D and 3D in vitro systems using primary hepatocytes, alternative hepatocyte sources and non-parenchymal liver cells and their use in investigating mechanisms of hepatotoxicity, cell signaling and ADME. *Archives of Toxicology*, 87, 1315–1530. <https://doi.org/10.1007/s00204-013-1078-5>
- Godoy, P., Schmidt-Heck, W., Natarajan, K., Lucendo-Villarin, B., Szkolnicka, D., Asplund, A., ... Hengstler, J. G. (2015). Gene networks and transcription factor motifs defining the differentiation of stem cells into hepatocyte-like cells. *Journal of Hepatology*, 63(4), 934–942. <https://doi.org/10.1016/j.jhep.2015.05.013>
- Gordillo, M., Evans, T., & Gouon-Evans, V. (2015). Orchestrating liver development. *Development*, 142(12), 2094–2108. <https://doi.org/10.1242/dev.114215>
- Hannan, N. R. F., Segeritz, C.-P., Touboul, T., & Vallier, L. (2013). Production of hepatocyte-like cells from human pluripotent stem cells. *Nature Protocols*, 8(2), 430–437.
- Hay, D. C., Fletcher, J., Payne, C., Terrace, J. D., Gallagher, R. C. J., Snoeys, J., ... Iredale, J. P. (2008). Highly efficient differentiation of hESCs to functional hepatic endoderm requires ActivinA and Wnt3a signaling. *Proceedings of the National Academy of Sciences*, 105(34), 12301–12306. <https://doi.org/10.1073/pnas.0806522105>
- Heiskanen, L. A., Suoniemi, M., Ta, H. X., Tarasov, K., & Ekroos, K. (2013). Long-term performance and stability of molecular shotgun lipidomic analysis of human plasma samples. *Analytical Chemistry*, 85(18), 8757–8763. <https://doi.org/10.1021/ac401857a>
- Hodson, L., & Fielding, B. A. (2013). Stearoyl-CoA desaturase: Rogue or innocent bystander? *Progress in Lipid Research*, 52, 15–42. <https://doi.org/10.1016/j.plipres.2012.08.002>
- Hu, C., & Li, L. (2015). In vitro culture of isolated primary hepatocytes and stem cell-derived hepatocyte-like cells for liver regeneration. *Protein & Cell*, 6(8), 562–574. <https://doi.org/10.1007/s13238-015-0180-2>
- Huang, H. -C., & Lin, J. -K. (2012). Pu-erh tea, green tea, and black tea suppresses hyperlipidemia, hyperleptinemia and fatty acid synthase through activating AMPK in rats fed a high-fructose diet. *Food & Function*, 3(2), 170–177. <https://doi.org/10.1039/C1FO10157A>
- Jensen-Ustad, A. P. L., & Semenovich, C. F. (2012). Fatty acid synthase and liver triglyceride metabolism: Housekeeper or messenger? *Biochimica et Biophysica Acta*, 1821, 747–753. <https://doi.org/10.1016/j.bbalip.2011.09.017>
- Kajiwara, M., Aoi, T., Okita, K., Takahashi, R., Inoue, H., Takayama, N., ... Yamanaka, S. (2012). Donor-dependent variations in hepatic differentiation from human-induced pluripotent stem cells. *Proceedings of the National Academy of Sciences*, 109(31), 12538–12543. <https://doi.org/10.1073/pnas.1209979109>

- Kamada, N., Kawashima, H., Sakuradani, E., Akimoto, K., Ogawa, J., & Shimizu, S. (1999). Production of 8,11-cis-eicosadienoic acid by a delta 5 and delta 12 desaturase-defective mutant derived from the arachidonic acid-producing fungus *Mortierella alpina* 1S-4. *Journal of the American Oil Chemists Society*, 76(11), 1269–1274. <https://doi.org/10.1007/S11746-999-0138-8>
- Katakura, M., Hashimoto, M., Okui, T., Shahdat, H. M., Matsuzaki, K., & Shido, O. (2013). Omega-3 polyunsaturated fatty acids enhance neuronal differentiation in cultured rat neural stem cells. *Stem Cells International*, 2013, 1–9. <https://doi.org/10.1155/2013/490476>
- Kia, R., Sison, R. L. C., Heslop, J., Kitteringham, N. R., Hanley, N., Mills, J. S., ... Goldring, C. E. P. (2012). Stem cell-derived hepatocytes as a predictive model for drug-induced liver injury: Are we there yet? *British Journal of Clinical Pharmacology*, 75(4), 885–896. <https://doi.org/10.1111/j.1365-2125.2012.04360.x>
- Kiamehr, M., Viiri, L. E., Vihervaara, T., Koistinen, K. M., Hilvo, M., Ekroos, K., ... Aalto-Setälä, K. (2017). Lipidomic profiling of patient-specific induced pluripotent stem cell-derived hepatocyte-like cells. *Disease Models & Mechanisms*, 030841. <https://doi.org/10.1242/dmm.030841>
- Kim, M. H., Kim, M. O., Kim, Y. H., Kim, J. S., & Han, H. J. (2009). Linoleic acid induces mouse embryonic stem cell proliferation via Ca<sup>2+</sup>/PKC, PI3K/Akt, and MAPKs. *Cellular Physiology and Biochemistry*, 23(1–3), 53–64. <https://doi.org/10.1159/000204090>
- Krueger, W. H., Tanasijevic, B., Barber, V., Flamier, A., Gu, X., Manautou, J., & Rasmussen, T. P. (2013). Cholesterol-secreting and statin-responsive hepatocytes from human ES and iPS cells to model hepatic involvement in cardiovascular health. *PLoS One*, 8(7), e67296.
- Kvilekval, K., Lin, J., Cheng, W., & Abumrad, N. (1994). Fatty acids as determinants of triglyceride and cholesteryl ester synthesis by isolated hepatocytes: Kinetics as a function of various fatty acids. *Journal of Lipid Research*, 35(10), 1786–1794.
- Livak, K. J., & Schmittgen, T. D. (2001). Analysis of relative gene expression data using real-time quantitative PCR and the 2<sup>-</sup>ΔΔCT method. *Methods*, 25(4), 402–408.
- Mallanna, S. K., & Duncan, S. A. (2013). Differentiation of hepatocytes from pluripotent stem cells. *Current Protocols in Stem Cell Biology*, 2 (Suppl.26), 1G.4.1–1G.4.13. <https://doi.org/10.1002/9780470151808.sc01g04s26>
- Manzini, S., Viiri, L. E., Marttila, S., & Aalto-Setälä, K. (2015). A comparative view on easy to deploy non-integrating methods for patient-specific iPSC production. *Stem Cell Reviews and Reports*, 11(6), 900–908. <https://doi.org/10.1007/s12015-015-9619-3>
- Massa, M. L., Gagliardini, J. J., & Francini, F. (2011). Liver glucokinase: An overview on the regulatory mechanisms of its activity. *IUBMB Life*, 63, 1–6. <https://doi.org/10.1002/iub.411>
- Medine, C. N., Lucendo-Villarin, B., Storck, C., Wang, F., Szkolnicka, D., Khan, F., ... Hay, D. C. (2013). Developing high-fidelity hepatotoxicity models from pluripotent stem cells. *Stem Cells Translational Medicine*, 2 (7), 505–509. <https://doi.org/10.5966/sctm.2012-0138>
- Meikle, P. J., Wong, G., Tsorotes, D., Barlow, C. K., Weir, J. M., Christopher, M. J., ... Kingwell, B. A. (2011). Plasma lipidomic analysis of stable and unstable coronary artery disease. *Arteriosclerosis, Thrombosis, and Vascular Biology*, 31(11), 2723–2732. <https://doi.org/10.1161/ATVBAHA.111.234096>
- Merrill, A. H., Jr., Sullards, M. C., Allegood, J. C., Kelly, S., & Wang, E. (2005). Sphingolipidomics: High-throughput, structure-specific, and quantitative analysis of sphingolipids by liquid chromatography tandem mass spectrometry. *Methods*, 36(2), 207–224. <https://doi.org/10.1016/j.jymeth.2005.01.009>
- Mesicek, J., Lee, H., Feldman, T., Jiang, X., Skobeleva, A., Berdyshev, E. V., ... Kolesnick, R. (2010). Ceramide synthases 2, 5, and 6 confer distinct roles in radiation-induced apoptosis in HeLa cells. *Cellular Signalling*, 22(9), 1300–1307. <https://doi.org/10.1016/j.cellsig.2010.04.006>
- Michalopoulos, G. K., Bowen, W. C., Mulé, K., & Luo, J. (2003). HGF-, EGF-, and dexamethasone-induced gene expression patterns during formation of tissue in hepatic organoid cultures. *Gene Expression*, 11(2), 55–75. <https://doi.org/10.3727/000000003108748964>
- Miyaoka, Y., & Miyajima, A. (2013). To divide or not to divide: Revisiting liver regeneration. *Cell Division*, 8, 8. <https://doi.org/10.1186/1747-1028-8-8>
- Moss, A. J. (1991). Cholesterol and atherosclerosis: Diagnosis and treatment. *Journal of the American Medical Association*, 266(20), 2910–2911.
- Ntambi, J. M. (1999). Regulation of stearoyl-CoA desaturase by polyunsaturated fatty acids and cholesterol. *Journal of Lipid Research*, 40(9), 1549–1558. Retrieved from. <http://www.ncbi.nlm.nih.gov/pubmed/10484602>
- Ohnuki, M., Takahashi, K., & Yamanaka, S. (2009). Generation and characterization of human induced pluripotent stem cells. In Schlaeger, T. (Ed.), *Current protocols in stem cell biology*. John Wiley & Sons, Inc. <https://doi.org/10.1002/9780470151808>
- Olsavsky, K. M., Page, J. L., Johnson, M. C., Zarbl, H., Strom, S. C., & Omiecinski, C. J. (2007). Gene expression profiling and differentiation assessment in primary human hepatocyte cultures, established hepatoma cell lines, and human liver tissues. *Toxicology and Applied Pharmacology*, 222(1), 42–56. <https://doi.org/10.1016/j.taap.2007.03.032>
- Rasmussen, T. P. (2015). Genomic medicine and lipid metabolism: LDL targets and stem cell research approaches. *Translational Cardiometabolic Genomic Medicine* (99–118). London UK: Academic Press. <https://doi.org/10.1016/B978-0-12-799961-6.00005-6>
- Ruhanen, H., Nidhina Haridas, P. A., Eskelinen, E. L., Eriksson, O., Olkkonen, V. M., & Käkälä, R. (2017). Depletion of TM6SF2 disturbs membrane lipid composition and dynamics in HuH7 hepatoma cells. *Biochimica et Biophysica Acta*, 1862(7), 676–685. <https://doi.org/10.1016/j.bbali.2017.04.004>
- Rui, L. (2014). Energy metabolism in the liver. *Comprehensive Physiology*, 4 (1), 177–197. <https://doi.org/10.1002/cphy.c130024>
- Santos, N. C., Figueira-Coelho, J., Martins-Silva, J., & Saldanha, C. (2003). Multidisciplinary utilization of dimethyl sulfoxide: Pharmacological, cellular, and molecular aspects. *Biochemical Pharmacology*, 65, 1035–1041. [https://doi.org/10.1016/S0006-2952\(03\)00002-9](https://doi.org/10.1016/S0006-2952(03)00002-9)
- Schwartz, R. E., Fleming, H. E., Khetani, S. R., & Bhatia, S. N. (2014). Pluripotent stem cell-derived hepatocyte-like cells. *Biotechnology Advances*, 32, 504–513. <https://doi.org/10.1016/j.biotechadv.2014.01.003>
- Schwartz, R. E., Trehan, K., Andrus, L., Sheahan, T. P., Ploss, A., Duncan, S. A., ... Bhatia, S. N. (2012). Modeling hepatitis C virus infection using human induced pluripotent stem cells. *Proceedings of the National Academy of Sciences of the United States of America*, 109, 2544–2548. <https://doi.org/10.1073/pnas.1121400109/-DCSupplemental.www.pnas.org/cgi/10.1073/pnas.1121400109>
- Si-Tayeb, K., Noto, F. K., Nagaoka, M., Li, J., Battle, M. A., Duris, C., ... Duncan, S. A. (2010). Highly efficient generation of human hepatocyte-like cells from induced pluripotent stem cells. *Hepatology*, 51(1), 297–305.
- Sprecher, H. (2000). Metabolism of highly unsaturated n-3 and n-6 fatty acids. *Biochimica et Biophysica Acta*, 1486, 219–231. [https://doi.org/10.1016/S1388-1981\(00\)00077-9](https://doi.org/10.1016/S1388-1981(00)00077-9)
- Stübiger, G., Aldover-Macasaet, E., Bicker, W., Sobal, G., Willfort-Ehringer, A., Pock, K., ... Belgacem, O. (2012). Targeted profiling of atherogenic phospholipids in human plasma and lipoproteins of hyperlipidemic patients using MALDI-QIT-TOF-MS/MS. *Atherosclerosis*, 224(1), 177–186. <https://doi.org/10.1016/j.atherosclerosis.2012.06.010>
- Sullivan, G. J., Hay, D. C., Park, I. -H., Fletcher, J., Hannoun, Z., Payne, C. M., ... Wilmut, I. (2010). Generation of functional human hepatic endoderm from human induced pluripotent stem cells. *Hepatology*, 51(1), 329–335. <https://doi.org/10.1002/hep.23335>
- Szkolnicka, D., Farnworth, S. L., Lucendo-Villarin, B., Storck, C., Zhou, W., Iredale, J. P., ... Hay, D. C. (2014). Accurate prediction of drug-induced liver



- injury using stem cell-derived populations. *Stem Cells Translational Medicine*, 3(2), 141–148. <https://doi.org/10.5966/sctm.2013-0146>
- Szkolnicka, D., Lucendo-Villarin, B., Moore, J. K., Simpson, K. J., Forbes, S. J., & Hay, D. C. (2016). Reducing hepatocyte injury and necrosis in response to paracetamol using noncoding RNAs. *Stem Cells Translational Medicine*, 5(6), 764–772. <https://doi.org/10.5966/sctm.2015-0117>
- Takahashi, K., & Yamanaka, S. (2006). Induction of pluripotent stem cells from mouse embryonic and adult fibroblast cultures by defined factors. *Cell*, 126(4), 663–676.
- Takayama, K., Inamura, M., Kawabata, K., Sugawara, M., Kikuchi, K., Higuchi, M., ... Mizuguchi, H. (2012). Generation of metabolically functioning hepatocytes from human pluripotent stem cells by FOXA2 and HNF1 $\alpha$  transduction. *Journal of Hepatology*, 57(3), 628–636. <https://doi.org/10.1016/j.jhep.2012.04.038>
- Tokuda, N., Numata, S., Li, X., Nomura, T., Takizawa, M., Kondo, Y., ... Furukawa, K. (2013).  $\beta$ 4GalT6 is involved in the synthesis of lactosylceramide with less intensity than  $\beta$ 4GalT5. *Glycobiology*, 23(10), 1175–1183. <https://doi.org/10.1093/glycob/cwt054>
- Wiśniewski, J. R., Vildhede, A., Norén, A., & Artursson, P. (2016). In-depth quantitative analysis and comparison of the human hepatocyte and hepatoma cell line HepG2 proteomes. *Journal of Proteomics*, 136, 234–247. <https://doi.org/10.1016/j.jprot.2016.01.016>
- Yang, D., Yuan, Q., Balakrishnan, A., Bantel, H., Klusmann, J., Manns, M. P., ... Sharma, A. D. (2016). MicroRNA-125b-5p mimic inhibits acute liver failure. *Nature Communications*, 7, 1–11. <https://doi.org/10.1038/ncomms11916>
- Younossi, Z. M., Koenig, A. B., Abdelatif, D., Fazel, Y., Henry, L., & Wymer, M. (2016). Global epidemiology of non-alcoholic fatty liver disease- Meta-analytic assessment of prevalence, incidence and outcomes. *Hepatology*, 64(1), 73–84. <https://doi.org/10.1002/hep.28431>
- Zhang, J. Y., Kothapalli, K. S. D., & Brenna, J. T. (2016). Desaturase and elongase-limiting endogenous long-chain polyunsaturated fatty acid biosynthesis. *Current Opinion in Clinical Nutrition and Metabolic Care*, 19(2), 103–110. <https://doi.org/10.1097/MCO.0000000000000254>

## SUPPORTING INFORMATION

Additional supporting information may be found online in the Supporting Information section at the end of the article.

**How to cite this article:** Kiamehr M, Alexanova A, Viiri LE, et al. hiPSC-derived hepatocytes closely mimic the lipid profile of primary hepatocytes: A future personalised cell model for studying the lipid metabolism of the liver. *J Cell Physiol*. 2018;1–18. <https://doi.org/10.1002/jcp.27131>

# **PUBLICATION**

## **III**

**Dedifferentiation of primary hepatocytes is accompanied with reorganisation of lipid metabolism indicated by altered molecular lipid and miRNA profiles**

Kiamehr M, Heiskanen L, Laufer T, Düsterloh A, Kahraman M, Käkälä R, Laaksonen R, Aalto-Setälä K.

Under review at Scientific Reports. 2018

**Publication reprinted with the permission of the copyright holders.**







